Automotive Collision Detection System Utilizing Distributed Polyvinylidene Fluoride Sensors

Ifthekhar Anwar

A Thesis

in

The Department

of

Mechanical and Industrial Engineering

Presented in Partial Fulfillment of the Requirements
For the Degree of Master of Applied Science at
Concordia University
Montreal, Quebec, Canada.

December 2005

Your file Votre référence
ISBN: 0-494-14295-2
Our file Notre référence
ISBN: 0-494-14295-2

ABSTRACT

Automotive Collision Detection System Utilizing Distributed Polyvinylidene Fluoride Sensors.

Ifthekhar Anwar

Vehicular bumper is a structure mounted at the front and rear of the vehicle to absorb the first impact and is designed to minimize its effect on the vehicle structure and its occupants. Although vehicle collision is an unavoidable fact, there are no reported attempts to date in exploring the feasibility of detection system utilizing sensors. For this investigation, PVDF (Polyvinylidene Fluoride) sensor for its sensitivity and dynamic range is selected for application to bumpers. A prototype bumper with PVDF sensors is fabricated to carry out tests under low level forces. A prototype bumper represented by a Plexiglass beam is mounted with a series of PVDF sensors across the length, while the bumper is mounted on a rigid structure through set of mounts. Each sensor is calibrated for various loads on and away from the sensor and tested to predict the magnitude of the force and corresponding position. Several configurations for the bumper with and without cover over the sensor surface are experimented to determine the collision detection capability of the bumper in terms of magnitude, duration and location of the impact. The time history response of each sensor and its characteristics are utilized to develop layouts for bumper systems with sensors. Two designs were fabricated and tested in the laboratory to establish methodology for establishing relationships between sensor responses with magnitude and location of collision. Based on the investigation, a final design is proposed for implementation of collision detection in automotive bumpers.

ACKNOWLEDGEMENTS

It is indeed a great pleasure for me to express my sincere appreciation and thanks to my respectable supervisors Dr. A.K.W. Ahmed and Dr. Javad Dargahi for initiating the study topic and for their continuous guidance, encouragement and support. Their profound knowledge and thoughtful instructions have always shed some light on my way to pursue this thesis work.

Thanks are due to the friends, colleagues, faculty and staff at CONCAVE Research Center of Concordia University and at the Department of Mechanical and Industrial Engineering, for their contributions in many intricate situations during the research work.

Finally, I would like to express special gratitude to my parents, Mohd. Abu Jafar and Dil Nahar, to my sibling Iqbal Anwar and Imrul Anwar for being enduring, encouraging and caring to my aspirations. I thank them for inspiring me to accomplish this work. To them, I dedicate this thesis.

TABLE OF CONTENTS

CHAPTER 3

AUTOMOTIVE BUMPER

CHAPTER 4

EXPERIMENTAL SET-UP AND TEST PROCEDURES

CHAPTER 5

EXPERIMENTAL ANALYSIS AND ANALYTICAL APPROACH

CHAPTER 6

CONTRIBUTIONS, DISCUSSIONS AND RECOMMENDATIONS

LIST OF FIGURES

LIST OF TABLES

NOMENCLATURE

Symbol	Unit	Description
Q	pC	Output charge
V	mV	Output voltage
A_e	m^2	Electroded area of PVDF film
A_a	m^2	Cross sectional area of the film perpendicular to the direction of the applied force
σ_1	N/m^2	Applied tensile stress in the drawn direction
σ_2	N/m^2	Applied tensile stress in the transverse direction
F	N	Applied force
d_{ij}	pC/N	Piezoelectric strain coefficient
d_{31}	pC/N	Piezoelectric strain coefficient in the drawn direction
d_{32}	pC/N	Piezoelectric strain coefficient in the transverse direction
d_{33}	pC/N	Piezoelectric strain coefficient in the thickness direction
d_{3h}	pC/N	Hydrostatic piezoelectric coefficient
d^*_{33}	pC/N	Function of piezoelectric strain coefficients in all the three Directions
P_y	$\mu C.m^{-2}.K^{-1}$	Pyroelectric coefficient
P_1	$\mu C.m^{-2}.K^{-1}$	Pyroelectric coefficient in direction '1'
P_2	$\mu C.m^{-2}.K^{-1}$	Pyroelectric coefficient in direction '2'

P_3	$\mu C.m^{-2}.K^{-1}$	Pyroelectric coefficient in direction '3'
dD/D	m/m	Average lateral strain
dL/L	m/m	Average axial strain
P	Volt	Peak magnitude of output voltage
T_r	mS	Rise time
T_f	mS	Fall time
X	mm	Position
A		Co-efficient of x^2 in a quadratic equation
B		Co-efficient of x in a quadratic equation
C		Constant of a quadratic equation

CHAPTER 1

INTRODUCTION AND LITERATURE REVIEW

1.1 Introduction

Automotive collision has been a subject of interest since the invention of the vehicle itself. Researchers in the field have been investigating and developing tools to prevent collisions. Through monumental development of sensor technology in the recent years, attempts are being made to use distance detection to minimize collisions. Collisions are however, a very frequent occurrence in city streets. In majority of vehicular collision, the first point of impact is the front and rear bumpers. In accident investigations and accident reconstructions, the bumper plays most important role. The damage to the bumper and its mounts are often used to establish the magnitude of impact force and its direction.

Over the years, there has been significant development of bumper technology and the mounting methods with isolators to minimize the effect of collision to the vehicle structure and its occupants. There are also regulations that dictate the minimum performance of a bumper system under collisions.

Although significant modern research has been directed towards intelligence in all aspects of vehicle systems, there has been no attempt in developing vehicle bumpers with built in collision detection system. With the advancement of sensor technology and economical production methods, it is feasible to incorporate sensors in the design and construction of bumper that can detect any impact it experiences. This investigation examines the feasibility of using Polyvinylidene Fluoride (PVDF) sensors on the bumper as a means to detect the magnitude and location of low level impact. For this a prototype

bumper with PVDF sensor is designed and built for extensive experimental investigation. The experiment is designed to determine if the bumper system can accurately determine the magnitude, location and duration of impact. A bumper system with such collision detection capability will definitely add to the development of intelligent vehicle system. Furthermore such technique can be applied for a wide range of other systems where such capability of force detection is desired.

Although there are some literature available on the bumper systems and collision testing, the author is not aware of any design with sensors or collision detection capability. This chapter therefore, presents a general review of work on collisions, bumper systems, impact tests and PVDF sensor technology. The chapter is concluded with objective of the proposed research and organization of the thesis.

1.2 Vehicle Collision Phases

Vehicle collision analysis techniques generally separate vehicle collisions into three different phases: pre-impact, impact and post-impact. The definition of the impact phase as the time the vehicles are in contact implies the definition of the pre-impact and post impact phases; i.e., the pre-impact is that time prior to vehicle to vehicle contact and the post impact is the time after the vehicles have separated. In order to analyze collisions, engineers have developed models which attempt to quantify the accident. Typically the pre-impact velocities of the vehicles involved in the accident are of particular interest. After an impact has taken place, it is difficult to gather information on the pre-impact phase. The post-impact phase is therefore usually taken as the starting point in the analysis of automobile collisions. From information obtained at the accident

scene, e.g., skid marks, debris, final resting points of the vehicles and vehicle deformation are the typical information that may be available for the analysis. Numerous models exists which can predict the velocity of each vehicle immediately after the separation of the two vehicles [3].The proposed research deals with impact phase only where the collision detection system can register data during impact.

1.3 Review of Relevant Literature

The phenomenon of automotive bumper impact conforms to the theory of classical physics. The initial parameters of impact are mass, velocity and geometry. The resulting variables of impact are force, acceleration, displacement, rebound velocity and impact energy. These parameters and variables can be recorded, measured and analyzed within a bumper test laboratory. Glance [4] discusses the methodology for testing and measuring automotive bumper performance in his study. Automotive bumper regulations have been established for tests to be carried out on bumper performance. Automotive industry have adopted pendulum and barrier (rigid flat face wall) impact tests and often surpasses the minimum standard recommended by the federal government. The considered and recorded variables are force, deflection, impact velocity etc versus time. The other measurement variables are acceleration, energy and rebound velocity. Displacement is measured with different devices including linear displacement transducers, lasers sensors, and antennae. Force is recorded with a single axis (or may be tri-axial) load cell placed behind the pendulum's impact ridge. Velocity is measured with an optical speed trap and accelerometers placed at the c.g. of the pendulum and cart to provide deceleration versus time data [4]. This procedure to introduce low, moderate or

high speed collision is quite popular among automotive manufacturers and the researchers. Szabo Thomas et al. [1] conducted several crash tests with Ford Escorts (Model years 1981-83). The responses of bumper to bumper impacts and under ride (generally defined as a portion of a passenger vehicle sliding under another vehicle) of one bumper under another are evaluated by equipping the Ford escorts with energy absorbing bumpers. Two impacts were conducted each at 2.23, 4.47 and 6.71 m/s. Bumper displacement, vehicle acceleration and vehicle velocity time histories were presented for both bullet vehicle (one which strikes) and target vehicle (one which is struck). Here underride which is a very important phenomenon had been uplifted by arranging the front bumper of the bullet vehicle to underride the rear bumper of target vehicle at a velocity of 4.47 m/s (16 Km/hr) and results indicated extended damage [1]. Some researchers experimented on Light commercial vehicles (LCV) bumpers and compare the damage produced by vehicle to barrier and vehicle to vehicle collisions of a similar severity. Heinrichs et al. [5] conducted impact tests on the front and rear bumpers of five pick up trucks where each one is subjected to an impact with fixed barrier and with a passenger vehicle. Measurements of speed, impact force, damage and high speed video were recorded for each test. The speed during the collision associated with each test was measured by attaching an MEA 5^{th} wheel (Macinnis Engineering Associates, Richmond, BC, Canada). The bumper considered in the study does not contain specific energy dissipating elements and is therefore referred as rigid bumper (Consists of a steel bumper beam attached to the vehicle frame either directly or by mounting brackets) [5]. Contemporary bumper systems are typically equipped with some form of impact absorber rather than having a simple rigid bumper (observed mostly in pickup trucks, vans, and

sport utility vehicles). The post collision condition of impact absorbers is a good measure of collision severity. Common impact absorbers are isolators (can be found on BMW, Chrysler, Datsun, Ford, General Motors, older Hyundai, older Honda, older Mazda, some Nissan, Mercedes, some Subaru, older Toyota, and Volvo cars), foam core (Polystyrene Foam-Acura, Honda, some Mazda and some Nissan cars and Polyurethane Foam-Hyundai, Toyota cars) and honeycomb cores (some newer General motors cars), deformable struts (some newer Volkswagens and some Dodge/Plymouth vehicles), rubber shear blocks (some older model Ford, Lincoln and Mercury vehicles) and leaf springs (older model General Motors vehicles). King et al. [2] measured the static properties of a group of 30 isolators. The dynamic properties of four of the isolators were measured. Those tests incorporated a pendulum and a displacement transducer to acquire the dynamic force displacement data. This assessment process continues with a number of vehicle to vehicle and vehicle to barrier collisions to judge the performance of different bumper types in low speed aligned bumper to bumper impacts. Both target and bullet vehicles were instrumented with MEA 5th wheels (Designed for low-speed impact testing and have sufficient downward force to prevent slip between the wheel and road surface during collision) and data were acquired from both 5th wheels simultaneously. On the whole the purpose of the study was to examine the low speed impact severity on automobile bumper systems and its correlation with the compression of bumper systems. Various aspects of the collision were examined including impact duration, speed change as a descriptor of impact severity, isolator compression, and coefficient of restitution [1, 2]. The coefficient of restitution (CR) can be defined as the ratio of the closing velocity (approach velocity) of the vehicles just before the impact to the post-impact separating

velocity. Consequently CR is able to demonstrate the post collision speeds of impact. For example if an aligned impact between a moving motor vehicle and a stopped motor vehicle occurs, the momentum transfer between the vehicles can result in three different outcomes for the post impact speeds. First, the vehicles can reach a common velocity following the impact. Second, the striking vehicle can come to a stop while the struck vehicle rolls away. Finally, and most commonly, each of the vehicles moves following the accident with some finite separation speed. All of these three outcomes depend on a property of collision which is CR. The CR for medium and high velocity collisions is low (approximately 0.1) whereas at extremely low velocity it approaches 1. Theoretically because actual magnitude had not been adequately established for very low speed, CR equals 1 for a purely elastic collision and 0 for a purely plastic collision (no rebound) and between this region the CR is taken below 0.4 for velocity 2.5 mph. For velocity in the range of 2.5-5 mph, in nine vehicle to vehicle collisions the average CR is 0.25, but in the case of vehicle to barrier collisions it becomes 0.3-0.4 for the same velocity range. For very low velocity like 1 mph CR is about 0.86 [6]. Similar work had been done for low, moderate and high speed. Tanner et al. [7] varied the speed in a range of 9.5 to 21 kilometers per hour (5.9-13 mph) for the barrier impact of Volvo 850 front bumper and the CR was found to be in the range of 0.2-0.4. In this elaborate study, a number of vehicles are examined for vehicle to barrier impact as well as vehicle to vehicle collisions and CR, acceleration and speed change have been justified as descriptor of collision. Coefficient of restitution is shown to decrease as the impact speed decreases. For the impact speed of 30 – 50 mph against a barrier and inline collisions the CR decreases from approximately 0.15 to less than 0.1 [6, 7, and 8].

Automotive bumpers are designed to prevent or reduce physical damage to the front and rear ends of passenger motor vehicles in low speed collisions. Bumpers are not typically designed to be structural components that would significantly contribute to vehicle crashworthiness or occupant protection during front or rear collisions. It is not a safety feature intended to prevent or mitigate injury severity to occupants in the passenger cars. Bumpers are designed to protect the hood, trunk, grille, fuel, exhaust and cooling system as well as safety related equipment such as parking lights, headlamps and taillights in low speed collisions. In recent times bumpers generally consist of a plastic cover over a reinforcement bar made of steel, aluminum, fiberglass composite, or plastic [9].

Contemporary researchers focused on fuel economy, high strength, cost effectiveness, aesthetical pleasure of customers etc. to continue their study for the advancement of bumper systems. Repair costs for bumpers are another issue that is becoming an increasingly important concern in bumper system design. The Insurance Institute for Highway Safety (IIHS) states that repair for minor incidents are a major factor in collision insurance costs. According to the IIHS bumpers play a significant role in minor incident repair costs and hence insurance costs. There are wide range of high strength and ultra high strength bumper steels available. These steels are reviewed as well as appropriate manufacturing methods for converting them in to bumper facebars and reinforcing beams are investigated, which can aid the bumper engineers of North America to meet the challenge. In the 1998 models 81 % of the bumper beams of North America were made from steel, 14.5 % from composites and 4.5 % from aluminum and in the 2001 models 84.2 % of the bumper systems were steel, 13.9 % were composites

and 1.9% was aluminum [9]. Sindrey [9] conducted a study with some commonly used bumper beams and found that steel weighs least except couple of composite beams, which improves fuel economy. Due to its low unit material cost, steel reinforcing beams are less expensive than composite and aluminum. Moreover vehicles with steel front and rear reinforcing beams have an average lowest repair cost [9]. Except these common steel bumpers, many design improvements are being created and slowly adopted. Increasingly stringent environmental demands are encouraging the automotive industry to look for ways of producing lighter and more fuel efficient cars. Using new technology, the VEK Project which focus on the weight optimization of energy absorbing components in vehicle industry (Involving: Innovatum, SAAB Automobile, Outokumpu Stainless, Finnveden Metal Structures and Epsilon are just some of the companies that have taken part in this project) has developed a bumper in high-performance stainless steel that is 26 percent lighter. Higher fuel prices and requirements for reduced carbon dioxide emissions have put automotive manufacturers under increasing pressure to produce lighter, more fuel efficient cars. Using a high performance stainless steel, the VEK project has succeeded in developing bumper system that at no extra cost and without sacrificing performance is 26 percent (35-40 kg) lighter than existing bumpers. The greatest weight reduction has been achieved in the collision boxes [10].

Besides steel the new trend of using Plastic bumper sets landmark in this field for few reasons. Plastic bumper provides significant weight advantages over any metal bumper due to its low specific gravity. Therefore, plastic bumper reduces vehicle weight and improves fuel economy. Furthermore, plastic can be made into complex shapes therefore manufacturers have greater design flexibility which can further enhance the

aerodynamic performance of the vehicle. Plastic bumpers contain reinforcement that allows it to be impact resistant as metals while being less expensive to replace than their metal equivalents. Plastic bumpers generally expand at the same rate as metal bumpers under normal driving temperatures and do not usually require special fixtures to keep them in place. Plastic product used in making auto bumpers can be recycled. This enables the manufacturers to reuse scrap materials in a cost effective manner. Test reveals that post-industrial recycled TPO (Thermoplastic Olefin) performs exactly like virgin material, converting hundreds of thousands of pounds of material destined for landfills in to workable grade A material, and reducing costs for manufacturers. Thus, re-conditioning and recycling plastic bumper covers is an important means to extend the life cycle of vehicle plastics. Another important advantage of plastic is that it does not get rusty, and can have longer material life [11].

A new invention in material technology was introduced with polymeric based composite materials (the fiber reinforcement is normally made from glass, carbon, aramid, boron or natural fibers while the matrix is normally thermoplastic or thermosetting materials), which offer high specific stiffness, low weight, corrosion free, ability to produce complex shapes, high specific strength, high impact energy absorption and aesthetically pleasing [12]. These advantages tend to incline the vehicle industry towards plastic and composite bumper. General Motor (Exterior Panels and Bumper Technology Group) developed an improved version of polymer bumper for their 1997 Saturn Coupe. Polymer bumper requires no adhesives; once fasteners are removed entire part can be reground and reused. This performs even better than their earlier Aluminium beam bumper model which was even cost effective and weighs 2.5 pounds less than

traditional one. The polymer version bumper weighs less and is also more cost effective than the previous version as 13 parts ware eliminated from aluminum beam model. To meet the stringent performance requirement of bumper federal standard, the new bumper had been made injection molded in one piece with optimized rib placement and thickness in the center of the beam. Optimizing thickness and rib structure allowed the bumper beam on a 2600 pound vehicle to withstand the point load of a pole in 5 mph impact testing.

As the automotive industry started implementing plastic bumpers as replacement of steel bumpers this inspires the researchers to examine different properties of plastic for use in automotive bumper. Rawson [13] of GE plastic performed a preliminary feasibility study that estimates the performance of the plastic part before tooling is cut. A study was conducted in order to correlate the predicted performance of thermoplastic bumper designs via hand calculations and detailed finite element analysis, and the obtained results were compared with actual physical testing. Actual injection molded thermoplastic bumper beams of a Polycarbonate-Polybutylene Terephthalatealloy was used [13]. Different works had been conducted by the insertion of different phenomenon such as the adoption of different energy absorption media, going through fatigue test in the plastic bumper system to realize superiority of this system over steel bumper. Following the demand of the customers the engineer are charged to reduce collision repair costs and enhance occupant safety further. As mentioned earlier, the majority of today's passenger-car bumper systems consist of a reinforcing bar either of steel, aluminum or composite construction and an energy absorption media. The most widely used energy-absorber construction is made from expanded-polypropylene foam, EPP

(more than 80%) and also another widely used energy absorber is honeycomb core which is made of ethylene vinyl acetate (EVA) copolymers. High strength to weight ratios and specific energies of engineering thermoplastics provide the opportunity to achieve energy absorption characteristics. It has been found that engineering thermoplastics provides good result in automotive application (automotive bumper and body panels) where structural integrity, crashworthiness and energy absorption are the key requirements. [14]. Chaudhuri et al. [15] designed, fabricated and tested the low cost prototype of sheet metal and fiber reinforced plastics (FRP) bumpers in four different types with various combinations of elastomers (can be stretched to many times their original length and can bounce back to their original shape without permanent deformation). The design comprises of several cuts throughout the length transversely at intervals for easy bending. The cuts are later welded together to from the shell. The joints are spot welded at intervals which turned out to be the weak spots in the shell. After testing it was concluded that if the cuts are continuously welded this problem can be overcome and the energy absorbing capacity can be increased by approximately 40 to 50 %. If the bumper is fabricated as a pressed or formed component in one piece then the energy absorbing capacity would have improved by 60-70 % [15]. This revolutionary footstep of the researchers goes further by using composite automotive bumper. Hendrickson International and Delphi Automotive Systems have announced a technology agreement to develop and manufacture a composite bumper for the medium- and heavy-duty truck and bus markets. A concept composite bumper, first unveiled by Hendrickson at the Great American Trucking Show in 2000, was developed using a hybrid glass and carbon fiber design weighing up to 70 pounds less than its steel equivalent. Composites can be

designed to conduct 50% less vibration than steel and to be more impact-resistant. The structural composite bumper is stiffer than plastic bumpers and requires less mounting hardware, enough to support headlights, fog lamps, collision avoidance sensors, or sight-sticks. Eliminating brackets will reduce the number of component parts, help shorten assembly time, improve warranty, and reduce maintenance costs. Gilliard et al. [16] proposed a lightweight, low cost, and high performance I-section bumper by new mineral filled glass mat thermoplastic (GMT) composite. Improved static loads and dynamic impact performance results had been achieved through the development of lower cost mineral filled/ chopped fiber glass GMT (40 %) [16].

Besides the experimentally obtained results in a multidimensional consideration another prospective way to bring researchers complacency is the simulation of vehicle impact through finite element method. Vehicle finite element models have been increasingly used in preliminary designs analysis, component design and vehicle crashworthiness evaluation. Numerous collision scenarios like barrier impact, pole impact, corner impact are simulated by the same post impact dynamics as mentioned before. Finite element study can further provide the flexibility to evaluate the variables like acceleration, velocity, deflection etc. for every part of the vehicles [17].

Due to the customer's demand, advancement towards easing injury during collision is also important priority among the vehicle manufacturers. By sensing crash severity it is possible to measure the magnitude of a vehicular crash event relative to injury of the occupant. In general, it implies the delta velocity of the crash. In early crash detection systems the only requirement was to determine if the crash was significant enough to deploy the airbags. Current crash severity systems normally employ an upfront

sensor(s), along with the passenger compartment accelerometer to obtain information on the severity of the crash. The up-front sensor provides required information for crash severity discrimination. There are currently three options: accelerometer, ball-in-tube and radar [18]. The accelerometer is the standard sensor for the passenger compartment for single point sensing and is also used for side impact sensing systems. The ball-in-tube is an alternative for use as an up-front sensor. However, in general ball-in-tube provides less information than an accelerometer. A radar sensor could be used as a replacement for either an up-front accelerometer or ball-in-tube sensor. The radar could provide two sources of information: closing velocity and shape. Velocity is relatively easy to estimate with accuracy, the shape information on the other hand could be a problem in general [18]. Gioutsos et al. [19] provides a solution for crash severity detection with the combination of two of the sensing system and termed it as ball-in-tube and accelerometer sensing system (BASS). The major components of the BASS are a ball-in-tube (BIT) sensor(s) in the front of the vehicle along with an electronic sensing module (ESM) in the passenger compartment. The ESM includes an accelerometer, a central processing unit with the BASS algorithm encoded and an input line(s) from the BIT(s). It should be pointed out that the system could work with an up-front accelerometer(s) transmitting a threshold crossing(s). This version of the system would be called MASS-multiple accelerometer sensing system [19]. Foo et al. [20] described the methods of computer modeling, occupant sensing and vehicle crash dynamics to define a crash sensing system. A multi-disciplinary effort for sensing system had been developed. Here the smart restraint sensing system get activated by the algorithm, necessary for predicting a

deployment event which are based on an approach of coupling the occupant kinematics in crash to the sensing technology [20].

Although there are no reported attempts to develop bumper system with collision detection capability, such a system can further enhance the accuracy of safety airbag deployment. Data recorded from such bumper can also be used to warn driver of contact with objects, as well as will provide indispensable information for accident reconstruction studies and insurance investigations. In 1969 the strong piezoelectric effect in the polymer materials, PVDF (Polyvinylidene Fluoride, consists of long chain molecules with repeated unit $CF_2 - CH_2$) was discovered. PVDF has the capability to determine the magnitude of the applied force and to identify its position and also can provide some information about the shape of the contacted object [21, 22, and 23]. Dargahi [22] conducted a study on a prototype tactile sensing system using three sensing elements to identify the position of applied force and termed the procedure as triangulation approach. The study also reported about the occurrence of crosstalk (the problem of evolving undesirable response from the nearest neighbor sensing element, when a force is applied to a certain sensing element) [22]. Thus there is the possibility that multiple sensors used over the length of bumper can be used simultaneously to estimate the applied load and its location.

1.4 Rationale for Using PVDF Sensor in Collision Detection System

This study focuses on the feasibility of developing a smart bumper capable of detecting very low to low level impact, the location of impact along the bumper, the duration of impact as well as the texture (softness) of the object. For this wide range of

detection capability with one sensor type, it was necessary to explore various sensor technologies. Use of piezoelectric material over the bumper surface is chosen as candidate sensing element for its sensitivity, large dynamic range and precision.

PVDF has been researched in the past in tactile sensing application [21, 22 and 23]. It was also used as a transducer in sensor system and actuator system [30], and in MIS (minimally invasive surgery), endoscopic grasper [41]. Use of piezoelectric material like PVDF as sensor element on the vehicle bumper could be considered as a new approach of collision detection. PVDF sensor exhibits good repeatability and impressive force sensitivity. The relationship between applied force and propagated charge is linear for stress up to 40 MPa. It has a very wide frequency (DC to MHz) and dynamic range. PVDF is very sensitive element but its sensitivity can be varied according to the mode of application [24]. In fact the capability of PVDF was the inspiring motivation for this project, where collision detection bumper system is an application. This may have many other application requiring sensing of forces and stress and location of force.

1.5 Objectives of the Present Research

The primary objective of the present thesis research is to further explore the force detection capabilities of a PVDF sensor, and to carry out feasibility investigations of using such sensors on vehicle bumper for collision detection. The experimental research is conducted in a systematic manner using a small scale prototype bumper. Several preliminary design and lay out of sensors were tried before arriving at the final design of the experimental set up. The objective in the design was to make the bumper collision

detection system capable of sensing magnitude, location and duration of the impact. The steps and specific objectives in each step are summarized in the following:

(1) To comprehend the characteristics of the PVDF (Repeatability, Linearity, Force Sensitivity, cross sensitivity etc.) through different experiments.

(2) To examine PVDF response characteristics and influence of duration of load application, size and softness of the impacting object.

(3) To design and manufacture different parts to construct a scale model of collision detection bumper and to integrate PVDF and instruments for the measurements of the responses to impact.

(4) To design and fabricate the test set up with the bumper such that impact force can be applied at any controlled location along the length of the bumper.

(5) To develop empirical relation of force by two sensors (two-sensor method) as a function of corresponding peak amplitude. Also to observe the corresponding rise time and fall time.

(6) To develop empirical relations of position of impact by using the two sensors where it was struck in between as a function of peak amplitude respectively for each load.

(7) To generate an accomplished collision model where the input is peak voltage of all sensors and the outputs are force and position.

(8) To validate the proposed model with experimental results.

1.6 Organization of the Thesis

Chapter 2 illustrates the history of piezoelectric material along with the basic characteristics of Polyvinylidene Fluoride (PVDF) have been briefly discussed. The concepts of piezoelectricity and pyroelectricity in PVDF are provided along with the basic phenomenon observed during the implementation of PDVF as sensor (force sensitivity, piezoelectric coefficients, linearity, repeatability, frequency & dynamic range, effect of temperature etc.).

Chapter 3 is composed by the information about the overall bumper system obtained from different literature has been gathered. Automotive bumper regulation history and associated safety standards applicable to individual continents have been accumulated too from the bumper legislations (incorporated by law governing organization like NHTSA, FMVSS etc.).All the components of contemporary bumper system have been described concisely. The idea of inserting this chapter is evolved just to accommodate the thesis with contemporary bumper system's assembly and associated safety regulations.

Chapter 4 comprises of experimental set-up design, instrumentation and test procedures. Precise description of the arrangement of set-up and the apparatus used are provided. The path of experimental methodology towards obtaining the most convincing way of vehicle collision detection is concisely explained. Besides these, to understand the sensor response several experiments are performed which are able to clarify the acceptability of the results. Only the characteristics related to the thesis are upheld.

Chapter 5 is the core chapter of the thesis. It includes the experimental and analytical endeavor of the thesis. It explicitly defines entire system for finding the applied

force and corresponding position of application. The chapter exemplifies the whole collision phenomena for better understanding of the system.

The thesis culminates with Chapter 6. The major contributions of the investigation are highlighted, and discussion and conclusions drawn are summarized in chapter 6. The scopes for further investigations with the generated system are presented.

CHAPTER 2

POLYVINYLIDENE FLUORIDE (PVDF) SENSOR

2.1 Introduction

Sensor can be defined as a generic name for a device that detects either the absolute value of a physical quantity or a change in value of the quantity and converts the measurement into a useful signal for an indicating or recording instrument. Simply a sensor accepts a particular form of input and converts the information into an electrical signal and delivers the signal to a data processing system [25]. The piezoelectric effect was discovered by the Curie brothers in 1880.They found that quartz changed its dimension when subjected to an electrical field and conversely generated electrical charge when mechanically deformed and they called this phenomenon "piezoelectricity"- derived from the Greek for "pressure electricity". Not long after, the same crystals were found to develop similar charge when exposed to incident thermal radiation and the term "pyroelectricity" was coined [26]. The practical use of piezoelectric materials became possible with Paul Langevin's discovery in 1916 of the piezoelectric characteristics of quartz crystals. Following this discovery, it was observed that some crystalline materials demonstrate a spontaneous polarization along one axis of the crystal, known as ferroelectric behavior. For many years, Rochelle salt was the only crystal that was known to have this ferroelectric property. The largest progress in this field was made in the sixties with the discovery of piezoelectricity in Polyvinylidene Fluoride (PVDF). In 1969 Kawai [24] found very strong piezoelectric effect in the fluoropolymer, Polyvinylidene fluoride (PVDF). While other materials like nylon and PVC (Polyvinyl Chloride) exhibit

similar effect, none are as highly piezoelectric as PVDF and its copolymer. Like other ferroelectric materials, PVDF is also pyroelectric (produce electrical charge in response to a change in temperature) [24]. The electrochemical coupling of PVDF is lower than that of piezoceramic, but since the foil thickness can be as little as 10 micrometers the vibration mass is extremely small. PVDF also has greater damping than ceramics, and the resulting dynamic characteristics allow very short pulses to be generated. This makes it possible to measure shorter ranges using PVDF than is possible with piezoceramic transducer. PVDF is a polymer of approximately 50-65 % crystallinity. This semi-crystalline polymer has drawn both scientific and technological attention because of the useful piezoelectric and pyroelectric properties it presents. The polymer consists of long chain molecules with repeated unit $CF_2 - CH_2$. The reason for the strong piezo-pyroelectric activity is related to the large electro negativity of fluoride atoms in comparison to the carbon atoms, thus accommodating a large dipole moment [22].

2.2 Piezoelectricity in PVDF

Piezoelectricity is electric polarization produced by mechanical strain in certain crystals, the polarization being proportional to the amount of strain. The reverse is also true [26]. β phase of PVDF has very good piezoelectric properties. PVDF is one of the rare polymers that exhibit diverse crystalline forms. It possesses at least four phases known as α, β, γ and δ, not all of which display the piezoelectric effect because of the different molecular packing. The alpha phase which is produced by cooling the melt is non polar, with adjacent chains antipallel. This form shows no spontaneous polarization. Beta phase has an orthorhombic structure and a large dipole moment leading to a

spontaneous polarization. The polar phase β is technologically the most interesting because of its better piezoelectric and pyroelectric properties. Crystallization of PVDF from the melt takes place predominantly in the α phase and the β phase is normally obtained by stretching or rolling the α phase films. The conversion from alpha to beta phase depends on the draw ratio and the temperature of the stretching process. Normally, the film must be stretched three to seven times at a temperature between $60^{o}C$ & $140^{o}C$ and allowed to cool in the elongated state. This results in a phase transformation due to the fact that polymer chains are stretched along their axis displaying a rotation and alignment of CH_2 and CF_2 groups. The gamma phase appears to be intermediate to the alpha and beta phases and can be produced by solvent crystallization or melt crystallization under high pressure. This form can also be converted to the beta phase by mechanical drawing. The delta phase is produced by poling the alpha phase at low field strengths. Useable piezoelectric films are produced by orientation of the film followed by poling, to produce the beta phase [27]. Recently it was demonstrated that β phase films are possible to obtain by solution crystallization with dimethylacetamide (DMA) at adequate temperature conditions [28].This beta phase of PVDF forms crystal symmetry of C_{2v} [27]. The piezoelectric coefficients for this form can be denoted by the following 3×6 matrix:

$$[d_{ij}] = \begin{bmatrix} 0 & 0 & 0 & 0 & d_{15} & 0 \\ 0 & 0 & 0 & d_{24} & 0 & 0 \\ d_{31} & d_{32} & d_{33} & 0 & 0 & 0 \end{bmatrix}$$

The axes are defined here in terms of the drawn direction (direction 1), normal to the drawn direction in the plane of the film (direction 2) and normal to the plane of the film

(direction 3).This is shown in Fig. 2.1.But for the bi-axially oriented beta form of PVDF (the one which was used in this study) , the crystal symmetry is $C_{\infty v}$, which implies a similar $[d_{ij}]$ coefficient matrix to that of the uni-axially oriented form, except that $d_{31}=d_{32}$ and $d_{15}=d_{24}$ [29].

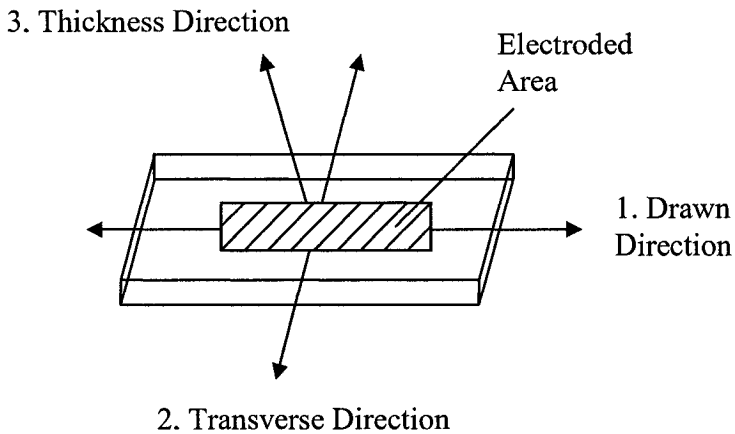

Figure 2.1: Schematic picture of a PVDF film showing the conventional identification of the axes [11].

When the film is compressed or stretched polarized PVDF generates a voltage from one metallized surface to the other, proportional to the induced strain. Infrared light on one of the surfaces has the same effect (will be discuss in the next section). Conversely, a voltage applied between metallized surfaces expands or contracts the material, depending on the polarity of the voltage.

2.3 Pyroelectricity in PVDF

Pyroelectricity is electric polarization induced by thermal absorption in certain crystals; the polarization being proportional to the level of thermal change [26].The PVDF can also exhibit a pyroelectric effect. When the thermal stress is applied on either surface of PVDF, pyroelectric effect can be observed. PVDF is cross sensitive (when the sensor is sensitive to more than one physical variable then the related phenomenon is called cross sensitivity) and its cross sensitivity exists with temperature stress along with mechanical stress. The coefficient of bulk polarization as a function of temperature is referred to as the pyroelectric coefficient i.e. $P_y = dp/dT$. Increment in the temperature results in an increase of crystalline volume together with a decrease in average dipole moment along the third orthogonal axis. Consequently the polarization in the 3rd direction is reduced. In this case the net dipole moment along axes 1 and 2 does not exist, thus P_1 and P_2 (i.e. the pyroelectric coefficient in 1 and 2 directions) are zero. This demonstrates that the pyroelectric coefficients for C_{2v} symmetry crystals are:

$$P_y = \begin{bmatrix} 0 \\ 0 \\ P_3 \end{bmatrix}$$ With a negative sign [29].

In addition to pyroelectric effect, piezoelectricity can contribute to the polarization due to the deformations that occur during heating, but this is not a true pyroelectric effect. The pyroelectric effect is separated in to primary Pyroelectricity and the effect due to the piezoelectric response is called secondary Pyroelectricity [30]. To overcome the effect of pyroelectricity is not to let PVDF films to be thermally stressed. Thermal shielding could help to overcome this effect and sustain the piezoelectric effect.

2.4 Basic Characteristics of PVDF Film Implementation as Sensor

This section deals with the characteristics observed upon incorporating PVDF film in sensor application.

2.4.1 Force Sensitivity

Piezoelectric materials are anisotropic (Material having mechanical properties that are not the same in all directions at a point in a body of it and there are no planes of material symmetry i.e. the properties are a function of the orientation at a point). Subsequently, depending upon the axis of applied electrical field or axis of mechanical stress or strain their electrical and mechanical responses differ. Calculations involving piezo activity must be taken into account for this directionality. The sensitivity of uniaxially oriented PVDF film depends upon the direction of measurement, i.e. drawn, transverse or thickness. If a tensile force is applied in the drawn direction (1-1) as shown in Figure 2.1, then the output charge can be expressed by:

$$Q / A_e = d_{31} F / A_a = d_{31} \sigma_1 \quad \ldots\ldots\ldots\ldots\ldots\ldots\ldots\ldots\ldots\ldots\ldots\ldots \quad (2.1)$$

Similarly the output charge in the transverse direction (2-2) is expressed by:

$$Q / A_e = d_{32} F / A_a = d_{32} \sigma_2 \quad \ldots\ldots\ldots\ldots\ldots\ldots\ldots\ldots\ldots\ldots\ldots\ldots \quad (2.2)$$

Where: Q = Output Charge;

A_e = Electroded area of PVDF film;

A_a = Cross Sectional Area of the film perpendicular to the direction of the applied force i.e. the area of the force application;

d_{31} = Piezoelectric strain coefficient in the drawn direction;

d_{32} = Piezoelectric strain coefficient in the transverse direction;

F = Applied Force;

σ_1 = Applied tensile stress in the drawn direction;

σ_2 = Applied tensile stress in the transverse direction;

If a PVDF film is compressed by a probe on a rigid flat surface, assuming that both the flat surface and the probe are friction free then the PVDF film is free to expand laterally in 1-1 and 2-2 directions. In this case the output charge can be stated as:

$$Q / A_e = d_{33} F / A_a$$

$$Q = d_{33} F \; ; \; [\because A_e = A_a] \quad \ldots\ldots\ldots\ldots\ldots\ldots\ldots\ldots\ldots\ldots\ldots\ldots \quad (2.3)$$

Where, d_{33} is the piezoelectric coefficient in 3-3 direction.

Here, the electroded area and the area of force application are same. But in the real world the friction does exists and moreover, in many applications the PVDF film is frequently glued to rigid substrate. In this condition the output charge is due to the combination of d_{31}, d_{32} and d_{33}, and it is very difficult to calculate the amount of contribution of each component. Thus when the PVDF film is glued (using nonconductive glue) to a rigid substrate, function of piezoelectric strain coefficient is obtained and is termed as d^*_{33}. It is interesting that for a specific applied force, the output charge from the film in the lateral direction is much higher than that of thickness direction. This is because of the extreme thinness of the PVDF film (Eqs. 2.1 and 2.2) [23].

2.4.1.1 Piezoelectric Strain Coefficients

It can be termed as proportionality constant between generated charges and applied force which are more or less proportional to each other. Determination of these strain coefficients has created a huge interest among the contemporary researchers

because of its difficulty in measurement especially in thickness mode which has been presented by different researchers in a wide range. Mathematically piezoelectric strain coefficient can be stated as:

$$d_{ij} = \frac{Q_i / A_i}{F_j / A_j} = \frac{C/m^2}{N/m^2}; \quad \text{..... ..... (2.4)}$$

$\Rightarrow d_{ij}$ = (Charge density produced in direction i)/ (Mechanical stress applied in direction j). The subscripts of the piezoelectric strain coefficient (d_{ij}) stand for the electrical direction and the normal stress direction respectively. In PVDF film, $d_{31} \& d_{32} > 0, d_{33} < 0$ and $-d_{33} \geq d_{31} > d_{32} > 0$. For commercially available uniaxially oriented PVDF film the approximate lateral mode piezoelectric strain coefficients are, $d_{31} = (18-20) pC/N \& d_{32} = 2pC/N$ [23].

Comparatively it's easier to measure the lateral mode piezoelectric strain coefficient of PVDF as it has convincing method of determining the $d_{31} \& d_{32}$ individually. Dargahi et al. determined the strain coefficient by using a dumbbell shaped specimen (often used for mechanical tensile test) and it was assumed that over the narrowed central part, the stress is constant. The study concluded with $d_{31} = 18.0 \pm 0.4 pC/N$ & $d_{32} = 2.0 \pm 0.1 pC/N$ [30].

It is however quite difficult to measure the piezoelectric coefficient d_{33} because of extreme difficulty in applying a normal force to the film without constraining the lateral movement of the film inducing other stresses within the film. The output can thus have contributions from both the applied stress and the induced friction stresses. So it is quite comprehensible that direct measurement of d_{33} associates a lot of difficulties. But couple

of indirect methods does exist to speculate the value of d_{33}. In one method named converse piezoelectric method, the change in thickness of a small sample is measured upon application of a known field. But the problem of this approach is to mount the sample in a way so that the lateral motion is not restricted. The restriction could affect the accuracy of measurement. In the second method, d_{33} is measured indirectly by measuring the hydrostatic piezoelectric coefficient d_{3h}. And then d_{3h}, d_{31} & d_{32} are used to calculate d_{33}. If 'P' is the hydrostatic pressure (The pressure which is exerted on a portion of a column of fluid as a result of the weight of the fluid above it and also pressure can be applied by piston) then the amount of charge is related to all three coefficients by: $\Delta Q / A = -(d_{31} + d_{32} + d_{33})3P$, in which $-(d_{31} + d_{32} + d_{33}) = d_{3h}$ [30, 31].

Dargahi et.al. also investigated the direct measurement of d_{33} as the thickness mode is used in many transducers. If the PVDF film is compressed (glued or clamped) between two surfaces, then the all the piezoelectric coefficients contribute to output charge unless the contact surfaces are frictionless. So they conclude that by reducing the friction forces to their minimum values, it is possible to eliminate the contribution of the two lateral modes and consequently the value of d_{33} can be calculated [30]. As friction force between PVDF film and the substrate surface would incorporate d_{31} & d_{32} along with d_{33} in the output charge, it is better to term it as d^*_{33} which is the function of all piezoelectric strain coefficients.

2.4.2 Linearity

PVDF exhibits very good linearity. The relationship between applied force and the output charge is linear for stress up to 40 MPa. In relation to linearity, two factors must be considered:

(a)The piezoelectric strain coefficient decays gradually with time (especially when thermal poling is used instead of corona poling [32].

(b)The thickness of the PVDF film could be varied from point to point across its surface. These factors suggest that the slope of the output charge against the applied force may vary with time, or from point to point across the surface of the PVDF film and this should not be confused with non-linearity [27].

2.4.3 Repeatability

Repeatability is the closeness between successive measurements of the same quantity, with the same instrument, by the same operator, over a short time span. Values quoted as sensor's repeatability or reproducibility indicate the range of output values that the user can expect when the sensor measures the same input values several times. PVDF possess quite negotiable repeatability [24].

2.4.4 Effect of Static Load on PVDF

PVDF sensors are ideally suited for measuring dynamic events; they cannot perform truly static measurements. Although the electrical charge delivered under a static load can be registered, it cannot be stored for an indefinite period of time. For static measurements highly insulated materials must be used for the sensor cables and

connectors to ensure maximum discharge time constant and optimal operation of the charge amplifier. So if the prolongation of time constant (represents the time required for a signal to decay to 70.7 % (-3dB) of its original amplitude) is desired then high input resistance and film capacitance can be used. This will however produce higher noise, requiring compensation through shielding etc. On the whole, because of the finite time constant, PVDF is suitable for dynamic measurements rather than static measurement (0.001 Hz min.) [24].

2.4.5 Frequency and Dynamic Range

PVDF exhibits a very wide frequency response ranging from DC to the megahertz region. Therefore both for slow motion (tactile manipulation) and fast motion measurements (surface texture measurement), PVDF films can be implemented. PVDF films also possess a very wide dynamic range. Depending on the mode of application the sensitivity (Under a fixed condition, sensitivity is the relationship between a change in the output of a device to the change in the input) of PVDF film can be varied. It is quite possible to measure the response of the PVDF film yielded for forces as small as 0.01 N by considering the value of the piezoelectric strain coefficient. The upper limit could be extended to thousands time of it. So there is a huge dynamic range exists (1000:1). There is however a limitation on the dynamic range and sensitivity. The product of those two parameters is a constant value related to the saturation voltage of electronic interface [27].

2.4.6 Effect of Temperature

Due to the cross sensitivity of PVDF film with temperature, when it is used for force sensing only, any change in temperature of the film (pyroelectric effect) is considered as an unwanted signal causing output error. To minimize this effect, an appropriate thermal shielding is required. This is normally done by shielding the PVDF film using thermally insulated materials. The PVDF film loses some of its piezoelectric and pyroelectric properties above $70^0 C$.Thus this is considered as maximum safe temperature limit [27, 33]. Dipole relaxation and degradation in PVDF begins at temperatures approaching 80°C [34].

2.5 Summary

This chapter introduced PVDF films as sensing element for force and position. Because of its large dynamic range, it is considered suitable for applications such as impact sensor in automobile bumper. Since it is essentially a three dimensional sensor, the relationship among directions are discussed. A brief discussion on various properties of PVDF sensor is also presented in this chapter.

CHAPTER 3

AUTOMOTIVE BUMPER

3.1 Introduction

Automotive bumpers are designed to prevent or reduce physical damage to the front and rear ends of passenger motor vehicles in low speed collisions. Bumpers are not typically designed to be structural components that would significantly contribute to vehicle crashworthiness or occupant protection during front or rear collisions. It is not considered as safety feature intended to prevent or mitigate injury severity to occupants in the passenger cars. Bumpers are designed to protect the hood, trunk, grille, fuel, exhaust and cooling system as well as safety related equipment such as parking lights, headlamps and taillights in low speed collisions. Mechanically the purpose of bumper is to control and absorb some of the kinetic energy involved in the crash of a vehicle, thereby reducing the level of forces transmitted to the body of the vehicle and ultimately occupants. Customers increasing demand to enhance the safety level compelled the vehicle manufacturer to adopt proper energy absorption device in the bumper system. It had been seen that the crashworthiness of the vehicle can be improved by increasing the energy-absorption capacity and efficiency of the bumper system. Additionally in order to reduce repair costs, the bumper should be able to sustain low speed impacts without allowing any damage to the body, chassis or any functional component. Most OEMs (Original Equipment Manufacturers) will allow the bumper system itself to obtain limited superficial damage that may require minor repairs but the bumper must be able to withstand multiple impacts without the loss of functionality [14]. Modern bumpers

generally consist of a plastic cover over a reinforcement bar made of steel, aluminum, fiberglass composite, or plastic. For a bumper to be effective there must be some distance between the reinforcement bar and the sheet metal it should protect [5]. Details of typical bumper design and its mountings is presented in section 3.3.

Over the years, code and standards have been established for the design and effectiveness of bumper systems in automobiles. Code of Federal Regulations (CFR)-Bumper Standard (Part 581) clearly states that the purpose of this standard is to reduce physical damage to the front and rear ends of a passenger motor vehicle from low speed collisions and the standard applies to passenger motor vehicles other than multipurpose passenger vehicles and low speed vehicles as defined in 49 CFR part 571.3 (b) [35].

In this chapter, the contemporary bumpers designs are categorized and the impact absorbers used in the bumper assembly are discussed. This chapter also includes automotive bumper regulations, added from different source, such as NHTSA (National Highway Traffic Safety Administration), FMVSS (Federal Motor Vehicle Safety Standard), CMVSS (Canadian Motor Vehicle Safety Standard), ECE (Economic Commissions of Europe), IIHS (Insurance institute for Highways Safety) etc. The discussion in this chapter is to merge the scattered information quoted in different publications, federal regulations and books which is useful for any research in the area of bumper systems.

3.2 Automotive Bumper Regulations

The bumper standard prescribes performance requirements for passenger cars in low speed front and rear collisions. It applies to front and rear bumpers on passenger cars

to prevent the damage of the car body and safety related equipments. The standard requires protection in the region 16 to 20 inches above the road surface. This is a major accomplishment of the bumper standard in the US because it helps to prevent over and under ride of impacting vehicles. The manufacturer can however provide the protection by any means they want [4]. For example some vehicles do not have a solid bumper across the vehicle, but meet the standard by strategically placed bumper guards and corner guards. Federal bumper standards do not apply on vehicles other than passenger cars i.e., sport utility vehicle (SUVs), minivans or pick up trucks. The agency has chosen not to regulate bumper performance or elevation for these vehicle classes because of the potential compromise to the vehicle utility in operating on loading ramps and off road situation. Moreover trucks with various tire size options create problems in fulfilling the height requirement although some OEMs (Original Equipment Manufacturers) test light trucks at mid bumper height.

3.2.1 History of Bumper Standard

In the 1960's car bumpers were of all types and sizes and were placed at various heights to the ground. The front bumper and rear bumper of some vehicles were not at the same height, and many bumpers were little more than chrome trimming moldings with poor impact performance. This trend led to bumper legislation. The first U.S. bumper legislation was enacted in 1969 and required to utilize an impact by a swinging pendulum against a flat wall [4]. On April 9, 1971 NHTSA (National Highway Traffic Safety Administration) issued its first passenger car bumper standard known as Federal Motor

Vehicle Safety Standard (FMVSS) 215, "Exterior Protection" which became effective on September 1, 1972.

3.2.2 Relevant Safety Standards

The North American bumper performance standards are more severe than the European ones. Thus, the bumpers on North American vehicles are considerably stronger than those on European vehicles. Although the North American bumper standards are set by legislation at the 2.5 mph (4 km/h) level for passenger cars, the North American OEM's (Original Equipment Manufacturers) voluntarily use a 5 mph (8 km/h) performance standard for passenger cars. At this impact speed, there must be no visual damage on a vehicle and there must be no damage to any safety items. However, damage to hidden components of the bumper system is acceptable. Current bumper systems are not designed to absorb energy under high speed impact. However systems are being developed that can absorb about 15% of the energy under high-speed impact. Europe has a greater concern about bumper repair cost than North American. Table 3.1 shows the comparison between North American safety standard and European safety standard [36].

Table 3.1: Safety Standards in North America and Europe [36]

NORTH AMERICA	EUROPE	KEY DIFFERENCES
Bumper Performance: (1)US standard passenger cars call for no visual damage and no damage to safety items at 2.5 mph (4 km/h); Canada calls for limited damage at 5 mph (8 km/h) for passenger cars. (2)Automakers have combined the more stringent aspects of each standard- no visual damage and no damage to safety items at 5 mph (8 km/h) for passenger cars.	**Bumper Performance:** No requirement standard, but most countries follow ECE 42, which calls for no serious damage (light bulbs may be changed) at 2.5 mph(4 km/h)	(1) 5 mph vs. 2.5 mph (8km/h vs. 4 km/h) (2) Law vs. recommendation. (3) Greater damage allowed in Europe.
Insurance Testing: (1)The IIHS (Insurance Institute for Highway Safety) conducts 4 tests at 5 mph (8 km/h) which measures repair costs for the bumper. The tests are front in to barrier, rear in to barrier, front in to angle barrier and rear in to pole. (2)Statistics are published in a newsletter.	**Insurance Testing:** (1)European insurance agencies have a test that measures costs for bumper repair (a credit is given for ease of replacement).The test is a 9 mph (15 km/h) impact at a 40% offset. In England, it's called the Thatcham Test, in Germany, it's called the Danner Test.	(1)5 mph vs. 9 mph (8 km/h vs. 15 km/h). (2)Europe gives credit for ease of replacement.
High Speed Crash Tests CFR 571.208 Occupant Crash Protection: (1)Frontal rigid barrier	**High Speed Crash Tests:** (1) 40% offset driver's side. (2) Front end collision. (3) 35 mph (56 km/h)	(1) Rigid vs. deformable barrier. (2) Head-on vs. offset collision.

collisions applied to passenger cars, MPVs, trucks and buses. (2)30 mph (48 km/h) frontal collision. No separation of any load bearing element of a seatbelt assembly or anchorage. (3)Lateral collision 20 mph (32 km/h) and impact both sides. (4) FMVSS 301, combination of 30 mph (48 km/h) frontal/rear and 20 mph (32 km/h) side.	(4) Deformable barrier/honey aluminum structure (proposed) (5) ECE 33 head-on collision unladen vehicle hits barrier at 30-33 mph (48-53 km/h) (6) ECE 32 rear-end collision impact or pendulum 22-24 mph (35-38 km/h)	

3.3 Contemporary Bumper Systems

Front and rear bumpers became standard equipment on all cars in 1925. At that time simple metal beams integrated with other engineering equipment are attached to the front and rear of a car in order to protect the vehicle in low speed collision. But by virtue of innovative research activity and government regulations this trend replaced with a huge variety of bumper system. Contemporary bumper systems of passenger cars are predominantly consists of a steel, aluminum, or reinforced plastic bumper beam which spans the width of the vehicle and some form of impact absorber. Common impact absorbers are isolators (similar to suspension shock absorber), foam and honeycomb cores, deformable struts, rubber shear block and leaf springs [2]. There are several factors involved in designing of bumper system. The prime consideration is to meet the federal standard as well as to satisfy the vehicle manufacturers whose ultimate goal is to satisfy the customer. It is interesting to be noted that California and Hawaii have bumper

performance disclosure laws, others are not bound to. The bumper arrangement should be capable of absorbing energy and stay intact at high speed impact. After NHTSA had reduced the bumper impact speed to 2.5 mph from 5 mph (1983 model year) a lot of manufacturers become inspired to replace the shock absorber with simple struts directly bolted in the body of the vehicle. In bumper design, weight, manufacturability, cost and type of materials used also play dominant role. Although each make of the cars have different components and layout for the formation of bumper systems, from the functional point of view they can be grouped under few common categories. In the literature, common bumper design had been classified under few different systems [9]. Modern car bumper design can be grouped under four common systems as shown in Figure 3.1: (A) Metal Face bar (B) Plastic Fascia and Reinforcing Beam (C) Plastic Fascia, Reinforcing Beam and Mechanical Energy Absorbers, (D) Plastic Fascia, Reinforcing Beam and Foam or Honeycomb Energy Absorber.

A metal face bar system consists of a single metallic bumper (Fig. 3.1A) that decorates the front or rear of a vehicle and acts as the primary energy absorber in a low speed collision. This system is widely used for light trucks including pick ups, SUVs and full size vans. Most metal face bars are stamped from sheet steel. They are fastened directly to the frame rails. For purposes of appearance and corrosion resistance, steel face bars are either plated with chromium or painted. Typical North American steel face bars system can withstand a 2.5 mph (4 km/h) impact with minimum visual damage and no damage to safety related items.

The second bumper system consists of a reinforcing beam covered by a plastic fascia (Fig. 3.1B). Steel is favored material for reinforcing beams. Steel reinforcing beams are

either hot rolled or stamped from sheet in to box, channel or hat cross-sections. All steel reinforcing beams receive corrosion protection. Some beams are made from hot dip galvanized or electro galvanized sheet that have a zinc metallic coating. Other beams are protected after fabrication with a paint system, such as E-coat. The reinforcing beam is fastened directly to the vehicle frame or motor compartment rails. This type of systems is primarily used in Japan and Europe, where bumper regulations are less stringent than those in North America. On many vehicles in Europe and Japan the reinforcing beam in this system also serves as the first structural cross member. If the reinforcing beam is part of the body –in-white, the favored material is steel because of the structural requirements associated with a cross member.

The third and fourth systems employ a plastic fascia (majority of plastic fascias are made from polypropylene, polyurethane or polycarbonate) over a reinforcing beam in conjunction with energy absorption (Fig. 3.1C & 3.1D). The systems differ only by the method of energy absorption (will be discussed later). These systems are widely used in North American passenger cars and minivans. They are commonly designed to withstand a 5 mph (8 km/h) impact with minimal damage and no damage to safety related items [36].

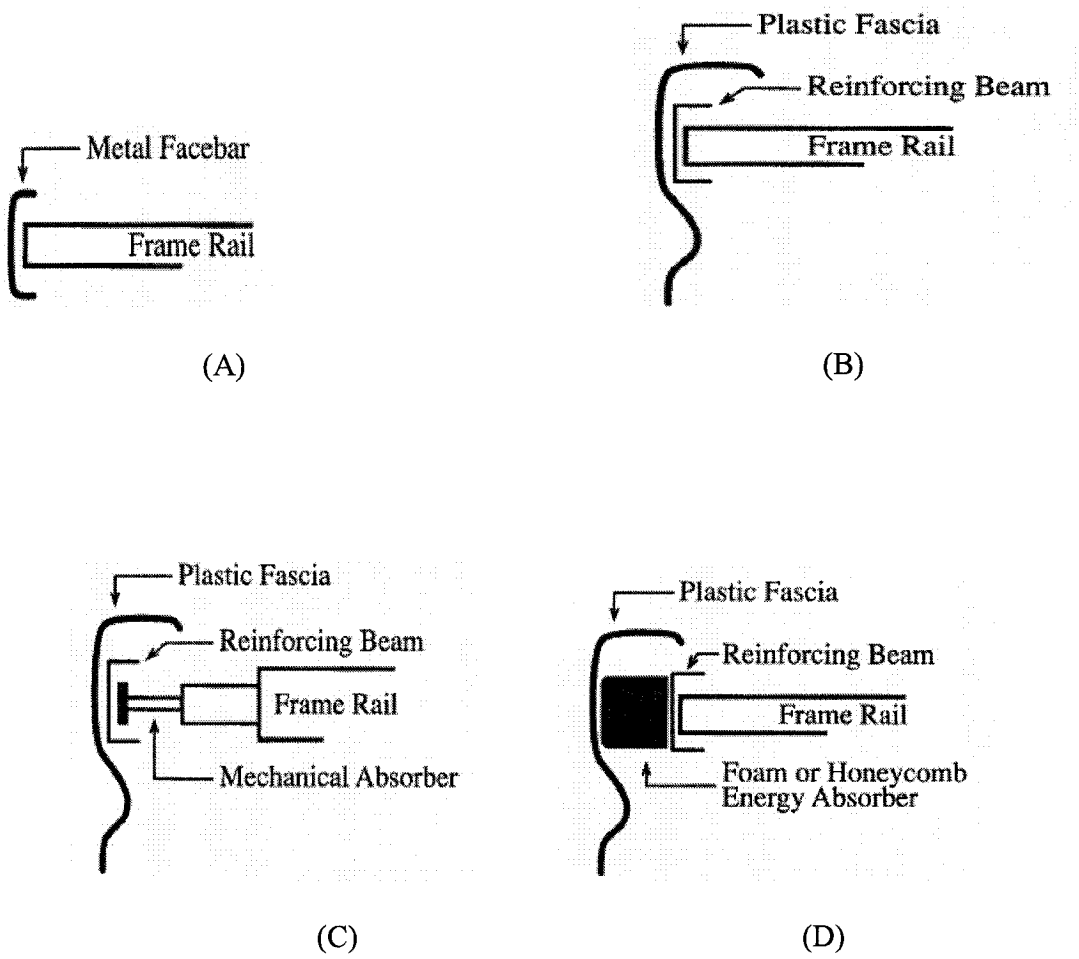

Figure 3.1: Common Bumper Systems. [36]

Based on these common systems, manufacturers are constantly looking for improvements for economical and safety related competitive edge over other manufacturer. Increasingly stringent environmental demands are encouraging the automotive industry to look for ways of producing lighter and more fuel efficient cars. Consequently researchers looking towards lighter steel, plastic, and composite materials which will serve the traditional purpose as well as satisfy customers while improve on fuel efficiency [10- 14, and 16].

3.3.1 Bumper Components

It is clear from the previous discussion that bumper system consists of different components. Major components are fascia, energy absorbers (isolators), face bar and reinforcing beam. Many papers describe the components of bumpers by emphasizing on certain parts according to individual interest [9]. The features of these components that form the bumper are discussed in the following subsections.

3.3.1.1 Fascia

Plastic used as the outer panel of a vehicle bumper is referred as fascia. This component does not have significant inherent strength and is only used to cover components underneath. For example, a bumper fascia has little strength itself but covers a steel beam, foam core or other energy absorbing component. Bumper Fascias are designed to meet several requirements. They must be aerodynamic to control the flow of the air around the car and the amount of air entering the engine which economizes the fuel requirement. It reduces the weight of the vehicle and improves fuel economy. They must be aesthetically pleasant too. Plastic is used because it can be made into complex shapes that cannot be duplicated by metal stamping; therefore manufacturers have greater design flexibility. Typical Fascias are styled with many curves and ridges to give bumper dimension and to distinguish vehicles from competing models. Important requirement of bumper fascias is that they are easy to manufacture, has some strength, and light in weight. The majority of bumper system's fascias are made by thermoplastic olefins (TPOs), polyesters, polyamides, polypropylene, polyurethane or polycarbonate and sometimes these are blended with glass fiber to increase strength and structural rigidity

[11, 12, 36]. A typical fascia of a modern vehicle bumper is shown in figure 3.2. This 1998 Ford Windstar (Ford Motor Company, Windstar product development team/ Exterior systems division) fascia represents the first application of a new blend of polymers having much higher flexural modulus than typical polypropylene or TPO compounded material. Ford realized 40% increase in tensile properties using this material, making the fascia stronger while taking out 5 pounds of weight from the earlier type. Recently some bumper fascias are produced with high durability, lightweight and capable of withstanding repeated impacts that would deform an aluminum or steel bumper. Even after repeated impacts, the appearance doesn't suffer due to a paint layer that's been chemically bonded to the part after molding. By utilizing an 'in mold' painting process, the finish color is applied to the interior of the mold surface prior to closing and urethane injection. Using this method (Trim System), the color layer becomes permanently bonded with the substrate material. Bumpers manufactured in this manner replace several fabricated metal parts; reducing both cost and weight of the finished part.

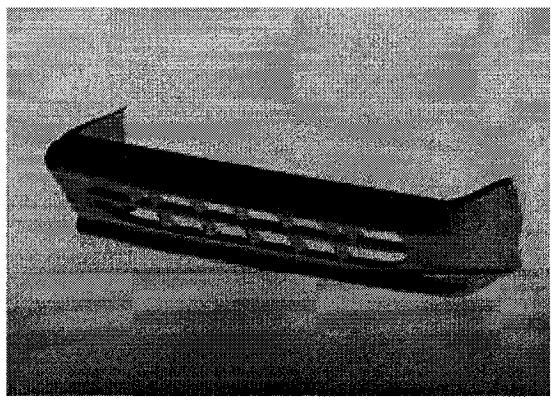

Figure 3.2: Bumper Fascia.

3.3.1.2 Energy Absorber

Energy absorbers absorb a portion of kinetic energy involved in a vehicle crash and help reduce the forces transmitted to the vehicle frames and occupants. Energy absorbers are primarily very effective in a low speed impact, where the bumper springs back to its original position. Energy absorber types include foam, honeycomb and mechanical devices. Some of the commonly used energy absorbers are discussed under the following sub headings.

Mechanical Absorber (Isolator)

Mechanical absorber (isolator) is a piston cylinder assembly mounted between the bumper and car. They are parallel to the vehicles longitudinal axis and having resemblance with shock absorber. Such isolators may be found on BMW, Chrysler, Datsun, Ford, General Motors, older Hyundai, older Honda, older Mazda, some Nissan, some Subaru, Mercedes, older Toyota and Volvo cars. There are many variations in the design of the isolators, principle of their application is however, very similar.

A typical design of a bumper isolator is shown in figure 3.3. The isolator is fitted with a metering pin and an annulus and a floating piston which separates the gas and fluid filled regions of the isolator. On compression, fluid forced through the annulus pushes the floating piston, which causes the gas to compress. As the compression continues, the annulus becomes smaller because of the tapered metering pin and the resistance to compression increases. When the compression force ceases, the expansion of the compressed gas returns the isolator to its pre compression state. The metering pin may have an initial region of constant diameter, followed by a tapered section in which the diameter increases, followed by a second larger constant diameter region. In the constant

diameter and tapered regions, the resistance to compression is provided predominantly by gas compression. As the large diameter of the tapered metering pin enters the annulus, the resistance to compression is provided by the fluid flow through the annulus and increases with compression rate. Some General Motors, Chrysler and Mazda isolators function in this manner.

Similar design of isolator with constant diameter metering pin or without metering pin can be found in the literature [2]. All such isolators essentially provide an element with visco-elastic property between the bumper and vehicle structure.

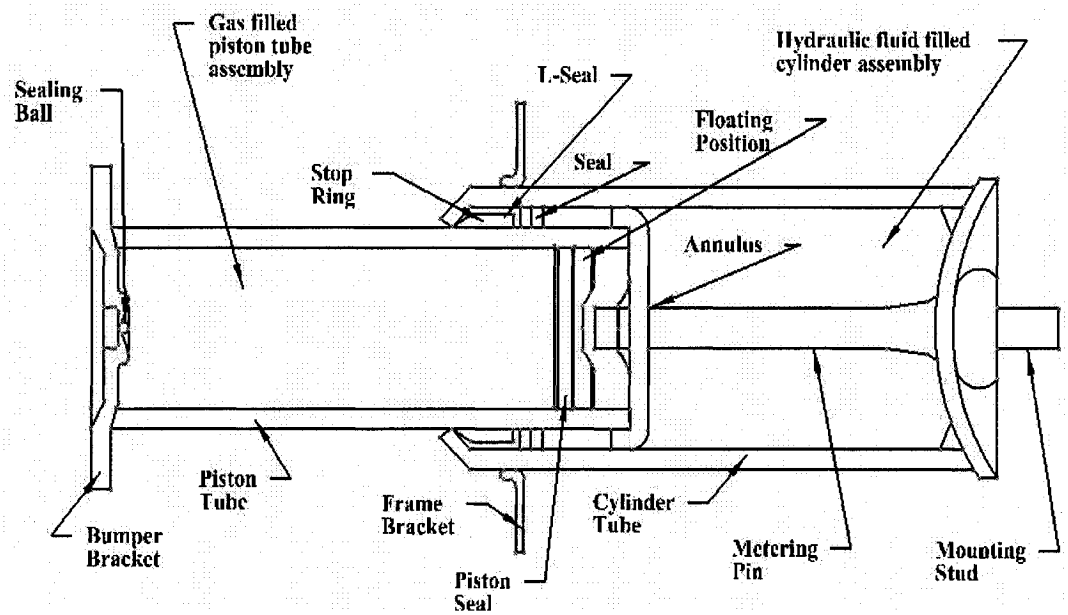

Figure 3.3: Typical Mechanical Absorber (Isolator) [2].

Vehicle manufacturers also use other energy absorbing elements to couple bumper to the vehicle. Some common ones include foam or plastic honeycomb core, deformable strut, rubber block as well as leaf spring [2].

Foam Core:

Large block of polystyrene, polypropylene, polyurethane or other foam is sandwiched between the bumper beam (rigidly fastened to the car) and a plastic cover that forms the bumper exterior. The foam will compress during an impact, and will usually recover its original shape. There is usually no indication that the foam core or the associated metal beam has experienced an impact, even when the impact is substantial. In some cases, a distinctive impression may be left on the cover. Structural damage to the vehicle may precede damage to the bumper. Polystyrene foam core bumpers may be found on Acura, Honda, some Mazda and some Nissan cars. North American vehicles are incorporating polystyrene foam in to their bumper designs to ensure the shape is not altered by an impact.

Honeycomb Core: A block of plastic honeycomb is inserted between an impact bar and a plastic cover that forms the bumper exterior. The walls of the honeycomb structure are oriented parallel to the vehicle's longitudinal axis. As the honeycomb compresses the walls buckle. The bumper exterior often shows no indication of an impact, though the honeycomb in the vicinity of the impact may be slightly deformed. In some high speed impacts, square holes can be cut in the bumper cover by the honeycomb. Honeycomb core bumpers may be found on some newer General Motors cars [2].

Deformable Struts:

The bumper bar is held in place with two rigid mounts, each of which is designed to yield plastically under load. Once deformed, the brackets need to be replaced. Some newer Volkswagen and some Dodge/Plymouth vehicles have been fitted with deformable struts [2].

Rubber Shear Blocks:

The bumper beam is attached to the vehicle by two I-beams. The 'I' shape beam slides in to a box-section frame which is fastened to the vehicle frame. Two rubber blocks are sandwiched between either side of the I-beam web and the walls of the box-section frame (Figure 3.4). The two rubber blocks provide resistance in shear. Typically this type of impact absorber will not show signs that motion of the bumper has occurred. Some older models Ford, Lincoln and Mercury vehicles have been fitted with this type of impact absorber [2].

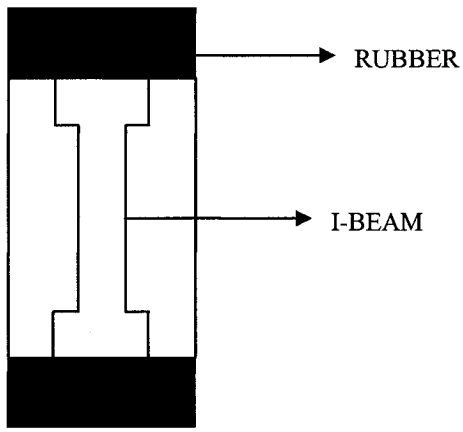

Figure 3.4: Rubber Shear Blocks.

Leaf Spring:

The bumper is held in place with two sets of leaf spring (Figure 3.5) that behave on impact like leaf spring suspension. Some systems have a rubber block mounted to the vehicle to provide a stop in case full compression of the springs occurs. The leafs in this case provide stiffness with progressively hardening characteristics, while friction between leafs generate damping properties. Some older model General Motors vehicles have been fitted with leaf spring bumper isolators [2].

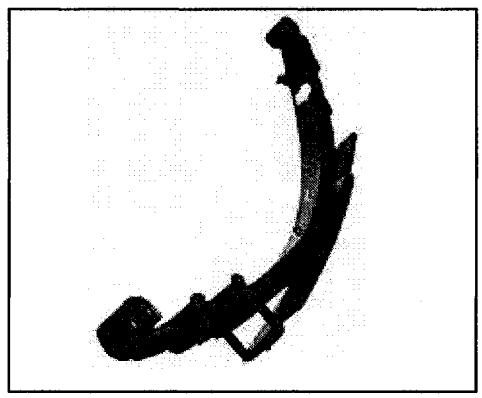

Figure 3.5: Bumper Leaf Spring.

3.3.1.3 Facebar

Face bars are usually stamped from steel with plastic or stainless steel trim to dress them up. A small volume of face bars is produced from aluminum. Steel face bars, for formability reasons are usually made from steels with a low to medium yield strength. Thus, face bars are quite thick. This thickness (plus the fact face bars are deep and have large wrap around ends) gives face bars a relatively heavy weight. After stamping, steel face bars are chrome plated or painted for appearance and corrosion protection reasons [36].

3.3.1.4 Reinforcing Beam

The reinforcing beam is a key component of the bumper systems which help in absorbing kinetic energy from a collision and provide protection to the rest of the vehicle. By staying intact during a collision, beams preserve the frame. Design issues for reinforcing beams include strength, manufacturability, weight, recyclability and cost. Steel reinforcing beams are stamped, roll formed or made by the Plannja process [a hot stamping process]. Typical cross sections are shown in figure 3.6. A stamped beam is advantageous in high-volume production and offers complex shapes. However, the stamping process is capital intensive and the process itself requires good formability of the steel. Roll formed beams account for the majority of the steel reinforcing beams used today. Common cross sections for roll formed beams are box, C or channel and hat. Typically these cross sections are made of ultra high-strength steels of very thin gauges. A back plate is sometimes welded to an open channel or hat section to create a box section. All steel reinforcing beams receive corrosion protection. Some beams are

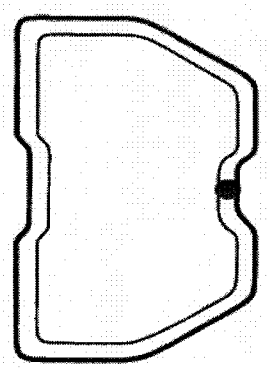

Figure: 3.6 A: Rolled Formed Box Section (Welded)

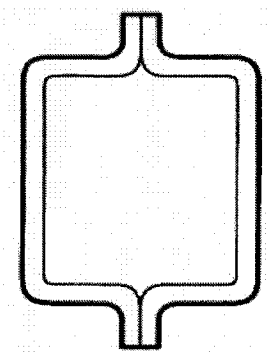

Figure: 3.6 B: Hat Box Section (Welded)

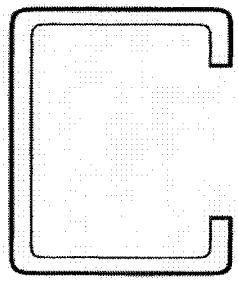

Figure: 3.6 C: C or Channel Section

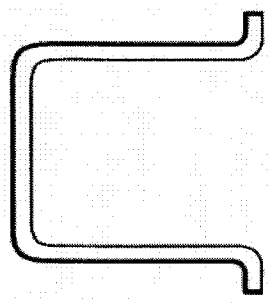

Figure: 3.6 D: Hat Section

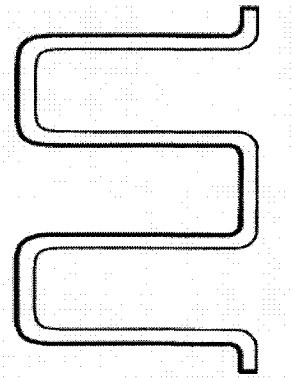

Figure: 3.6 E: Double Hat Section

Figure 3.6: Cross Sections of a Reinforcing Beam. [36]

made from hot dip galvanized or electro galvanized sheet. The zinc coating on these products provides excellent corrosion protection. Other beams are protected after fabrication with a paint system such as E coat [36].

3.4 Summary

For the development of bumper system with sensors to detect collision, it is essential to first understand the purpose and design of bumper system for vehicles. This chapter outlines the historical development of bumper, and rules and regulations that dictates the performance the bumper must provide. For this a survey is carried out to

establish common designs of bumper system and its components. Commonly used bumper system, its components and their characteristics are discussed in this chapter. This will help to establish a prototype scale model of a bumper that can be used in this investigation to explore the potential of PVDF as a sensing element for bumper system.

CHAPTER 4

EXPERIMENTAL SET-UP AND TEST PROCEDURES

4.1 Introduction

Based on the objectives outlined in chapter 1 and the considerations of bumper systems and their layout discussed in chapter 3, the bumper test set-up and experimental procedure was developed. To represent the bumper, a Plexiglass beam with two mounting locations was selected and mounted on a rigid structure through a set of rubber mounts. A number of PVDF sensors discussed in chapter 2 were mounted along the length of the bumper. Each sensor was independently instrumented with charge amplifiers to record data using a data acquisition system. An elaborate test set-up was developed with an electro-dynamic shaker capable of providing impact force to the bumper through different size probes at any location along the length of the bumper.

Response of each sensor to impact force was tested individually to observe the response characteristics and to verify force sensitivity, repeatability and consistency from sensor to sensor. Throughout the experimental process, modifications to the bumper setup were carried out to realize the detection system's full capability to measure both force and location of impact.

This chapter presents the components of the bumper and test setup used in the experimental investigation. In addition, it presents the experimental procedure and test results for individual sensors. Tests were carried out to determine the sensor's capabilities and its sensitivity to duration of impact, probe size and the softness of the probe. Based on the initial tests of the instrumented bumper for predicting impact magnitude and

location, final designs are proposed in this chapter. The results of tests with final design and their analysis are presented in chapter 5.

4.2 Prototype Impact Detection Bumper

In order to represent the bumper, a beam of Plexiglas with dimensions of 30.48 x 3.175 x 2.413 cm (12 x 1.25 x 0.95 inch) was selected (Figure 4.1). The size represents a 1:5 scale size of a typical passenger car bumper. Like the bumper prototype, the PVDF sensor cover was made of Plexiglass. It is an electrical insulator and its trade name is Acrylic. The density of Plexiglass is1.18 gm/cm ^{3} (1180 kg/m^3) and its Poisson ratio (the ratio of average lateral strain dD/D and average axial strain dL/L) is 0.4. Plexiglass was selected because of its ease of manufacturing, its rigidity, its low density, and because it is an insulator.

Two holes were drilled in the Plexiglas beam, 5.842 cm (2.3 inch) away from each vertical edge such that it can be mounted on a rigid structure through two isolators.

Five bi-axially oriented rectangular Polyvinylidene-fluoride (PVDF) films of 25 μm (4.33e-3 inch) thickness were placed on the bumper as shown in Figure 4.1. The PVDF sensors were metallized on both sides with aluminum (Good Fellow, USA) with dimensions of 52.07 x 12.7 mm (2.05 x 0.5 inch) glued in a non-conductive way to the Plexiglass bumper. Each sensor (quoted piezoelectric coefficients are d_{31}=18-20pC/N, d_{32}=2pC/N [38]) is longer than the frontal length of the bumper prototype. Here 6.35 mm (0.25 inch) is kept on both the top and the bottom sides. The connections are glued in a conductive way with the PVDF sensor on the top and bottom side of the bumper. Sensor placement on the bumper has been designed by incorporating an inline approach (detects

collision only by unveiling 'X' co-ordinates of bumper) and have been incorporated at 2.54, 10.16 ,15.24 , 20.32 , and 27.94 cm (1.0, 4.0, 6.0, 8.0, and 11.0 inch) from the reference (left) end of the bumper prototype.

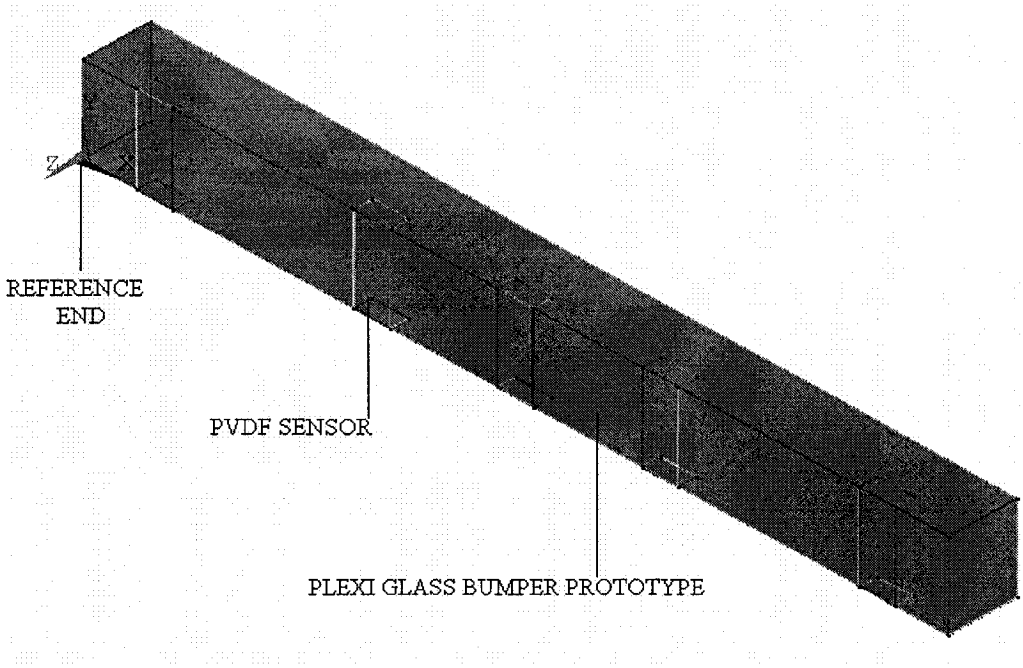

Figure 4.1: Plexi Glass Bumper Prototype Attached with Five PVDF Sensors.

4.3 Test Set-Up

The test setup consisted of three main components: the base frame, the shaker system and the bumper holder. Engineering drawing for the fabrication of the components are presented in Appendix-A. The features of each of these components are described in the following:

Base Frame: The base frame was made of mild steel beams and plates (density: $7850\,Kg/m^3$) as shown in figure 4.2. The total size was 152.4 cm (5 ft) long by 50.8 cm (20.0 inch) wide. The system was design to ensure all the units could be incorporated in the base frame such that the system was potentially vibration free. The beam had an I-

cross section with a weight of 90.0 kg. The bumper holder, the bumper prototype, and the electro-dynamic shaker were bolted into this frame as shown.

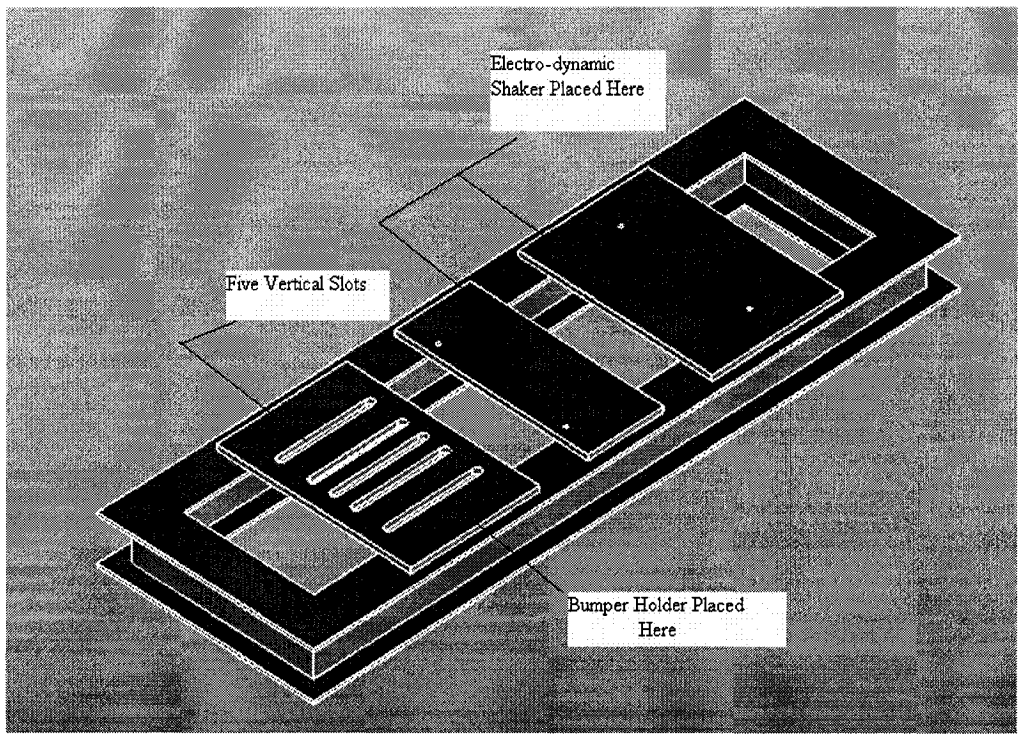

Figure 4.2: Model of Base Frame with Five Vertical Slots Provide the Flexibility to Move Vertically.

It consisted of a slotted bumper support section for mounting of the bumper holder. Each of the five slots was 22.86 x 1.905 cm (9.0 x 0.75 inch) and fabricated vertically using a milling machine. The slots were provided to allow for the adjustment of the distance of the bumper from the shaker. As shown in figure 4.2, the two other plates were designed to secure the electro-dynamic shaker system firmly on the base frame. This whole base frame stood upon four wheels that were locked, which made it reasonably vibration free.

Bumper Holder: To hold the bumper prototype, a bumper holder (figure 4.3) was designed which upheld the bumper at approximately 45.72 cm (18.0 inch) high; the standard is that the bumper should be 16.0 to 20.0 inch above the ground [3], although this would not affect the study. The height of the bumper holder was 40.64 cm (16.0 inch) and its width was 44.45 cm (17.5 inch). It was made of mild steel (density 7850 Kg / m^3). The holder possessed three horizontal slots; each one was 12.7 x 1.651 cm (5.0 x 0.65 inch) in dimension and gave the frame flexibility to move horizontally so that it became possible to strike the bumper in every possible horizontal position. Moreover, three slots enable the bumper holder to be attached with the base frame by means of nut and bolts.

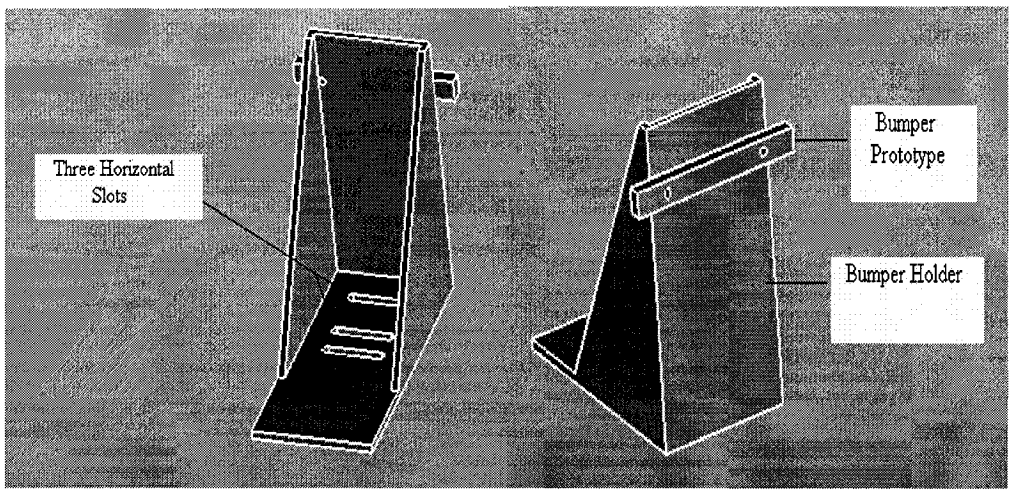

Figure 4.3: Model of Bumper Holder with Bolted Plexiglass Bumper.

Shaker System: The vibration exciter system (a Bruel & Kjaer-Exciter body type 4801 with general purpose exciter head 4812) was used to strike the sensor on the bumper prototype through the probe. It could generate a maximum of 445 N (100 lbf) of dynamic force and a maximum of 135N (30 lbf) of static force. The displacement, peak to peak

(stroke length) was 12.7 mm (0.5 inch). This electro-dynamic shaker was bolted to the base frame (figure 4.4). It was designed to be driven by a power amplifier (a Bruel & Kjaer- Type 2707) with a frequency range from DC to 1000 kHz.

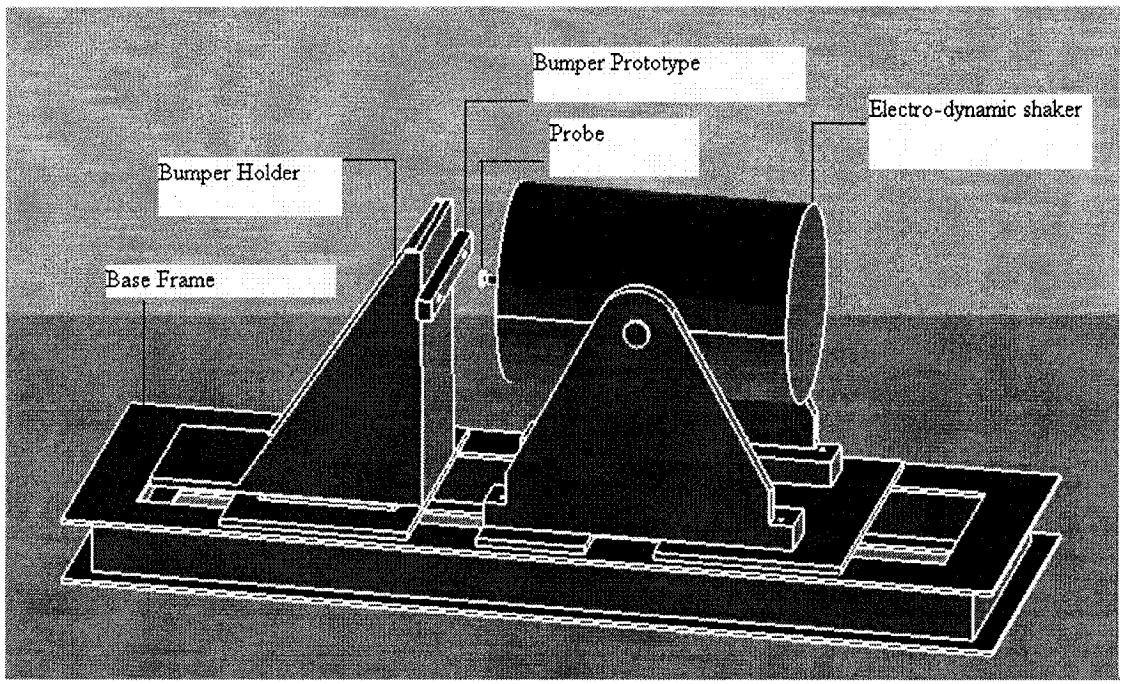

Figure 4.4: Model of Vibration Free Unit of the Set-Up Mounted on Base Frame.

Instrumentation: Five bi-axially oriented 25 μm PVDF films were glued with non-conductive glue to the bumper prototype. When a force was applied to the bumper, the PVDF film acted as a transducer, converting the force to charge by the following relation (See section 2.4.1):

Output Charge, $Q = d^*_{33} F$

Where,

F = Applied Force

d_{33} =Piezoelectric Strain Co-efficient in the 3-3 Direction.

d^*_{33}=Summation of Piezoelectric Strain Co-efficient in all the Three Direction.

A few micron thin copper wires were glued by conductive glue (Circuit Works) to the PVDF films. The output from each PVDF film was fed to a charge amplifier (a Kistler Instrument Corporation-Model 5004) via coaxial cables which were connected to the copper wires through thermoplastic terminals.

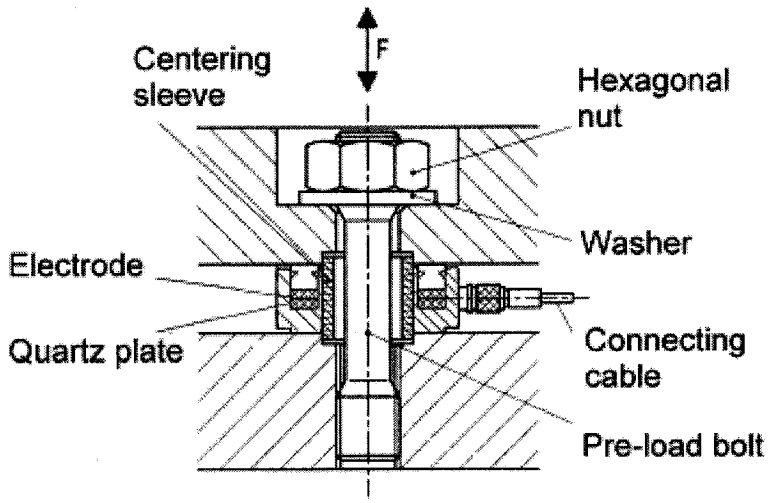

Figure 4.5: Piezoelectric Crystal Force Transducer.

The vibration exciter system described earlier was used to strike the sensor through the probe and was driven by a power amplifier. The power amplifier was connected with a 20 MHz function and wave form generator (an Agilent 33220 A) so that the vibration unit would produce a series of impact forces (with different magnitude) through the probe on the PVDF sensors. The charge generated due to the impact was fed through charge amplifiers (Kistler Instrument Corporation-Model 5004) with the predetermined sensitivity, time constant and range set-up. A charge amplifier is a charge-to-voltage converter, so the converted voltage was monitored in real time on an oscilloscope (an Agilent 54624A) and recorded in a computer. Each sensor was attached with a single charge amplifier to identify the amount of charge generated by each sensor individually

in different scenario of testing procedure. The magnitude of the force applied was determined by a piezoelectric force transducer (a Kistler Instrument Corporation- Model 912, see figure 4.5), which was positioned between the probe and the vibration unit (the shaker). It had the capacity to measure from 0 to 22.2 kN which was well within the range sought for. The maximum load applied was 400 N due to the stringent capability of the shaker.

Two probes made of Aluminum and Plexiglass were used, with a probe head diameter of 1.0 inch. Besides that 0.4, 0.5 inch diameter probe and also 0.346 x 0.2 inch probe made of Aluminum were used. In some experiments, silicon rubber and recycled rubber were glued to the Aluminum probe head to examine the effect of softness on the PVDF sensor placed on the bumper. A Shore 'A' Durometer (Fig. 4.6) was used to measure the hardness of these rubbers; it was designed to measure the ASTM type A hardness of rubber, elastomers, and other rubber like materials (neoprene, silicon, vinyl, butyl etc.).

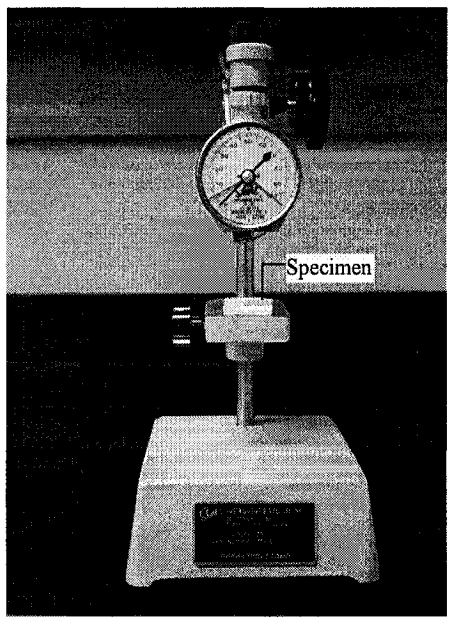

Figure 4.6: Shore A Durometer.

The organization of the complete experimental set up is shown in Figure 4.7.

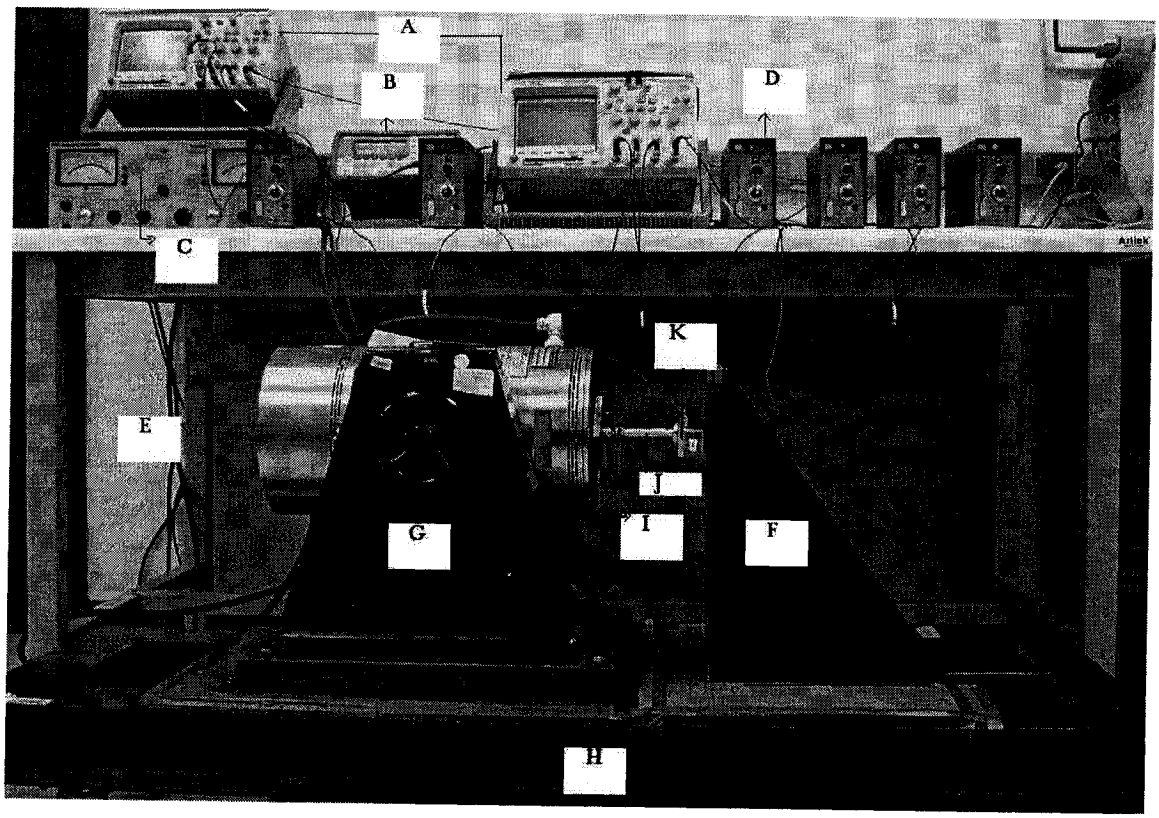

Figure 4.7: Photograph of Complete Experimental Set-Up.

Here,

A) Oscilloscope (Qty: 2).

B) Signal Generator.

C) Power Amplifier.

D) Charge Amplifier (Qty: 5).

E) Vibration Exciter Head

F) Bumper Holder.

G) Vibration Exciter Body.

H) Base Frame.

I) Load Cell.

J) Probe.

K) Bumper Prototype.

4.4 Test Procedures

Each PVDF sensor was tested by applying numerous step loads. Forces were applied by the probes on the sensor and off the sensor. The responses from the PVDF sensors were recorded and examined. The stroke of the shaker (i.e. the force trend) was sent through a signal generator and the contact time was also controlled to observe the effect of duration (time of load application). The electro-dynamic shaker was adjusted to apply horizontal forces with various magnitudes. The position of impact was adjusted through the slots created in both the bumper holder and the base frame. The schematic of the setup is shown Figure 4.8.

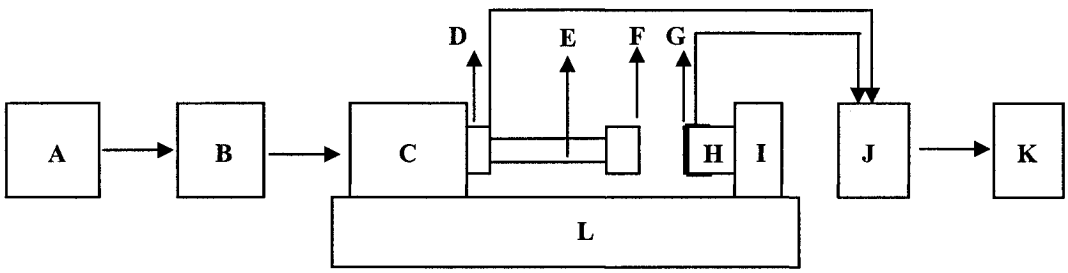

A- Signal Generator
B- Power Amplifier
C- Vibration Exciter
D- Load Cell
E- Probe Rod
F- Exchangeable Probe Head
G-PVDF Sensor
H-Plexi Glass Bumper Prototype
I-Bumper Holder
J-Charge Amplifier
K-Signal Analyzer
L-Vibration Free Base Frame

Figure 4.8: Block Diagram for the Entire System for Collision Detection.

The transient signals were obtained for each impact and were analyzed. The analysis was initially based on the peak amplitude (P), the rise time (T_r) and the fall time (T_f) of the signals.

The test procedure must acknowledge the probable experimental error. The errors in the measurements were estimated as about 20%, arising from both variations in film thickness and glue thickness of about 5%. In addition, error could be introduced due to the positioning of the center of the probes on the intended points on the bumper. Considering the diameter of the probes, an error of 1.5 mm is estimated. This introduced a possible error of 10%. Since a level meter was used to ensure that the shaker was horizontal, so that the probe was applied perpendicular to the sensor, a possible reading error of 3% is also estimated. Variation in room temperature would further effect in output of PVDF film of about 2%. The spread of the results for various tests is within this error band.

4.4.1 Measures of Collision Detection

Peak Amplitude: In the experimental transient response of PVDF film, the peak value is considered to be the first peak magnitude.

Rise Time: The rise time is defined as the time required for the response to rise from 0 to 90 % of the transient response peak value.

Fall Time: Fall time is the time required to decrease the peak value from 90% to 10%.

A sample response of the PVDF sensor by indicating P, T_r and T_f for a force of 320 N is shown in figure 4.9.

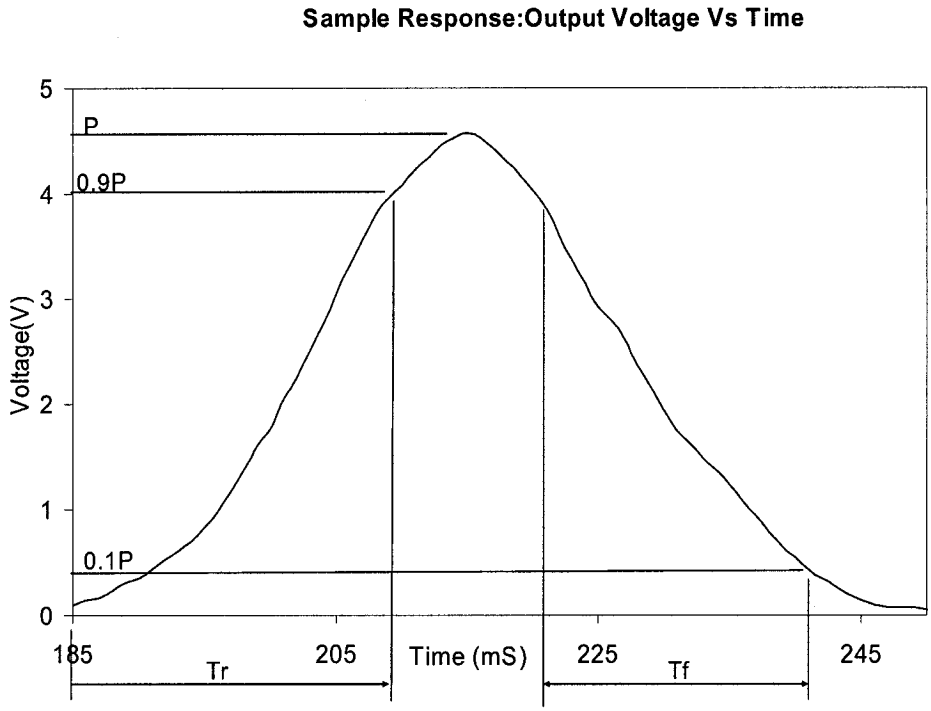

Figure 4.9: Sample Response of 320 N load on PVDF Sensor Showing Peak Voltage Amplitude (P), Rise Time (T_r) and Fall Time (T_f).

4.4.2 PVDF Sensor Test

The test procedure began with the calibration of the different systems used in the test set-up, such as the charge amplifiers, the load cell and the PVDF sensors. Each PVDF film was calibrated separately by applying known step loads and recording the output voltage. It was also important to consider the pyroelectric effect of the PVDF film so that any spurious results would be avoided. The following tests were conducted to characterize the PVDF film and to lead the study in a right track.

Linearity: The linearity of the sensor was examined by applying various loads and recording the output voltages. It was shown that there is a linear correlation between the applied force and the output voltage. The result is shown in Figure 4.10.

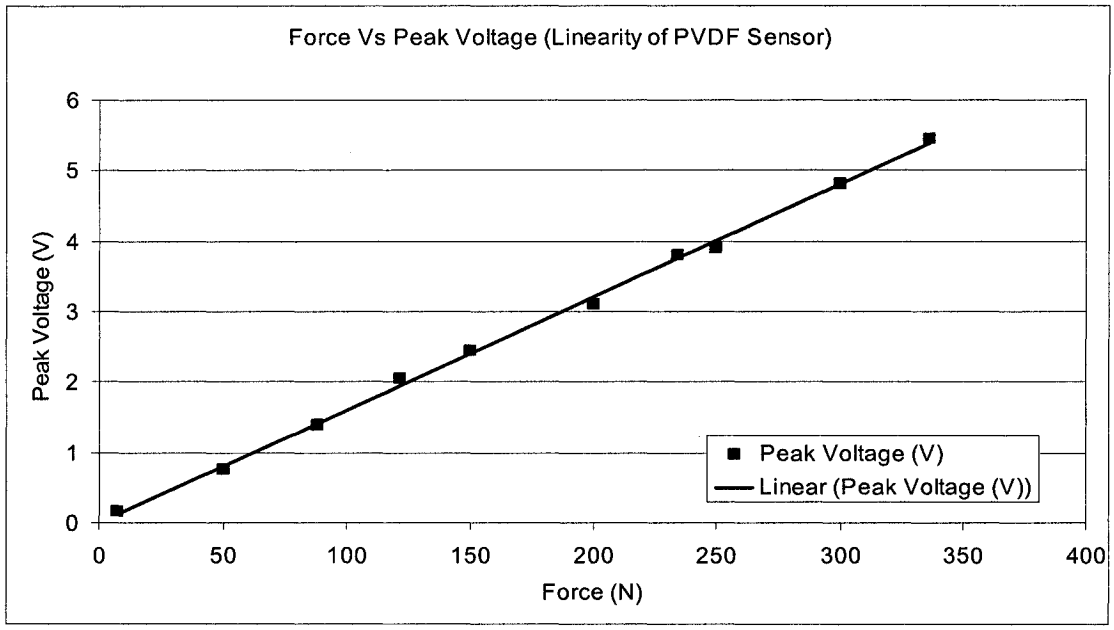

. Figure 4.10: Linearity in PVDF Sensor.

Repeatability: In order to check for the repeatability of each sensor, the above linearity experiment was repeated three times. The results show that the sensors are linear within

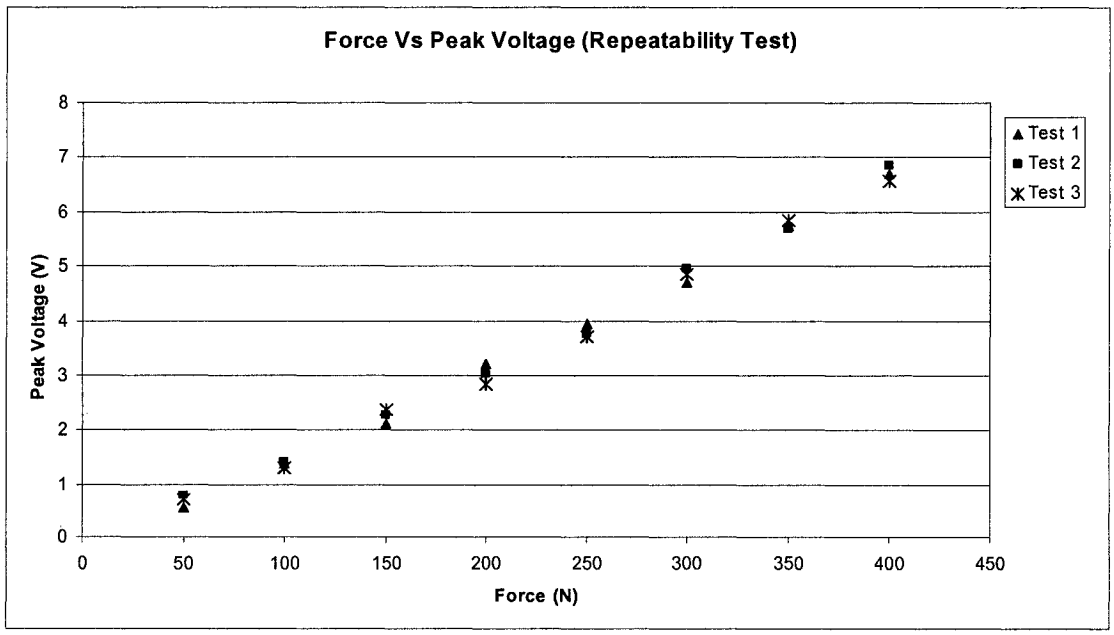

. Figure 4.11: Repeatability in PVDF.

10% error band. Hence we can conclude that the repeatability of the sensor is 10%.

Besides experimenting on these common characteristics of PVDF sensors, some distinct phenomena of the PVDF sensors of the set-up have also been narrated below. These are significant in order to remove the controversies of the proposed collision detection system:

Effect of Probe Size

Numerous probes with different size and shapes were examined. Four probe sizes were examined, three of which were smaller than the sensor and one of which was larger. The results show that the contact area did not significantly affect the output voltage of the PVDF sensor especially for the probes which are smaller than the width of the sensor. The result is shown in figure 4.12.

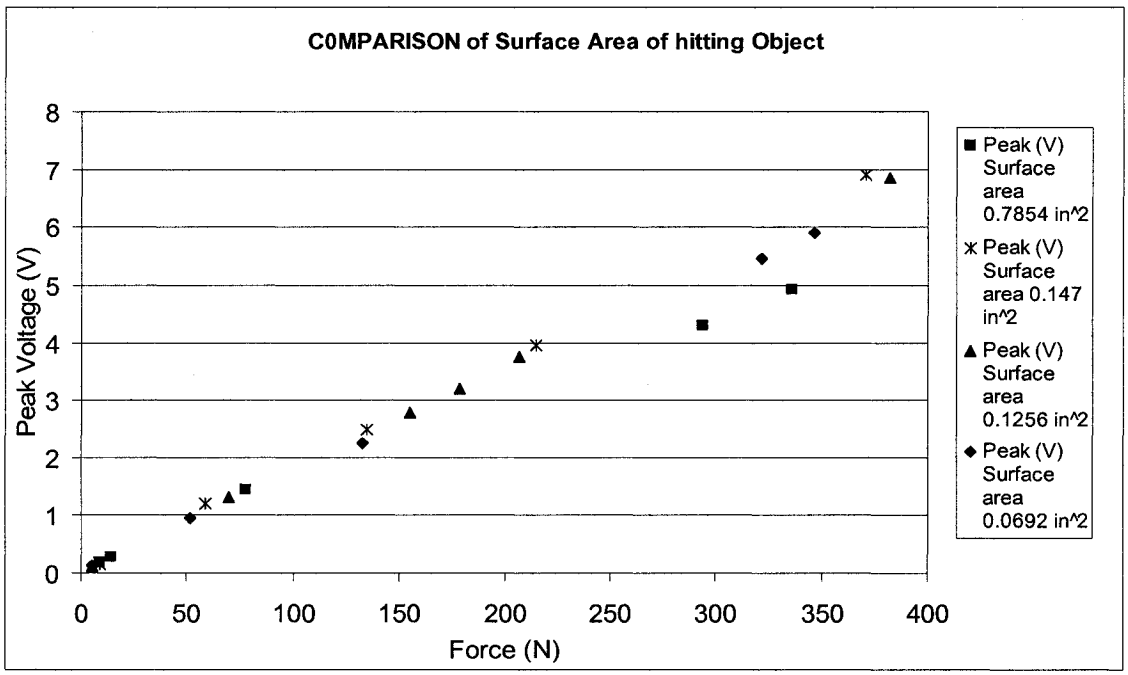

Figure 4.12: Variation in Output Voltage upon Changing Contact Area.

Effect of Compliance of Contact Objects

Three materials were tested by keeping the potential collision situation in mind.

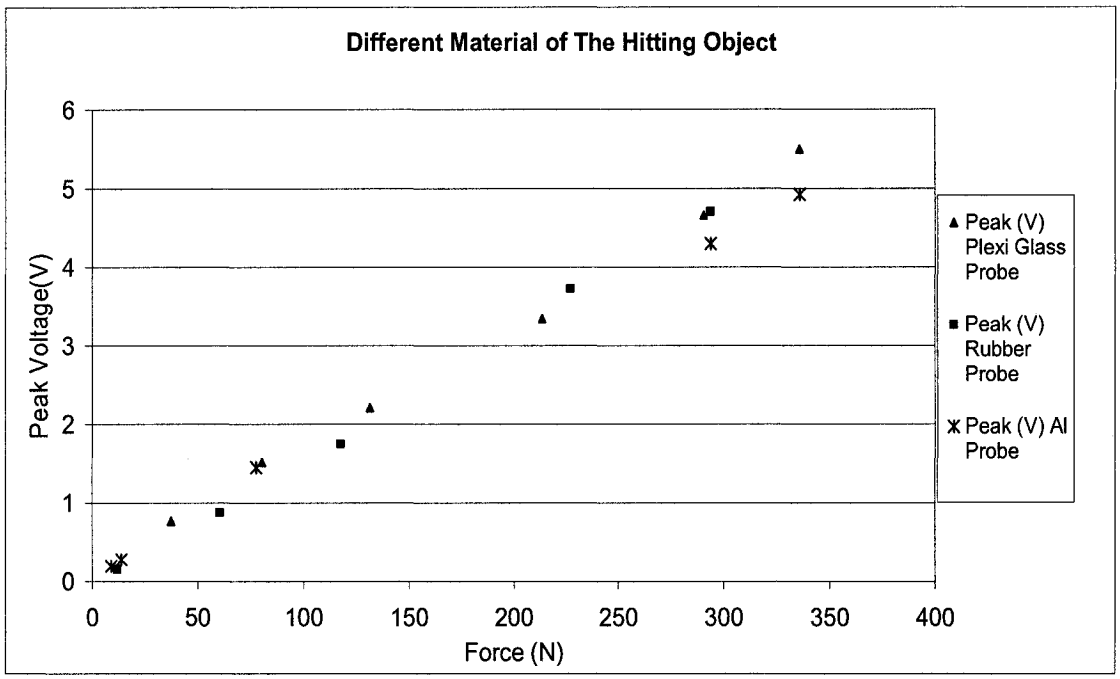

Figure 4.13: Variation in Output Voltage by Varying Probe Material.

The materials were aluminum, Plexiglass, and hard rubber; they had modulus of elasticity of $70\times10^{9}, 3.08\times10^{9}, 3\times10^{6}$ Pa respectively. It was assumed that the hard rubber would represent human contact. The result is shown in Figure 4.13. It was observed that relatively soft material (hard rubber) generates less smooth signals than hard material (Plexiglass or Aluminum) but the peak voltage remains approximately same for the same load.

Pyroelectric Effect

In order to avoid a pyroelectric effect, a strip of Mylar film was positioned on top of the PVDF sensors by a non-conductive tape. This Mylar film not only prevented the damage to the PVDF sensors, but also prevented a pyroelectric effect due to the change in surface temperature of the contact probes of various materials.

Effect of period of load application

Due to the inherent characteristics of the PVDF film, which does not sustain a static load, when a step load was applied to the sensor, the output was a transient response. For the combined effect of the PVDF film and the type of the charge amplifiers used, the transient peak time was approximately varies from 0.2 to 0.225 seconds. Therefore, regardless of the length of contact time, the transient peak value remained the same. This result is shown experimentally in Figure 4.14.

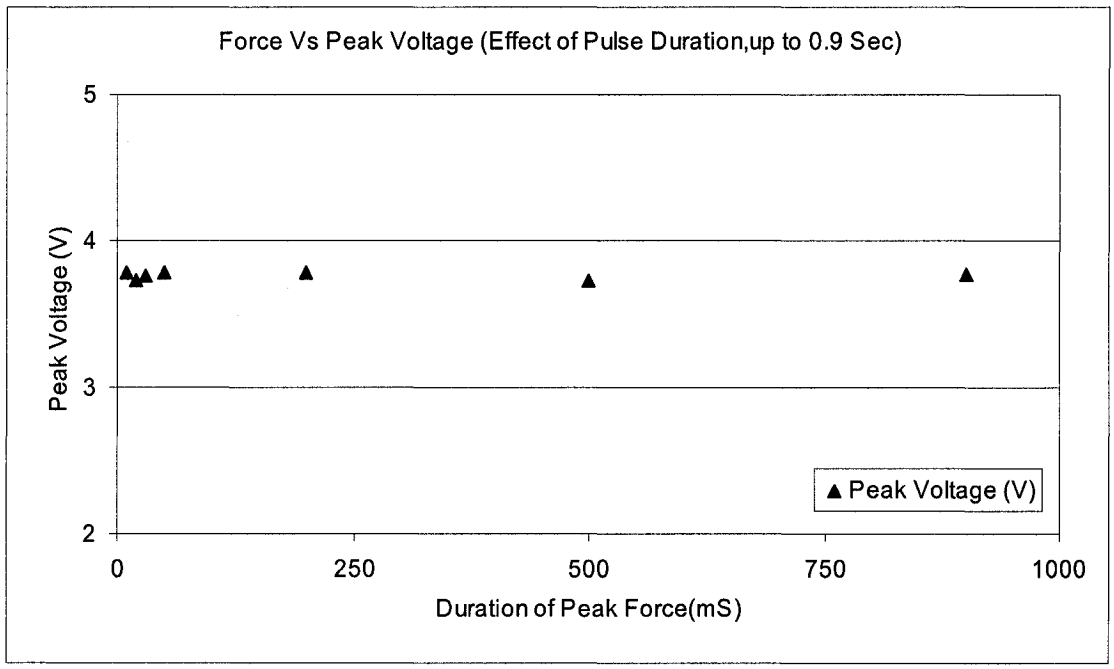

Figure 4.14: Effect of Duration of Load on PVDF.

4.4.3 Preliminary Set-Up Results

In this set-up (Figure 4.15), a strip of Mylar film was placed on top of the entire bumper sensor system. In these experiments, an arbitrary signal was applied from the

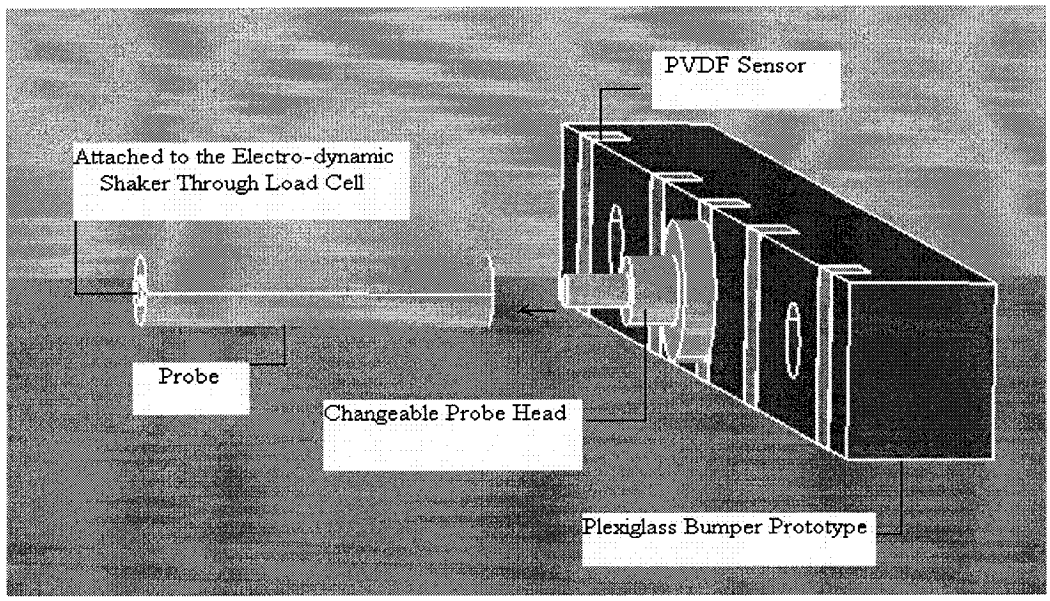

Figure 4.15: Model of Initial Set-up.

signal generator. A typical signal is shown in Figure 4.16. The shaker was activated by this signal via the power amplifier. In addition, the pulse width was adjusted so that the probe hit each sensor for a period of 5 seconds.

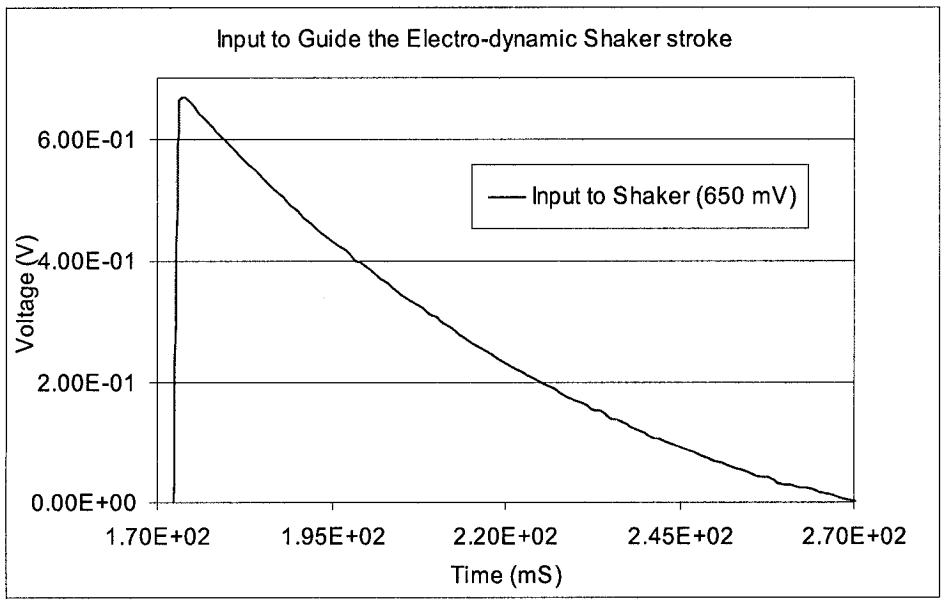

Figure 4.16: Arbitrary Input to the Electro-dynamic Shaker by the Function Generator.

Series of loads had been applied to the bumper prototype as mentioned earlier and had been measured by the load cell. A sample output of the piezoelectric load cell (the input force to the bumper) is shown in Figure 4.17. Using the calibration method for the force transducer, the peak voltage corresponds to 122 N of input force.

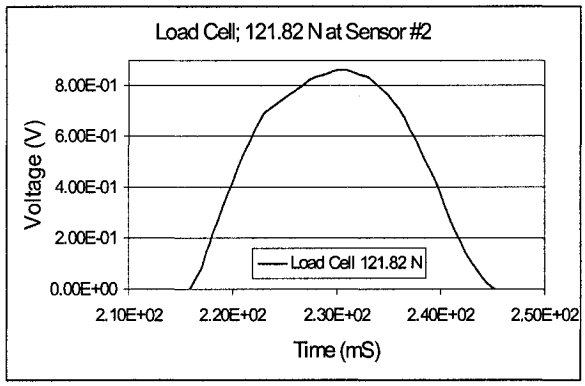

Figure 4.17: A Typical Output of the Force Transducer.

The applied loads to each PVDF sensor and their output were recorded on an oscilloscope and then analyzed on a computer. The magnitude of the load was varied from

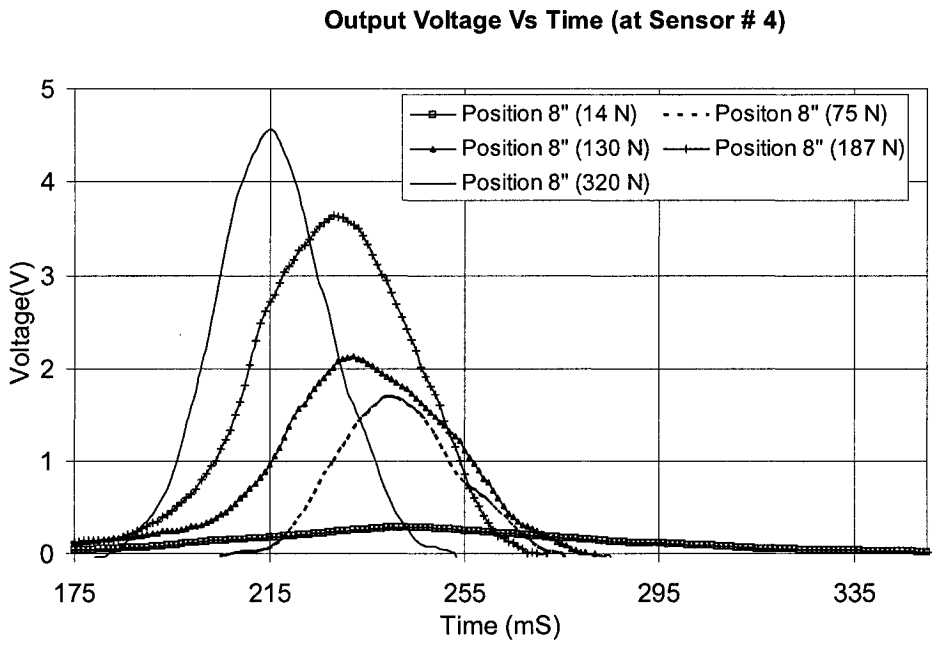

Figure 4.18: Voltage Output of the Sensor 4 (Force on the Sensor 4).

10 N to 350 N. The outputs from the PVDF sensors were consistent, within the experimental error. A typical output signal from one of the PVDF sensors upon the applications of different loads is shown in Figure 4.18.

Considering various output results, it was observed that the time it took for the signal to reach their peak value was the same, within the experimental error. This was also true for the fall time. The shape of the transient was related to the characteristics of the charge amplifier and will not be discussed further. As a result of this experiment, it was concluded that the focus of the further experiments would be directed towards peak value analysis. The schematic of preliminary design of the bumper is shown in Figure 4.19.

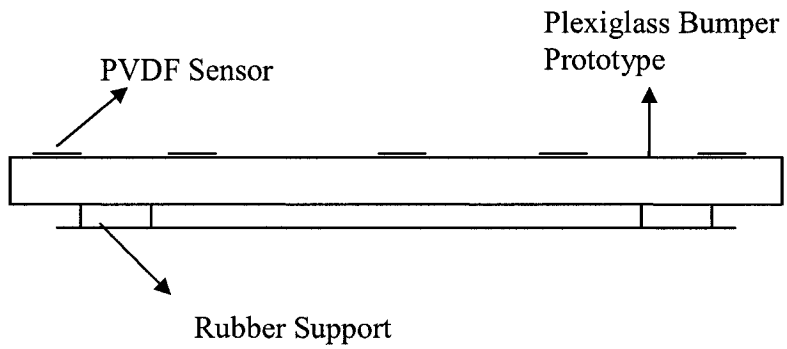

Figure 4.19: Bumper and Sensor Arrangement without Sensor Cover.

Several loads of varying magnitudes were applied directly to each PVDF sensor and the output peak value was recorded; these are shown in Figure 4.20. Using this Figure, it is possible to find the magnitude of the force applied right upon the PVDF sensors of the bumper prototype.

A set of experiments were also conducted to determine the effect of the applied load away from the sensing elements (PVDF sensors). No significant measurable output was observed from any of the PVDF sensors. It was thus concluded that this initial prototype

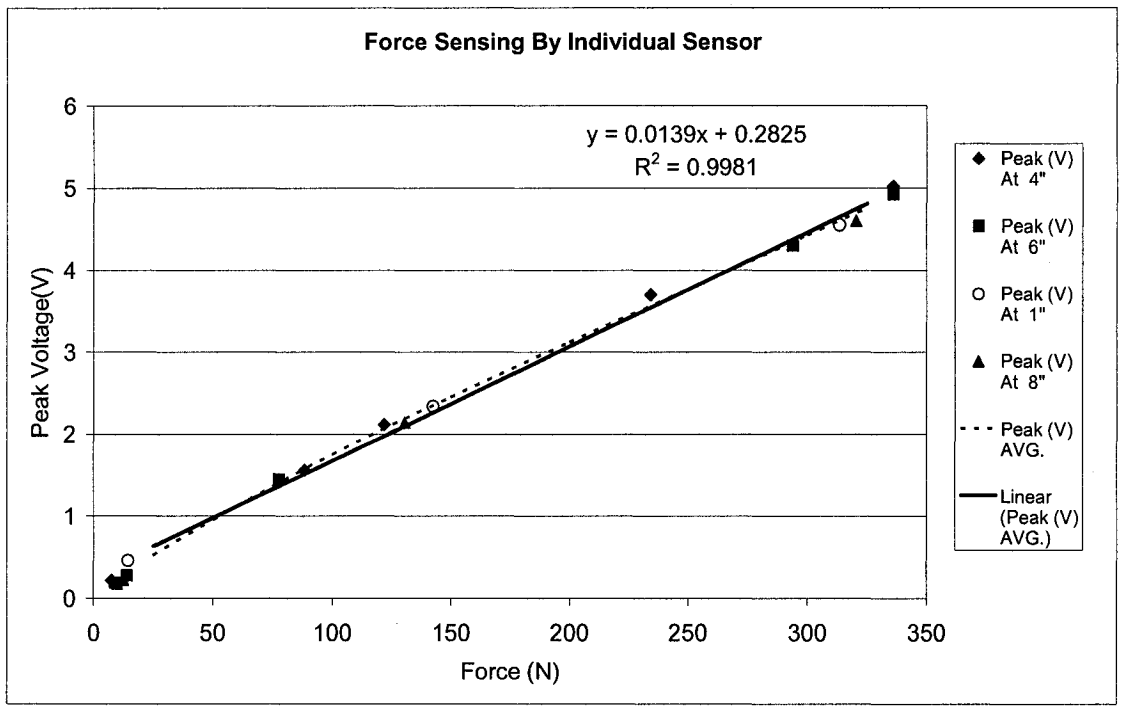

Figure 4.20: Force Detection only when Struck upon Sensors.

bumper system neither can measure the magnitude nor the position of the force, applied away from sensors. So it was compulsory to move towards a better collision detection system capable of sensing the degree of impact and its position. As a result the final two designs were evolved. In the following section, the proposed design approaches are concisely explained in order to determine the magnitude and the position of the applied force, both on and away from the sensor.

4.5 Final Design of Impact Sensing Bumper

In order to overcome the deficiency of the previous design, thus being able to detect output from the PVDF sensors when the force was applied away from the sensor, two design approaches were taken. One was to use a cover plate with teeth and another was without teeth. The teeth were fabricated using a hard plastic material and they were

positioned directly upon the PVDF films. The schematic setups of the two designs are shown in Figure 4.21.

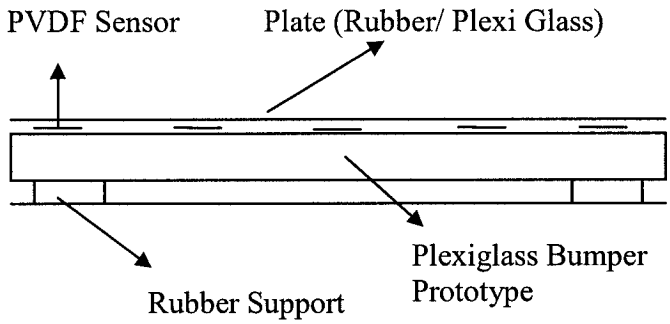

(a) Design 1:Without Teeth.

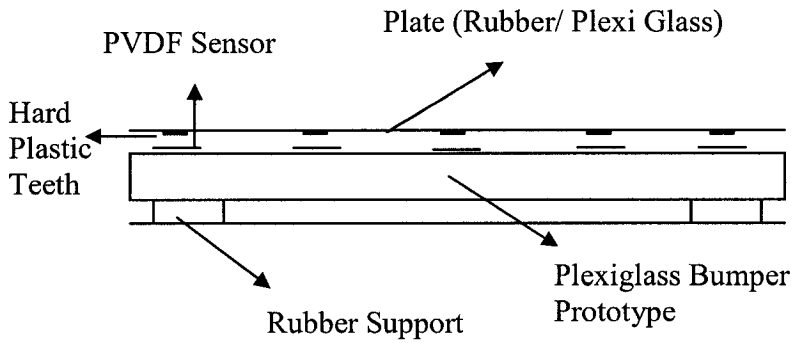

(b) Design 2: With Teeth.

Figure 4.21: Final Designs; Bumper and Sensor Arrangement with Sensor Cover (With and Without Teeth).

4.5.1 Design 1

In this design, a Plexiglass plate of 3.175 x 30.48 x 1.27 cm (1.25 x 12.0 x 0.5 inch) in dimension was placed on the top of the sensors along the bumper (Figure 4.22).

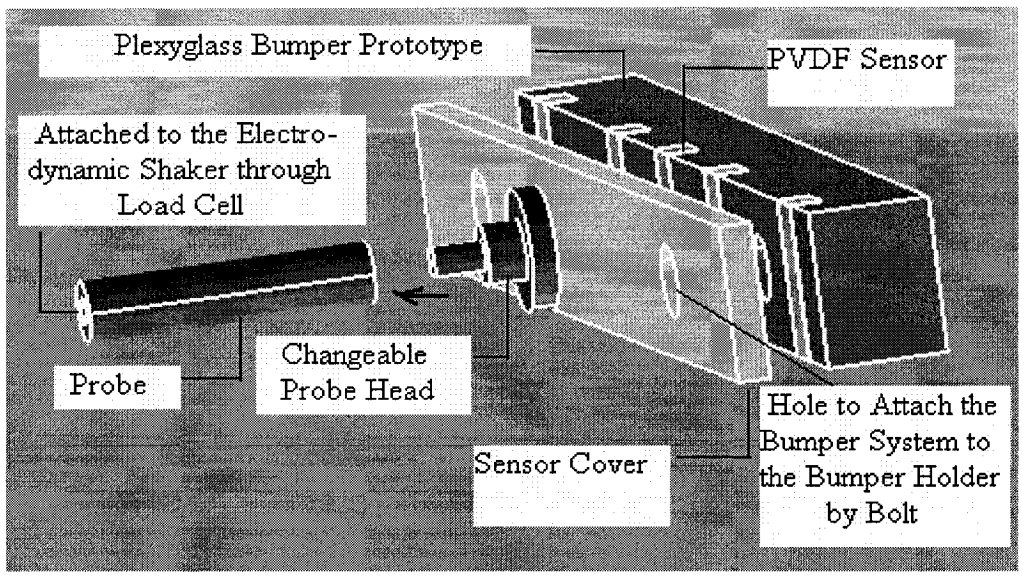

Figure 4.22: Model Design 1 Showing the Cover Plate Placed on the Sensors along the Bumper.

Series of impact loads (step loads), were applied with different probe sizes on the cover plate. The loads were applied both directly upon the sensors and away from the sensors. When the load was applied, all five sensors showed output responses. The magnitude of the applied load and its corresponding position was obtained by detecting the outputs of two adjacent PVDF sensors. The highest transient response peak showed the closeness of the position of the applied force to the particular sensor. The applied load on the bumper prototype had been calculated through two highest peak voltage generating sensors. Right after the collision occurs the two highest peak voltages were summed up to find the force as, F=f (P). The position of impact can also be sensed by the help of two sensors. Here two highest output peak voltage generating sensors could sense the position individually but to be sure, two sensors approach is incorporated to observe whether both results intersect at a common point or not. The remarkable point is to detect the position of the impact, force should be determined at first because the position graph will work only

after the force is known as each load has individual trend of response. After the detection of the force by two sensors method, any of the position sensing graphs of the two adjacent sensors will be able to find the position right away. Empirical relations were also developed by applying a series of specific force at different locations such as X1, X2, X3, X4, and X5 along the bumper prototype. Then position stated as a function of peak voltage i.e. $X = f(P)$. Each empirical relation is suitable for an individual load.

One of the problems with this design was that the results did not show a very good repeatability. This is because the cover plate did not make full contact with the 25μm PVDF sensors and the load is shared by the whole structure. It would be possible to increase the thickness of the cover plate to improve the contact phenomena of the sensors; however, this would lead to an increase in the thickness of the total bumper system. Another problem was that the outputs from the sensors were not sensitive enough for small load applications. Hence a measurable response for small loads was not obtained. Based on the above problems, a modified design is proposed using a cover plate with associated plastic teeth. The design is described in the following section.

4.5.2 Design 2

As mentioned above, five hard plastic teeth, each of which is 6.35 x 31.75 x 3.81 mm (0.25 x 1.25 x 0.15 inch), were glued to the cover plate. This cover plate associated with teeth is shown in Figure 4.23. Besides that the same test procedure to find the degree of impact and its corresponding position was implemented as it was done in design 1.

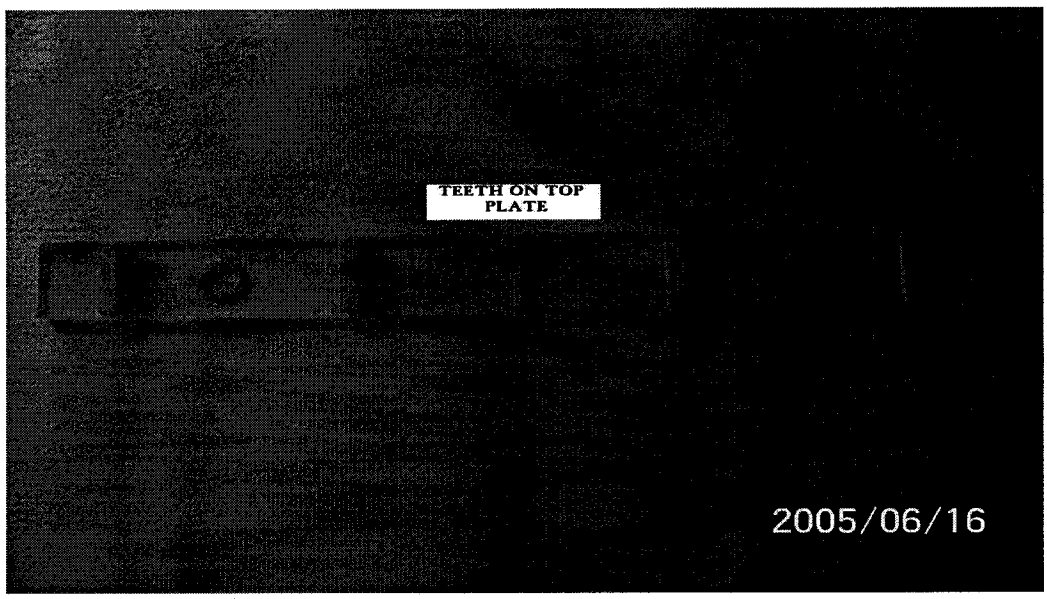

Figure 4.23: Photograph of Top Plate Teeth.

The complete cover plate attached to the bumper is shown in Figure 4.24 along with the electrical connection.

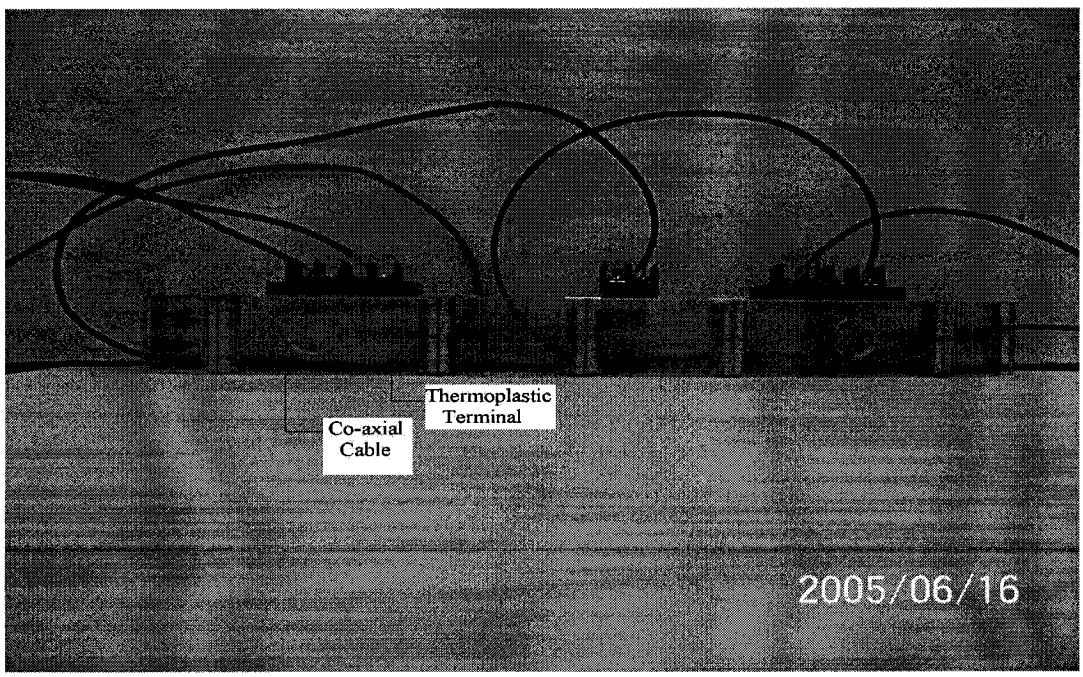

Figure 4.24: Photograph of Top Plate with Teeth on Bumper Prototype.

In this design, the plastic teeth were positioned directly on the sensors. Consequently, the entire load on the sensors is carried by these teeth. As a result, the tests showed a very good repeatability. In addition, since the applied load was transferred directly to the sensors through the teeth, the sensitivity was increased and the dynamic ranges of the sensors in bumper system were also increased.

4.6 Summary

This chapter defines the method of experiment, provides a concise description of the instruments used, and also explains the procedure to find the desired collision force and its position. Various models of the individual parts and the whole assembly were designed using the CATIA R13. The complete fabrication of the collision detection setup was done in the workshop of Concordia University. The design of the system was sufficiently flexible so that the bumper can be moved as close as possible towards the probe. The bumper can also move sideways. The response characteristics of the PVDF sensor were experimentally examined by testing each individual sensor. It was found that the responses of PVDF are linear and the duration of the load application did not have any significant effect on the output transient responses. Through repeatability tests, it was shown that PVDF can measure the force to within a 10% error band. The typical response of PVDF proves that it is possible to characterize the response in terms of only peak voltage amplitude (P). The rise time and fall time of the transient responses did not exhibit significant variations; thus they were not studied further. Since the peak values showed consistent results, they were used as a measure of collision. When the force was applied away from the sensing elements, the magnitudes of the transient response were

used to obtain the position of the applied force. Because of poor repeatability and the inability to measure the position of the applied load between the sensors, two new designs are proposed. One is with the sensor cover only and the other is improved by attaching teeth to it.

The following chapter presents the results of the tests carried out with the proposed bumper systems.

CHAPTER 5

EXPERIMENTAL ANALYSIS AND ANALYTICAL APPROACH

5.1 Introduction

In the preceding chapter, PVDF sensors were characterized by applying step loads directly on the sensors. In this chapter, the magnitude and position of the applied load will be studied when it is applied at any point along the bumper. Two approaches were taken. The first was a bumper with a cover plate with no teeth, representing a contemporary bumper system. The second was a bumper with a cover plate with associated teeth, contacting directly on the PVDF sensors along the bumper system. Using the two approaches, the complete bumper system was calibrated to determent the magnitude and the position of the applied load at any point along the bumper.

This chapter describes a new concept termed as "Two-Sensor Method". This involves arranging a set of PVDF sensors along the vehicle bumper prototype and measuring the severity and the position of the collision as a function of peak magnitude of voltage output. After difficulty in the preliminary design of the collision detection system, two methods were proposed in Chapter 4. An extensive study has been performed here in this chapter with those two designs. Sensing a load and its position in between two sensors was impossible; this propelled the study to find an alternative solution. By incorporating a top Plexiglass plate on the PVDF sensors, it became possible to detect the in between loads and locate their position. Also, the insertion of the top plate removed the existing ambiguity of the effect of the surface area and material properties of the impacting object upon the PVDF sensors. This made the system independent of the size and the softness of the striking probe. At the beginning of the analysis it was decided

to consider the output peak voltage of all the sensors. The collision detection system was to be calibrated by means of addition of all sensor responses (peak voltage). However, it was seen that this approach created inequality in the summation of the total output peak voltage of all the sensors from position to position. For instance, when the bumper was struck in the middle, then the summation of all the sensors peak voltages was much higher than the summation of the output voltage peak when the bumper was hit on the corner. Furthermore it was determined that the addition of only the two highest peaks served the purpose perfectly; this was termed the "Two-Sensor Method". The common activity in all the set-ups used so far in the study was to make each sensor act similarly, by tuning the amplification rate (sensitivity and scale) of each charge amplifier attached to each sensor. Thus, the structural difference could be overcome. Without achieving this, the purpose of this work could not be considered successful. Only when all the sensors act the same we could conclude that, independent of position, the severity of the impact can be measured and the position graph will provide the distance away from the peak magnitude of the impact-generating sensor. Establishment of empirical relations makes the whole system handy where it is very easy to simulate any impact and its position through these equations.

5.2 Collision Detection Design 1

A cover plate made of Plexiglass with dimension of 3.175 x 30.48 x 1.27 cm was bolted to the bumper. The plate covered the PVDF sensors along the bumper. Two of the PVDF sensors were placed at the outside of each bolt and three of the sensors were positioned in between the bolts. A technique was developed to determine the magnitude and the

position of the applied force in between the bolts using only two sensors. Since this technique could easily be used for the areas of the bumper outside of the bolts by providing an additional sensor at each corner of the bumper prototype, this technique was not re-tested for outside of the bolts.

Initially it was believed that only one sensor was sufficient to determine the magnitude and the position of the applied load. Hence, the bumper was calibrated for various magnitudes of the force away from each sensor. This method was proved to be unacceptable because it was possible that at some points along the bumper, the output from the sensor would show confusing results. This was because, it would be difficult to determine whether a high load was applied at a large distance from the sensing element or a low load was applied close to the sensor.

Another technique was developed by considering the output from all the sensing elements. Numerous step loads were applied at different positions and the output of all the sensors was recorded. These loads were applied at the end of the bumper and gradually moved towards the other end. The outputs from all the sensors were recorded. The aim was to sum the peak values of all the sensors; this would indicate the total load applied to the bumper. However, this proved to be ineffective. When the load was applied in the middle of the bumper, the sum of the output peak values from all the sensors was greater than the sum of the peak voltages when the load was applied at the end of the bumper.

A final technique was developed in which the summation of the outputs of two adjacent sensors close to the point of application of the load was considered. This method was named as "Two-Sensor Method". The bumper was calibrated by applying loads through

a 10 mm (0.4 inch) diameter probe along the bumper and between the two bolts. The output peak values from the two adjacent sensing elements were recorded. Experimental results showed that for a known load, the sum of the output voltages of the two adjacent sensors were the same along the bumper within the experimental error band. This output sum was independent of the position of the applied load.

Initially, the bumper area between the two bolts was calibrated by applying varying magnitudes of step loads by the probe directly on the sensors. A typical input pulse to the shaker by the signal generator is shown in Figure 5.1

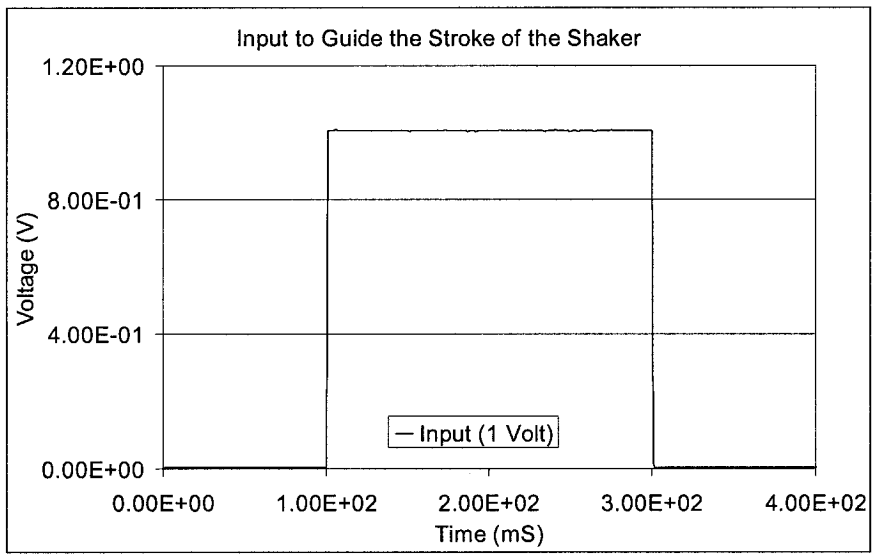

Figure 5.1: A Typical Output of the Signal Generator.

The applied loads were 100, 200, 300 and 350 N. A typical output from the force transducer for 350 N is shown in Figure 5.2

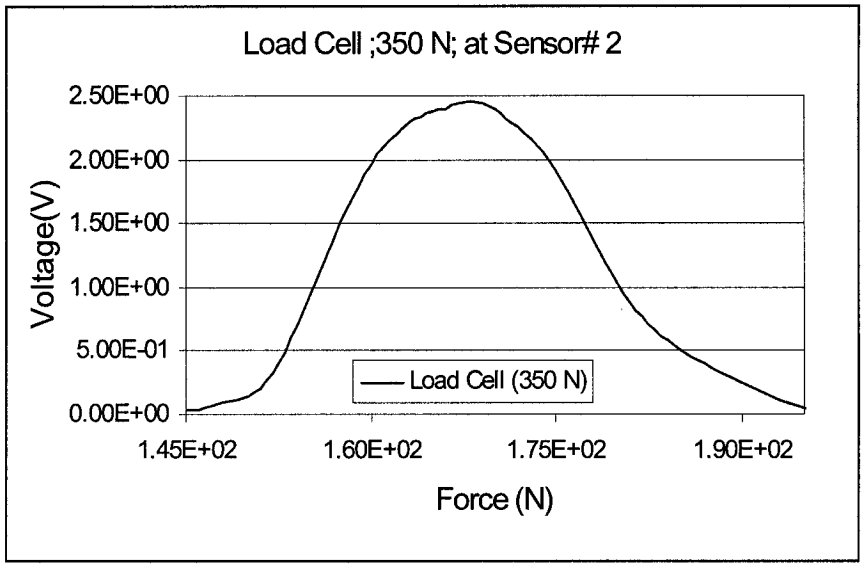

Figure 5.2: A Sample Response of the Force Transducer.

The output from each PVDF sensor was recorded. The results showed that for a given applied load the peak values were approximately same. A result for one of the sensing elements is shown in Figure 5.3.

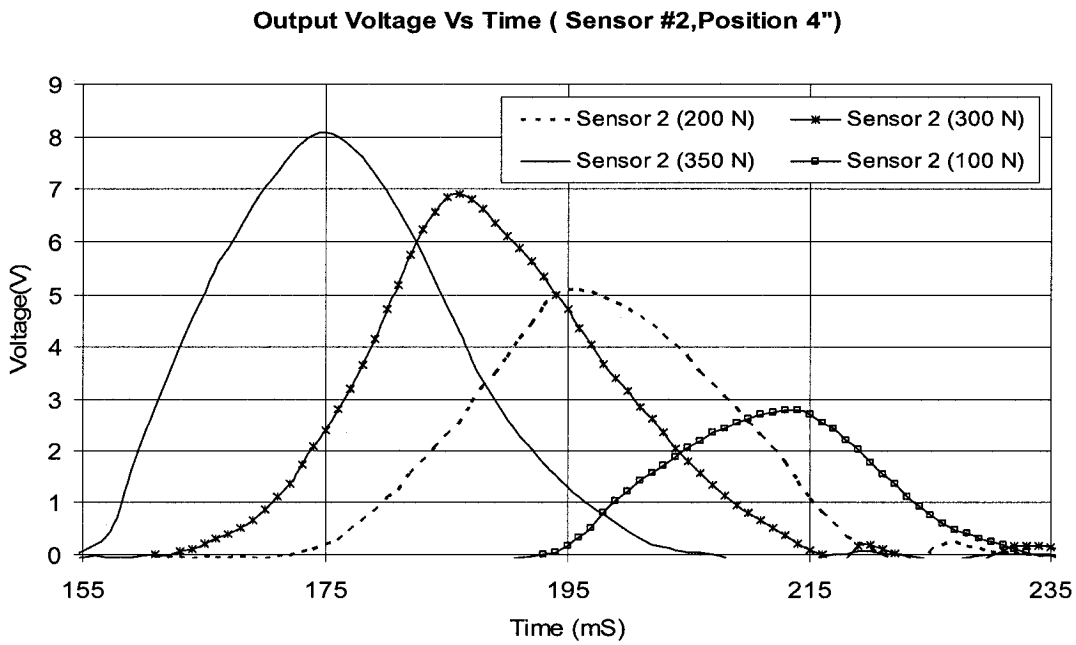

Figure 5.3: Sample Output Response from the PVDF Sensor for Different Loads.

In order to calibrate the sensors, the various forces were applied directly on them and the peak values were recorded. Each specific load was plotted against corresponding peak output voltage. Like the preliminary design, the applied force and thus generated peak voltage also proved to be proportional (Figure 5.4). The empirical relation developed based on readings of each sensor is

$$y = 0.021x + 0.7793 \quad \ldots\ldots\ldots\ldots\ldots\ldots\ldots\ldots\ldots\ldots\ldots\ldots \quad (5.1)$$

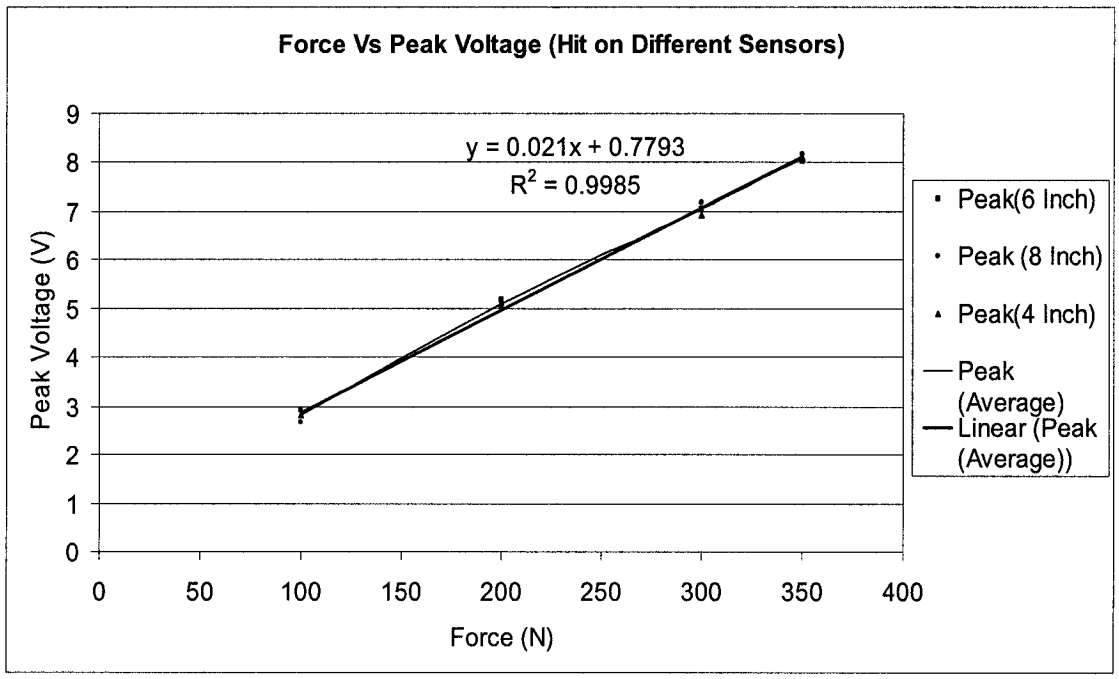

Figure 5.4: Calibration of Each Individual Sensor.

5.2.1 Two-Sensor Method

After calibration of the individual sensors, the two-sensor method was used to determine the magnitude and the position of the applied load at any point along the bumper. The two-sensor method was developed based on the experimental results. It was

observed that the sum of the outputs from two adjacent sensors is the same (within the experimental errors), regardless of the position of the application of the force. The system was calibrated by applying loads of 100 N, 200 N, 300 N and 350 N individually at 10 mm (0.4 inch) intervals between the two sensors. The outputs of the two highest peak generating sensors were recorded for each position and the peaks were added together. The complete results for the distance between sensor number 2 and 3 is shown in Figure 5.5. The following empirical relation was developed using linear regression.

$$y = 0.0371x + 0.8479 \quad \ldots\ldots\ldots\ldots\ldots\ldots\ldots\ldots\ldots\ldots\ldots\ldots \quad (5.2)$$

Here x is the desired force and y is the summation of the two generated output voltages.

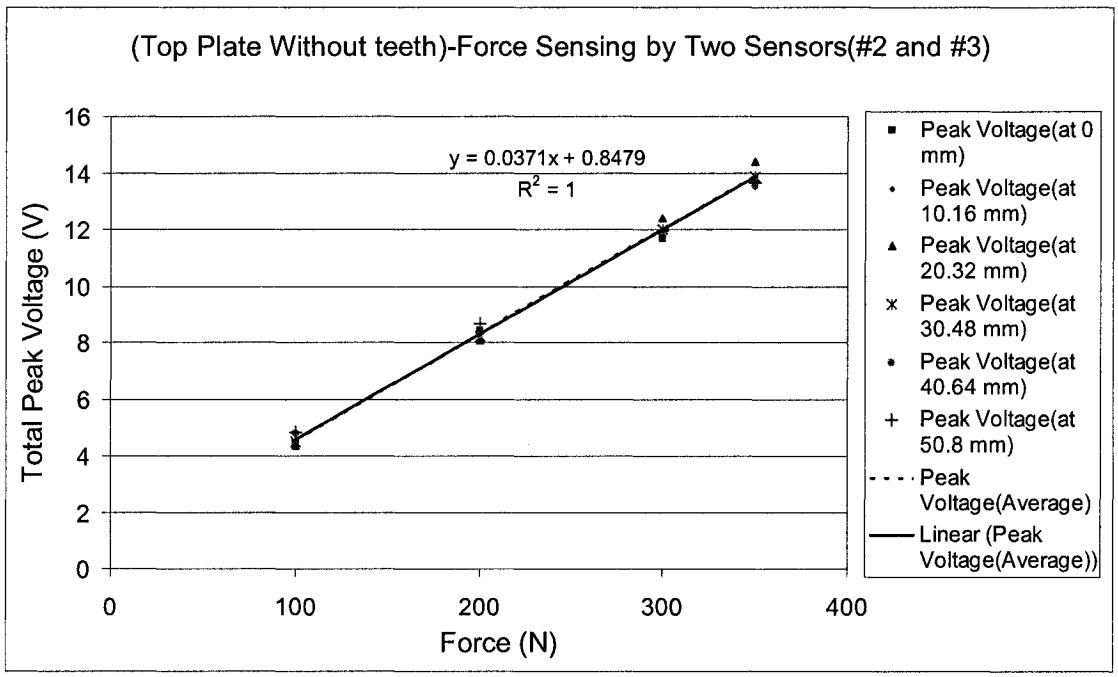

Figure 5.5: Calibration of the Bumper between Sensors 2 and 3 for Force Detection by the Two-Sensor Method.

The same technique was used to calibrate the bumper prototype between sensor 3 and 4. The result is shown in Figure 5.6.

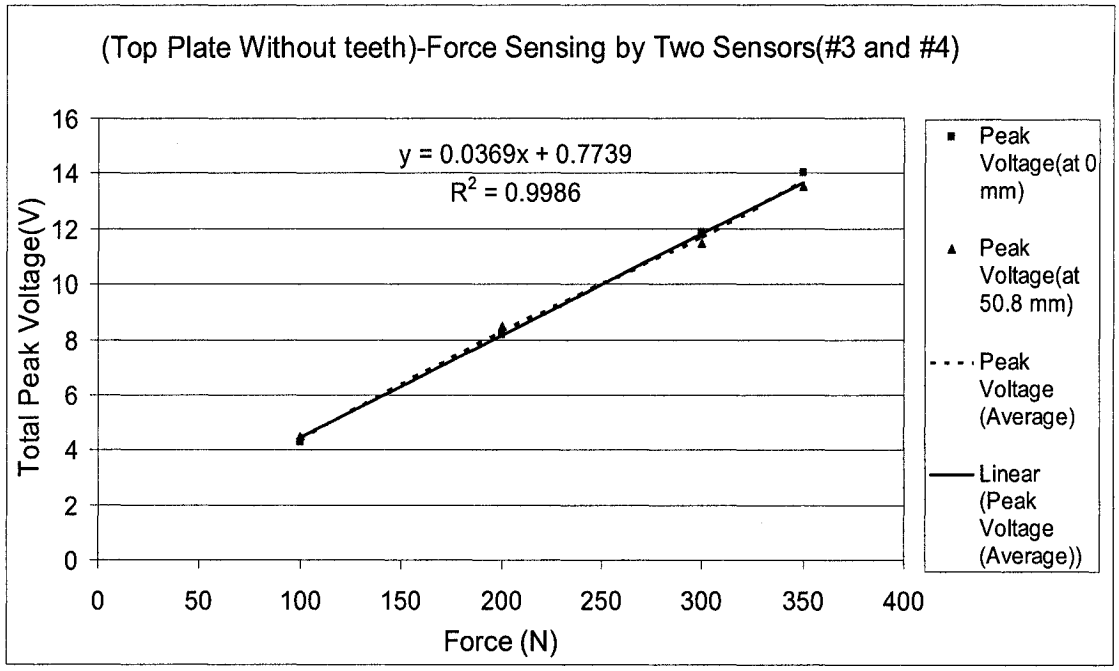

Figure 5.6: Calibration of the Bumper between Sensors 3 and 4 for Force Detection by the Two-Sensor Method.

The empirical formulation for this graph is shown by the following equation.

$$y = 0.0369x + 0.7739 \quad \text{..... .....} \quad (5.3)$$

Considering equations (5.2) and (5.3), it can be seen that they are very similar and that the difference in the coefficients of the equation is due to experimental errors. Thus, either of the equations could be used to determine the magnitude of the applied force between the two bolts along the bumper.

In order to determine the collision position, each specific load was applied individually on and away from the sensors. The peak value of the output of each sensor was plotted against the position of the applied loads away from each sensor. The results for both sensors 2 and 3 are shown in Figures 5.7 and 5.8 respectively. Any of the two highest peak generating sensors are able to indicate the position of the applied load away from the corresponding sensor.

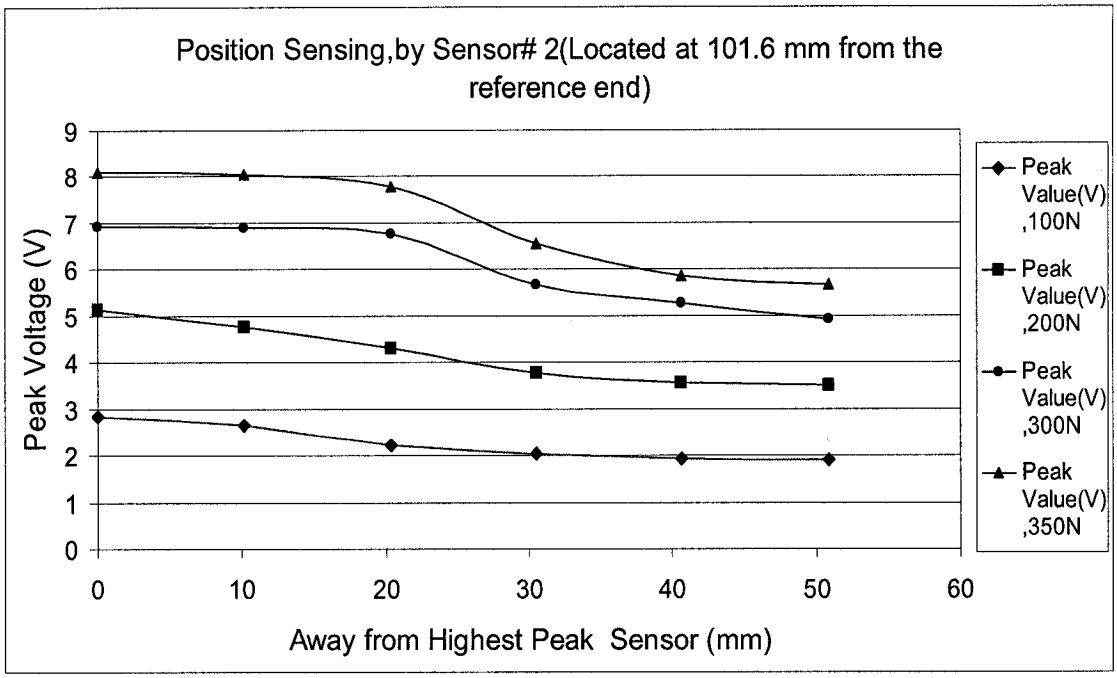

Figure 5.7: Output of the Sensor 2 for Various Loads on and away from the Sensor.

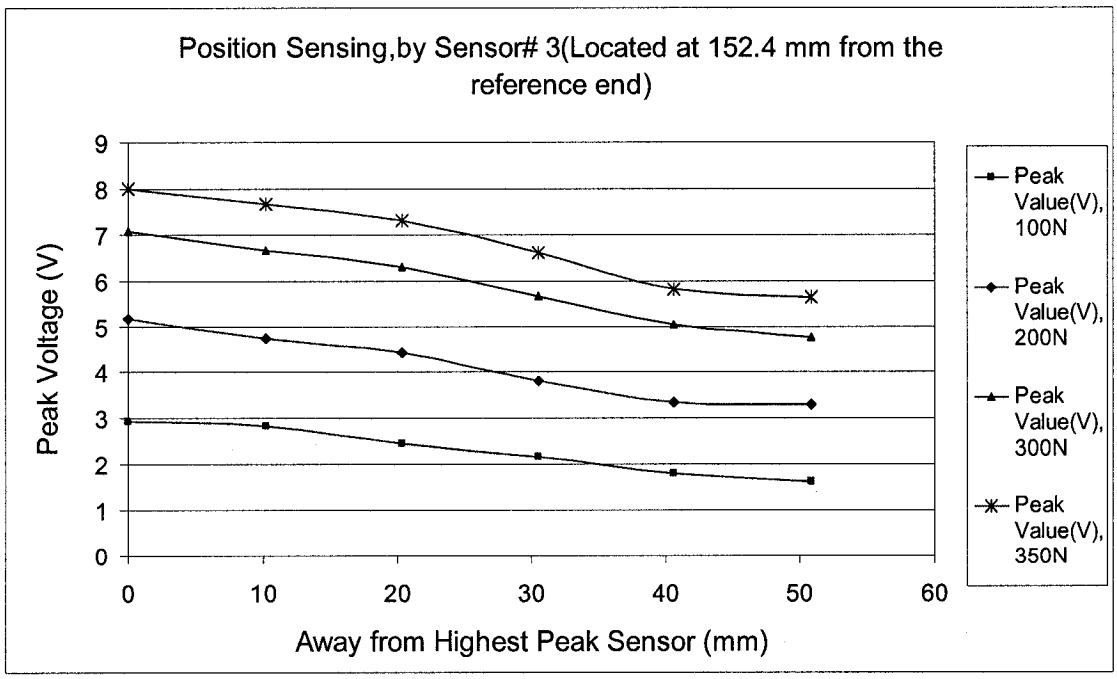

Figure 5.8: Out put of the Sensor 3 for Various Loads on and away from the Sensor.

In a typical collision with the proposed bumper prototype, initially the two highest peak voltages will be identified and added together. Using Figure 5.5 or 5.6 the magnitude of the applied load can be determined (this can also be obtained using either equation 5.2 or 5.3). Knowing the total load applied, the position of the impact can be obtained from either figure 5.7 or 5.8. Where the magnitude of the total load is not apparent on the above two figures, an interpolation method should be used to plot the appropriate graph related to the load. The position of the load could be found by considering the highest peak voltage and then by drawing a horizontal line on the graph. From the position of the intersection, a vertical line can be drawn which determines the position of the applied load. Similar results were obtained for the pair of sensors 3 and 4. Since the results were identical within the experimental error, they are not reported.

Since the above graphical method could be time consuming, an attempt was made to fit an equation for each individual load in Figures 5.7 and 5.8. The results are shown in Figures 5.9 and 5.10. The equations generated from the curve fitting technique are limited for certain tested loads only, which are shown in the following page.

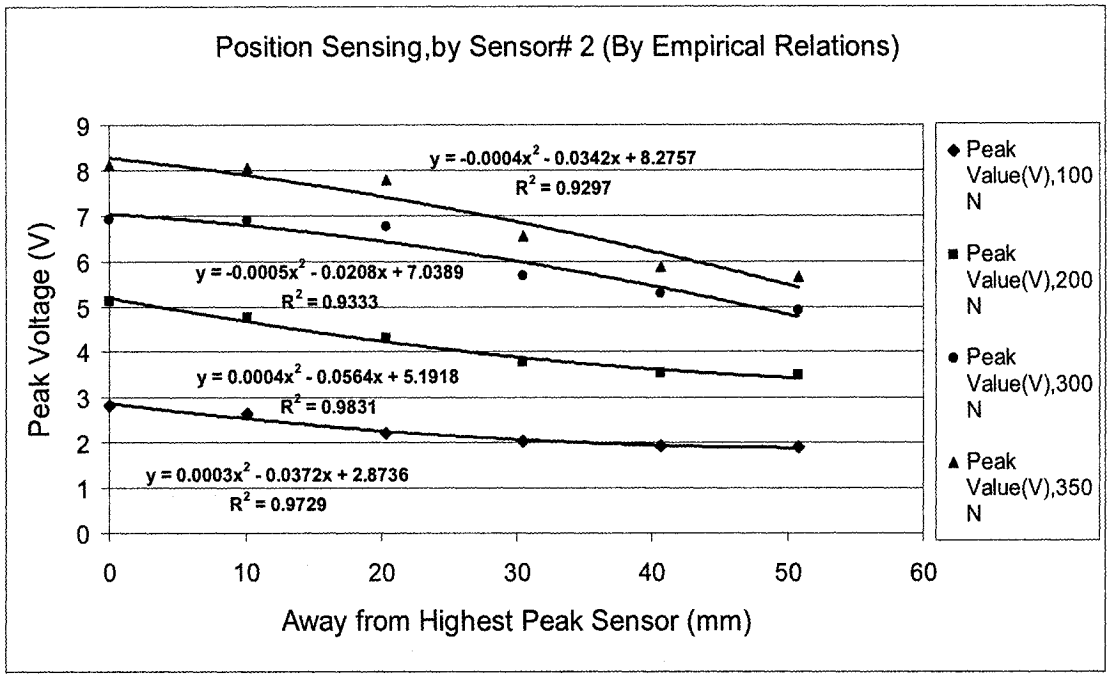

Figure 5.9: Curve Fitting Results for Sensor 2.

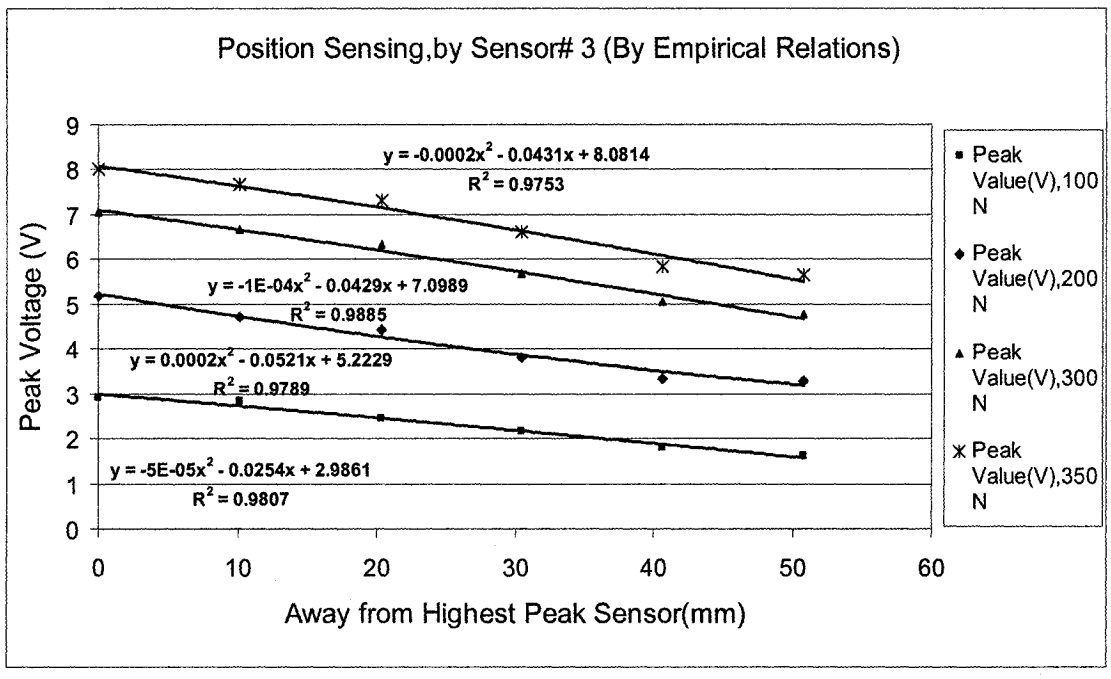

Figure 5.10: Curve Fitting Results for Sensor 3.

The coefficients of the above regression equation were used to develop the following approximation method.

5.2.2 Approximation Method

The empirical equations discussed in the earlier segment can only find the position away from the sensors for four known loads such as 100 N, 200 N, 300 N and 350 N. To generalize this position sensing system i.e. to find the position for any given load, this "approximation method" was evolved and will be discussed in this section. The coefficients of the above quadratic equation were plotted against the force obtained by the two-sensor method. Then a curve was fitted for the coefficients of x^2, x and the constant of the quadratic equations individually against the applied load. The results obtained and the empirical relations for each coefficient against the applied load are shown in Figures 5.11, 5.12, 5.13.

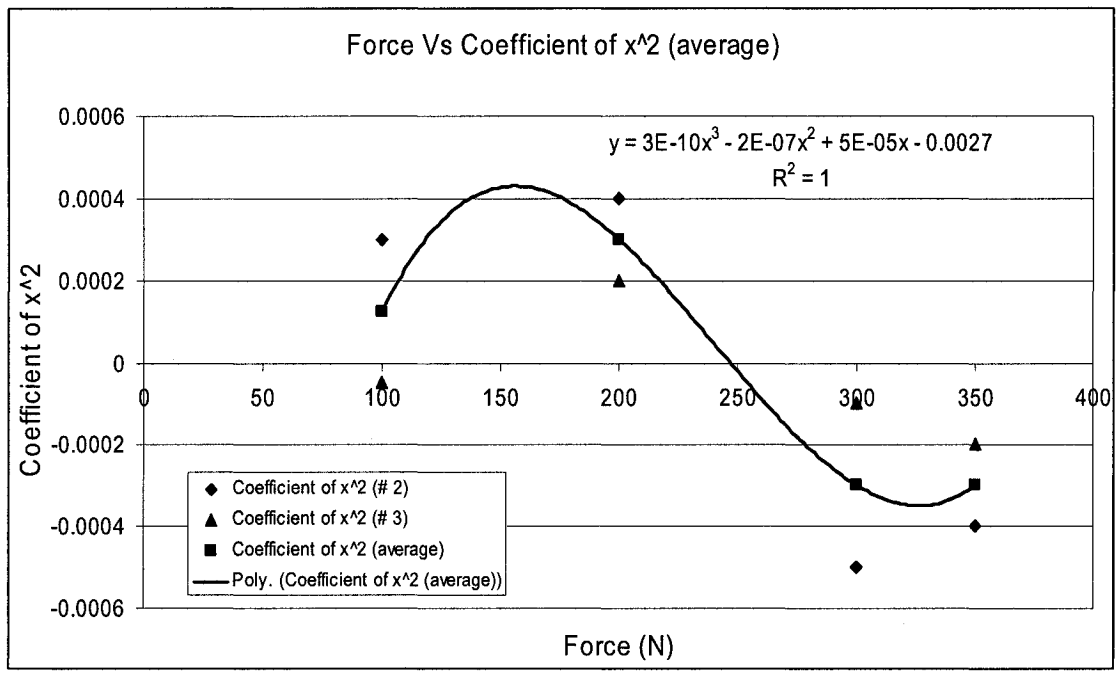

Figure 5.11: Empirical Relation to Find the Co-efficient of x^2.

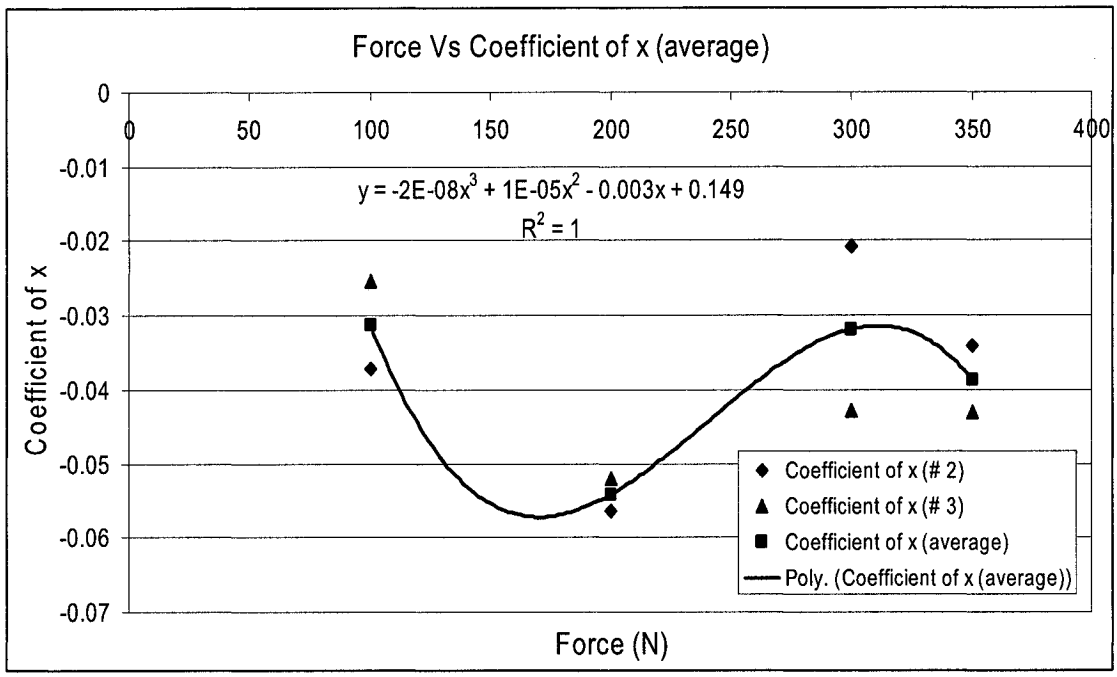

Figure 5.12: Empirical Relation to Find the Co-efficient of x.

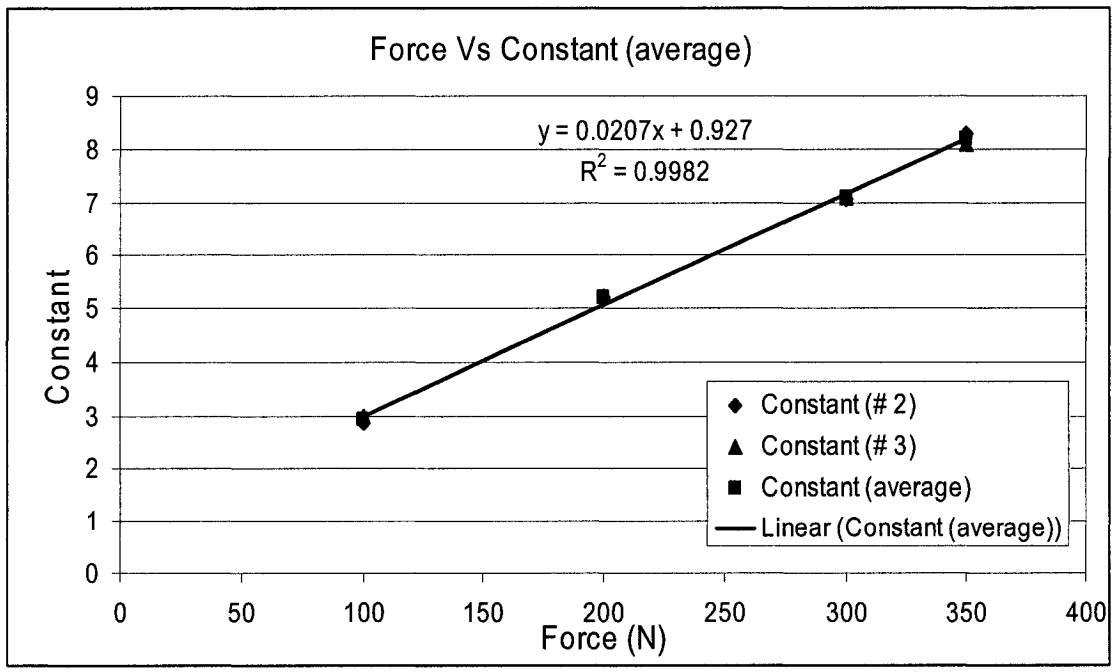

Figure 5.13: Empirical Relation to Find the Constant.

Using the above method, the coefficients A, B, and C of the quadratic equation, $y = Ax^2 + Bx + C$ were obtained, where y represents the highest peak value and x represents the position of the impact. By knowing the y value, the x value can easily be determined.

The calculation procedure of design 1 is clearly described in Appendix-B with numerical values obtained from a sample test.

The poor repeatability of this top plate on sensor set up (design 1) propelled the study towards a better alternative solution. In this set up when a load is applied on the bumper prototype, load is shared by the entire structure. So most probable case of this poor repeatability is every time when the prototype is struck with a specific load in a specific position the sensor does not feel the same amount of force every time. This problem was greatly felt during position detection where the detection system did not perform satisfactorily. As the top plate is thin, the bending of the plate comes in to the action which creates obstacle in proper sensing. But more rigid or very thick top plate could be able to solve this problem which however is not desirable for a bumper system. Although design 1 with proper calibration is capable of predicting the magnitude of the impact well, it is unlikely that such design can satisfy the location detection feature within small error band. This is due to the fact that in design 1, the load is distributed over the entire bumper while the sensors only sense the loads over them. Design 2 evolved as a solution to the distribution of load such that total load is sensed by the sensors alone.

5.3 Collision Detection Design 2

As it was mention in Section 4.5.2, in this system the cover plate had teeth that were positioned directly on the PVDF sensors. The dimensions of each tooth were 6.35 x 31.75 x 3.81mm (0.25 x 1.25 x 0.15 inch). The approach in detecting the magnitude of the applied force and its position was similar to that of design 1. A typical output from the force transducer and the PVDF sensor when a 350N step load was applied directly on the PVDF sensor over the bumper is shown in Figure 5.14

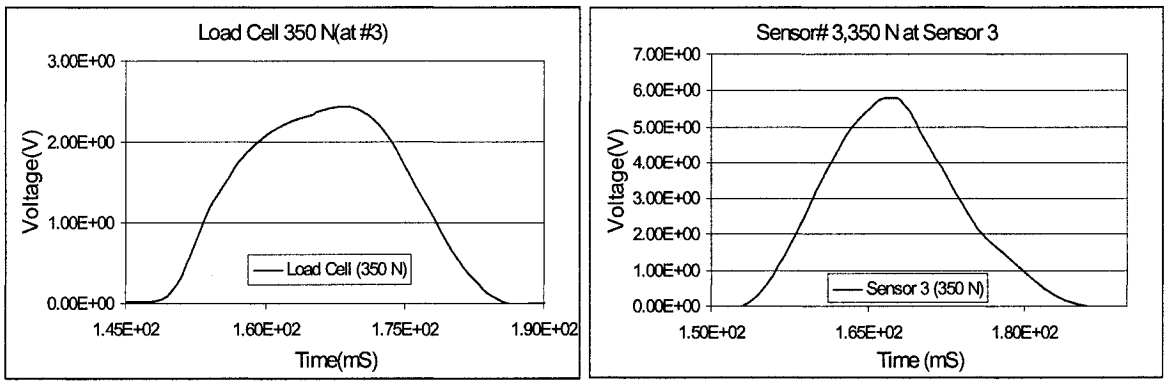

Figure 5.14: Sample Output from the Force Transducer and the PVDF Sensor.

Similar to design 1, each individual sensor was calibrated. Each peak value was plotted against the applied load on sensors individually; the result is shown in Figure 5.15.

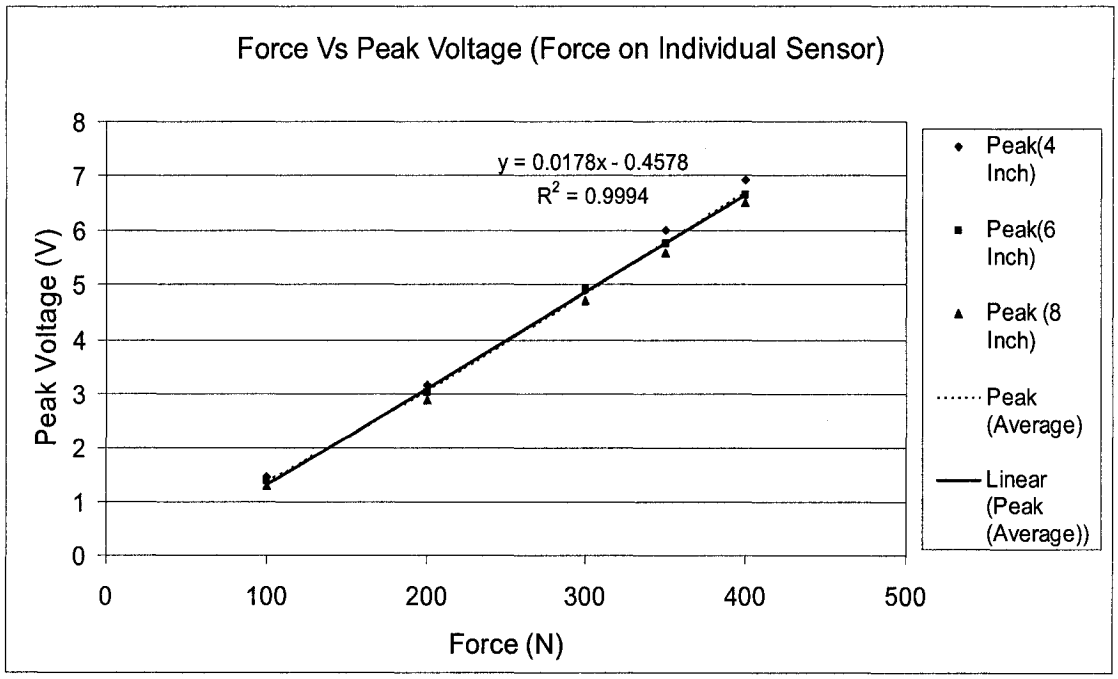

Figure 5.15: Calibration of Each Individual Sensor.

After fitting the average value the following empirical relation was obtained

$$y = 0.0178x - 0.4578 \quad (5.4)$$

This equation can only find the force when applied upon sensors. Subsequently two-sensor method was proposed as it is capable of determining the magnitude of force and its corresponding position graphically as well as analytically.

5.3.1 Two-Sensor Method

After calibration of the individual sensors, similar to design 1, the two-sensor method was used to determine the magnitude and the position of the applied load at any points along the bumper prototype. The system was calibrated by applying 100 N, 200 N, 300 N, 350 N and 400 N loads at 10 mm intervals between the two sensors. The complete results for the distance between sensors 2 and 3 are shown in figure 5.16.

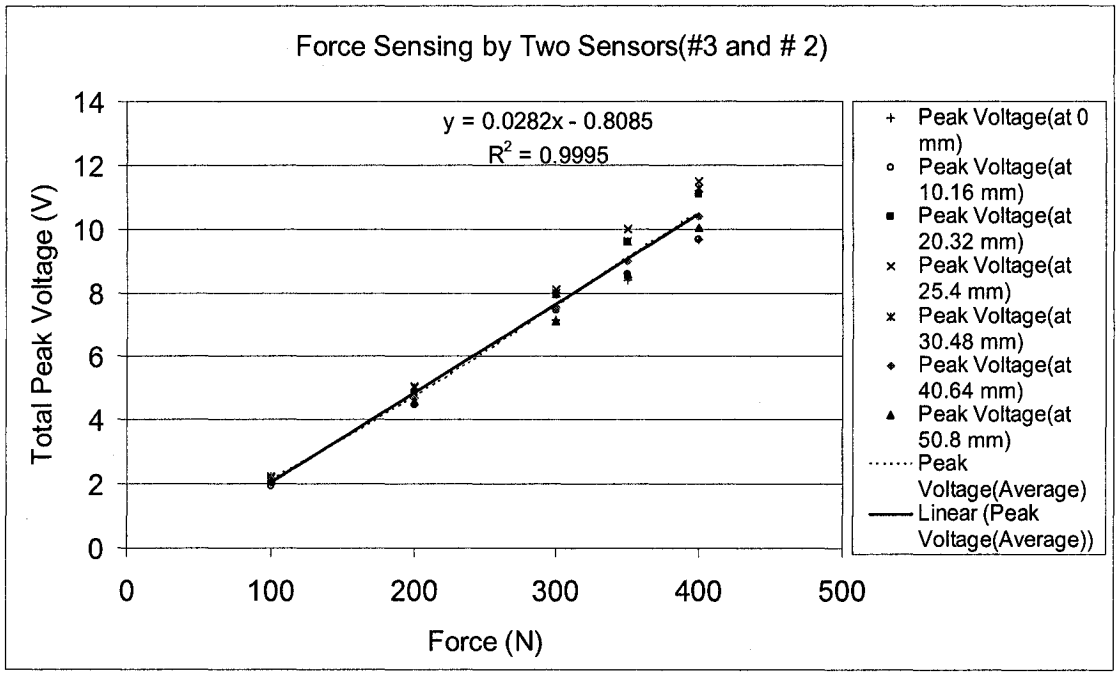

Figure 5.16: Calibration of the Bumper between Sensors 2 and 3 for Force Detection by the Two-Sensor Method.

Here using linear regression the empirical relation developed for force detection by sensor 2 and 3 was found to be $y = 0.0282x - 0.8085$ ..... (5.5)

The same technique was used to calibrate the bumper distance between sensors 3 and 4. The result is shown in figure 5.17

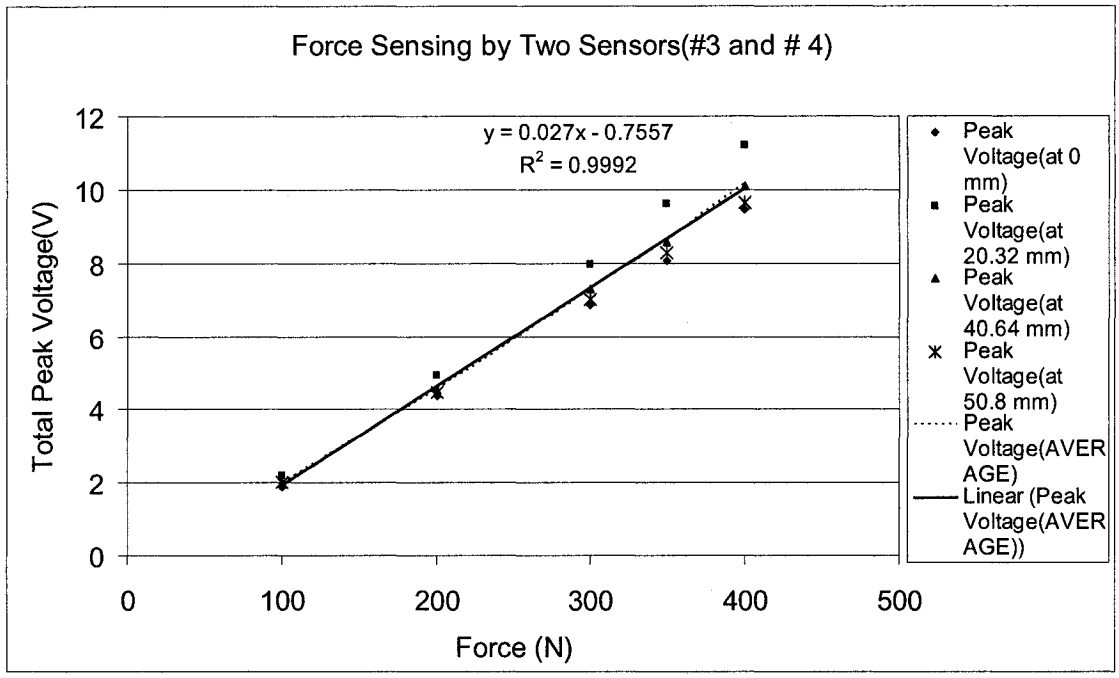

Figure 5.17: Calibration of the Bumper between Sensors 3 and 4 for Force Detection by the Two-Sensor Method.

The empirical formulation for this graph is shown by the following equation.

$$y = 0.027x - 0.7557 \quad \text{..... ....} \quad (5.6)$$

Two equations (5.5) and (5.6) are very similar. The difference exists in the coefficients of the equation and can be attributed as experimental errors. Thus, either of the equations could be used to find the applied load.

This two-sensor method is applicable to determine any normal load independent of how big the structure is. In the above figures (5.16 and 5.17) it can be clearly stated that independent of where the normal force is applied, the addition of the two highest peak generating sensors' output is capable to detect the magnitude of the force.

In order to determine the collision position, the output of each sensor was plotted against the position of the applied load away from each sensor. The results for both sensors 2

and 3 are shown in figures 5.18 and 5.19 respectively. Similar results were obtained for sensor 4 and hence not reported. In all these position sensing graphs, depending on the

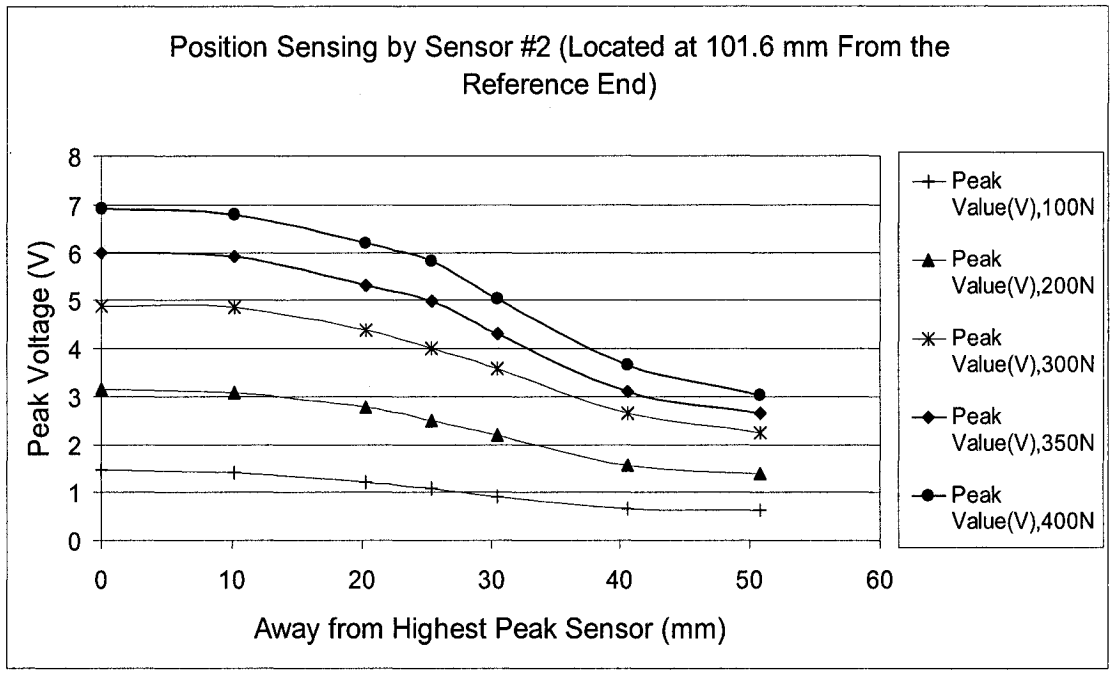

Figure 5.18: Output of Sensor 2 for Numerous Loads on and away from the Sensor.

load, several curves were obtained which is able to detect any position when force lies between 100N to 400N and expected to be so on by extrapolation. Because the trend clearly indicates that even the higher load should support the graphical position indication system.

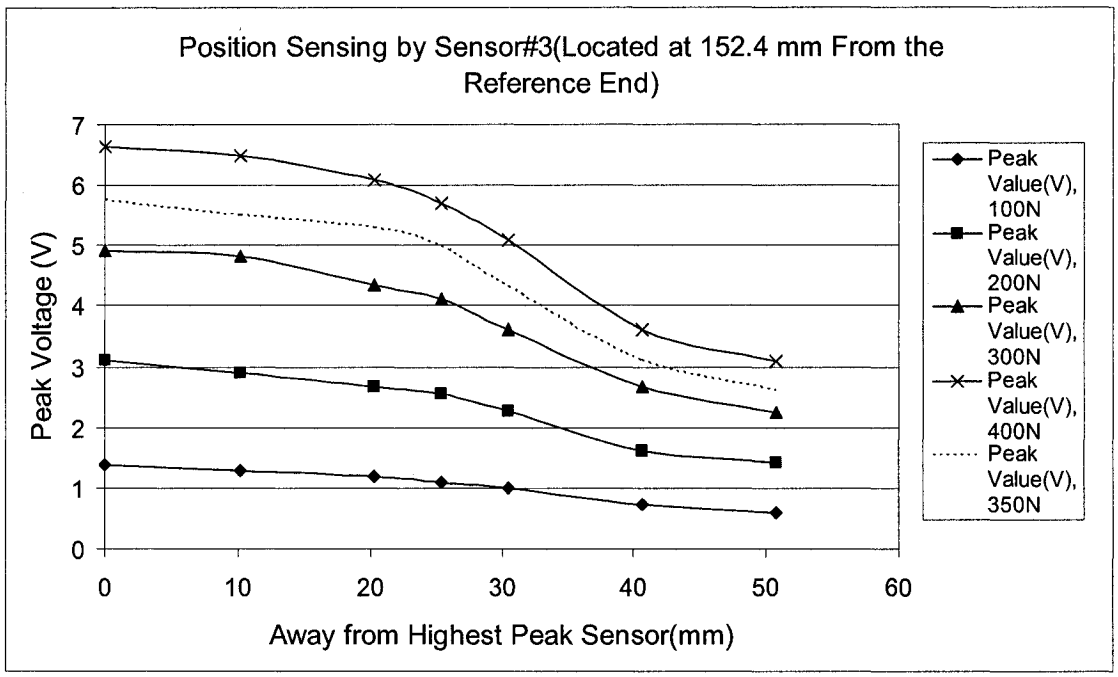

Figure 5.19: Output of Sensor 3 for Various Loads on and away from the Sensor.

A similar analysis was conducted to determine the position of the applied load. The procedures for determining the position of the applied load is described in section 5.2.1 Although the graphical results provided with the better accuracy expectedly but the method could be time consuming so an attempt was made to fit an equation for each individual load in Figures 5.18 and 5.19. The results are shown in the following page in Figures 5.20 and 5.21. This curve fitting technique reveals the idea of approximation method and will be described in the next section for design 2.

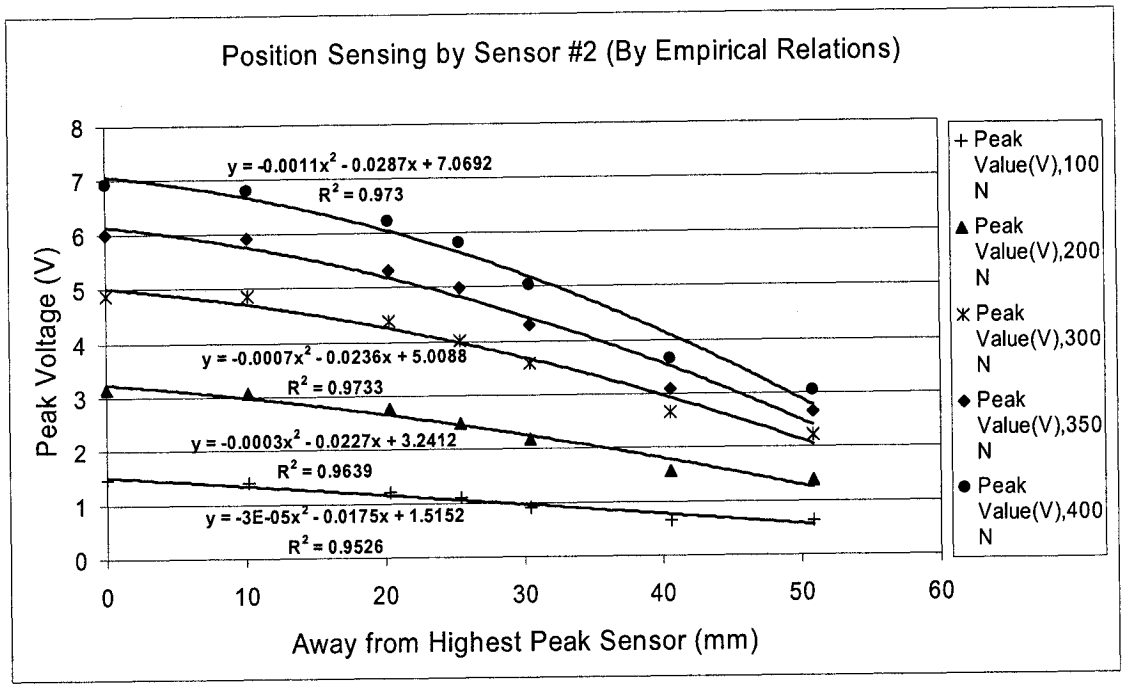

Figure 5.20: Curve Fitting Results for Sensor 2.

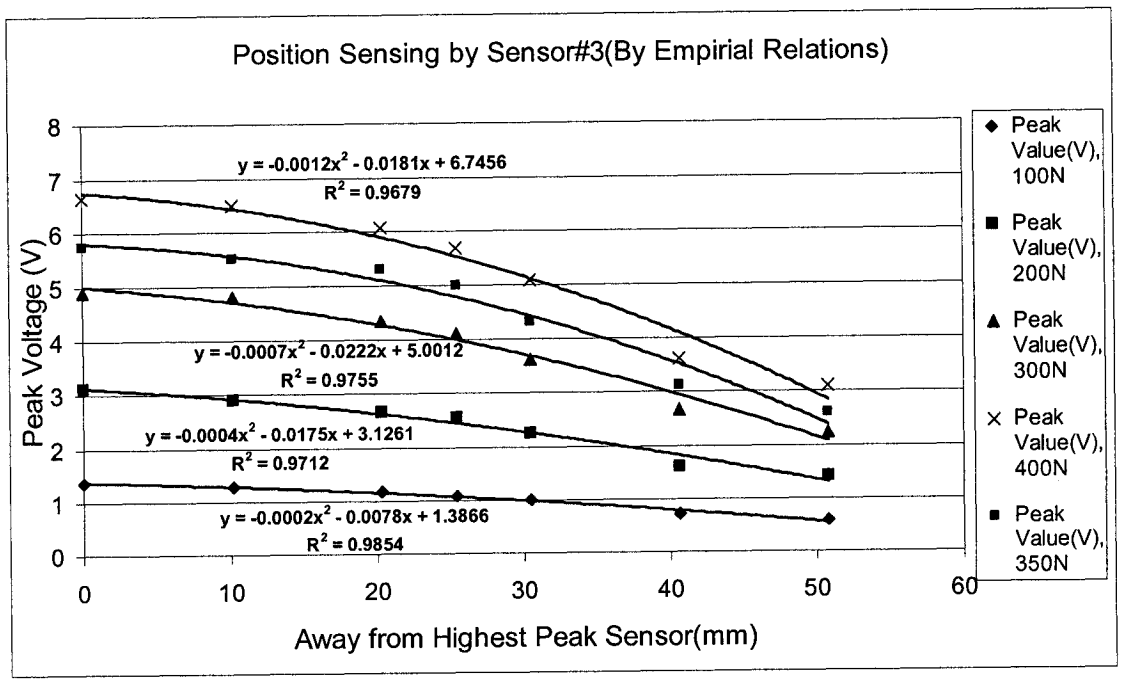

Figure 5.21: Curve Fitting Results for Sensor 3.

The coefficients of the above regression equation were used to develop the approximation method which is described in detail in section 5.2.2. Like earlier the coefficients of x^2, coefficients of x and the constants obtained from the empirical relations developed by each sensor have been averaged to find a single equation to find these constants for any load. This phenomenon ended up with the position of impact for any normal load analytically. These empirical relations for the coefficients are developed to generalize the model rather than finding the position from graphs by interpolating several readings. The results obtained and the empirical relation for each coefficient against the applied load is shown in figures 5.22, 5.23, and 5.24.

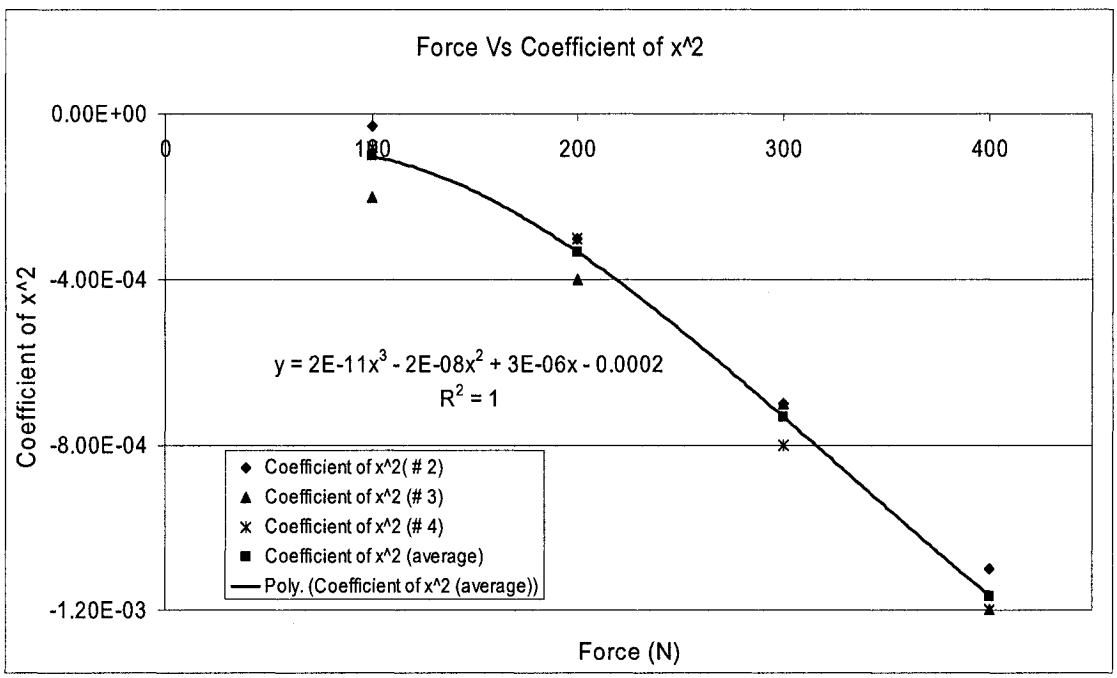

Figure 5.22: Empirical Relation to Find the Co-efficient of x^2.

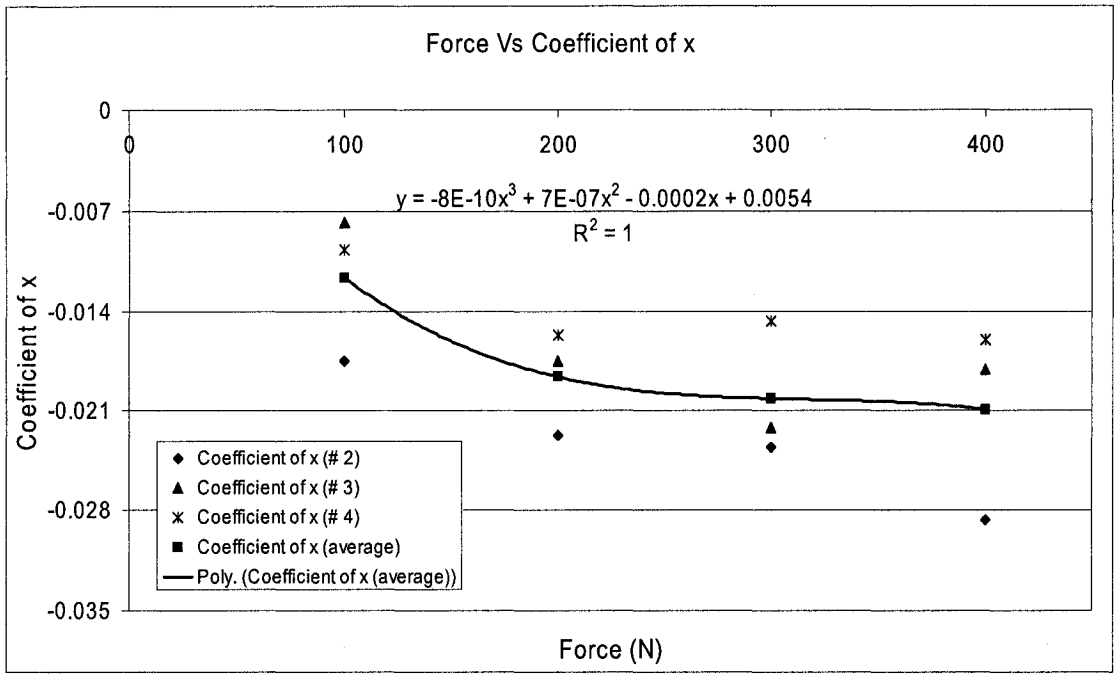

Figure 5.23: Empirical Relation to Find the Co-efficient of x.

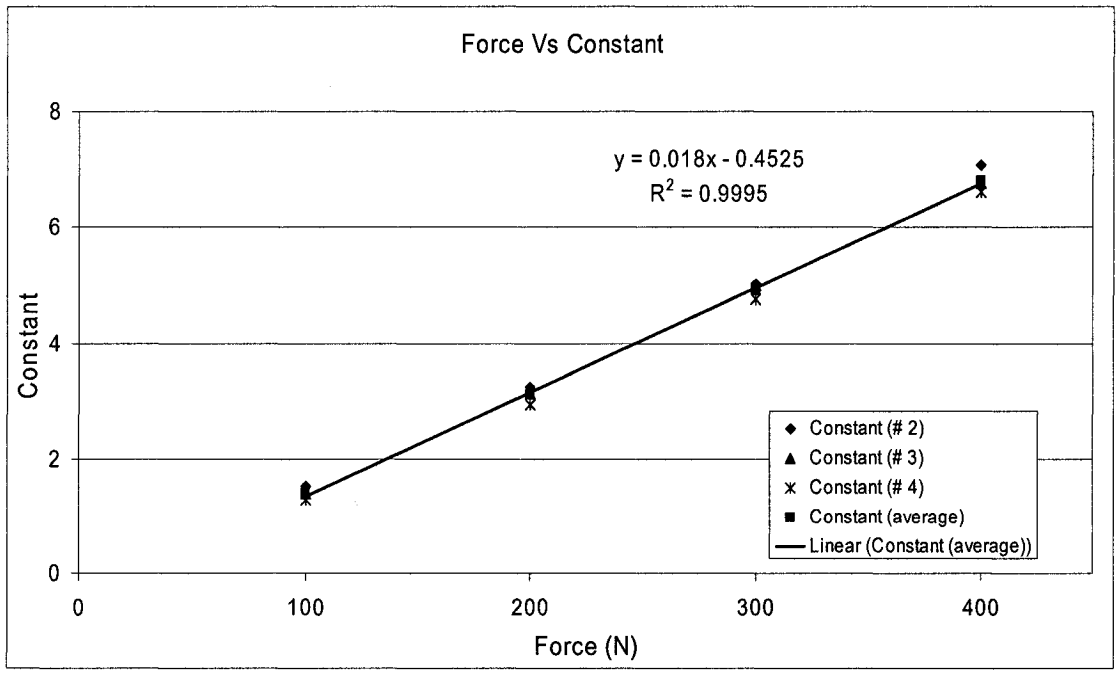

Figure 5.24: Empirical Relation to Find the Constant.

By this approximation method, the coefficients A, B, and C of the quadratic equation i.e. $y = Ax^2 + Bx + C$ can be obtained. Here y represents the highest peak value and x represents the position of the impact.

5.4 Comparison of Designs 1 and 2

A sample test was conducted determine the difference between the two designs. A known load was applied at a known position and the two peak values were recorded. The procedures that were described in section 5.2.1and 5.2.2 were used to determine the magnitude of the applied force and its position on the bumper. The results show that for a known force and position, design 1 showed 3% and 11% errors for the force and position respectively. However, for the same loading, design 2 showed 3% and 5% errors respectively. This suggests that design 2 is more accurate in determining the position of the applied force.

5.5 Summary

This is the core chapter of the thesis. In this chapter two design approaches were described for determining the magnitude and position of the applied force during collision. The essential difference between designs 1 and 2 was that design 2 had a cover plate with teeth positioned directly on the PVDF sensors. A new two-sensor method was developed to characterize the bumper system in terms of the applied load and the corresponding position. A graphical method was developed to detect the impact position. In order to simplify the graphical method, an approximation method was developed. The

results of the experiment showed that design 2 determines the position of the impact load more accurately than design 1.

CHAPTER 6

CONTRIBUTIONS, DISCUSSIONS AND RECOMMENDATIONS

6.1 Highlights of the Investigation

The overall objective of this dissertation was to identify the contemporary methodology of measuring the severity of vehicle impact (as described in Chapter 1) and then to propose a new, effective and feasible measure of vehicle collision that could be incorporated in a vehicle bumper system to state the magnitude of an impact force and its position. The specific objectives involved a detailed understanding of the vehicle bumper system and the characteristics of PVDF sensor so that this sensor could be adopted in a vehicle bumper system successfully as a collision detector. Rapid enhancement of vehicle collision phenomena compelled vehicle manufacturers to innovate a smart and handy way towards solving this problem. This study could be an effective idea to measure the impact phenomena in a very impressive way. The thesis leads the automotive industry towards using PVDF (piezoelectric polymer) as a sensing element for vehicular collisions. This concept has been adopted in a bumper prototype made with a Plexiglas material (follows the lightweight concept of using plastic material as bumper beam) and after a series of experiments it was made possible to develop a successful collision detection system that is able to measure collision force and position. The system is designed, manufactured and assembled in such a way that right after the collision, the force and position can be evaluated as outputs. The peak amplitude of the force indicated in a signal generator is used as the input. This adds an option for the vehicle industry. Three traditional upfront sensors prevail in the bumper system as mentioned in chapter 1 (accelerometer, ball-in-tube and radar). Among them, radar is

capable of detecting the shape of the impact object and could be used as an alternative to one of the other two previously mentioned up-front sensors in future vehicles. Besides possessing dynamic characteristics to prove its validity in a bumper system (as described in Chapter 2), the proposed PVDF sensor is capable of detecting the shape of the impact object and the degree of impact and it is frequently used in tactile sensing [21, 40, and 41]. So, the idea of approaching PVDF as a sensing element in a bumper system will add a new dimension in the advancement of crash severity sensing techniques. The major contributions of this dissertation are below:

- The general characteristics of a PVDF sensor (repeatability, linearity, force sensitivity, nullification of cross sensitivity etc.) that are essential for impact measurement were re-established through different experiments.
- This thesis reveals the idea of using a PVDF sensor for detecting low speed to very low speed vehicle collision.
- A set-up was designed, manufactured and the necessary instruments were calibrated and assembled to complete the process of collision detection. A prototype of a bumper beam was designed in 1:5 ratios to investigate vehicle (generally low speed) collisions (i.e. to obtain the normal collision force and position) by implementing Polyvinylidene fluoride sensors on a vehicle bumper prototype by an inline approach (all the sensors are attached in a row in the middle portion along the bumper).
- This thesis proposes a new set of collision measures. This innovative methodology is incorporated by determining the degree of impact and location of impact as a function of peak voltage (the sensor's output is fed to a charge

amplifier to obtain peak magnitude of voltage). This new collision measure could replace the widely accepted characteristics to define collision, such as force, acceleration, displacement, and rebound velocity & impact energy.

- A new technique to evaluate the collision force was developed and termed the *two sensor method* where the magnitude of normal force and its position of application are evaluated by the help of two sensors (two concerned sensors where the normal force is applied in between).
- An approximation system was developed to determine the position of the applied force in a more versatile form.
- The entire collision detection was generated where the input is simply the summation of two concerning sensors (in between which the impact is applied) output. This new approach is believed to be useful to omit the controversy in determining the fender bender phenomena.

6.2 Discussions and Conclusions.

The reason for choosing the PVDF film as the transduction principle is that it is durable, rugged, and is potentially low cost. In addition, it can easily be deposited on the bumper using micro electro-mechanical (MEMS) techniques. Using this technique, the cost will reduce dramatically. Furthermore, the same transducers could be used to transmit and receive ultrasound that could be used as collision avoidance transducers. The combination of these attractive characteristics make PVDF films the prime candidate for transduction. To avoid the pyroelectric effect of PVDF sensor, a Mylar film was used to cover it. Additionally in the two-sensor method, a cover plate was placed on the top of

the Mylar film. As a result of this, the pyroelectric effect of the PVDF film was isolated. Thus any spurious results due to a pyroelectric effect were avoided.

The wire connection to the 25μm PVDF film was challenging. For this purpose, conductive glue was used. Since the impact load was high, disconnection occurred due to vibration. This problem was partially overcome by bending the PVDF film and gluing it to the substrate. The use of MEMS deposition would overcome this problem more effectively.

Considering the above advantages of the PVDF film and illuminating to the fact that there is no study on the use of this transducer on the bumper of vehicles according to the best knowledge of the author, makes this work a worthwhile contribution.

Using the approximation method, curve fitting technique was used. Although many attempts were made to fit the best curve, the fitted curves did not seem to fully represent the experimental data. A more advanced curve fitting method would result in a better approximation, hence reducing a possible error due to position detection.

Although the results obtained from design 1 was sufficient; but design 2 in which the teeth of the bumper directly contacted to the PVDF sensors, improved the signals obtained from the PVDF sensors significantly. The sensors exhibited better repeatability, high dynamic range, and high signal-to-noise ratio. This is because in design 2, the applied load was directly transmitted to the PVDF sensors via the teeth of the cover plate. Hence, reducing structural vibration and reducing noise.

In this investigation, a new concept was employed for collision detection using PVDF film as the transduction medium. An innovative two-sensor method was developed for detecting the magnitude of the impact load and its position on the bumper. Considering

the promising results obtained in this study and the potential of the PVDF film, further study in this area would be worthwhile.

6.3 Recommendations for Future Work

- In this study, a rigid probe was used to apply the impact load. The study could be expanded towards impact by various soft probes. The soft object introduces a spring and damping effect. This effect could be detected by the PVDF sensor, resulting in various output transient signatures. Research could be conducted to determine the rise and fall time of these signals. The characterization of these signatures could enable the investigators to distinguish various soft-contact objects. The results of such a study could be useful to determine the object with which the vehicle collided.

- This study reports on a collision detection using a circular probe of 0.4 inch (10 mm) diameter. However in a real collision situation, the collision is normally bumper to bumper, thus the impact area is lager than 0.4 inches. This effect should be investigated.

- As was mentioned in the discussion, PVDF film can be used as a transmitter and receiver of ultrasound. Hence the system described in this study could also be used as a collision avoidance system. Further study is required to adopt this approach. In addition, the pyroelectric effect of the PVDF film could also be used to measure the temperature. This information could be useful in obtaining

additional information about the severity of the collision. This would require that additional PVDF films to be integrated on the surface of the cover plate. The pyroelectric effect could also be used in collision avoidance by detecting the intensity of light. Further study could be conducted in this area.

- In this study, vertical loads were applied to the bumper. In a real collision, it is possible for the impact to be at an angle. Thus, a study should be performed to investigate the effect of an inclined load.

- The dynamic range considered in this study was between 100 N and 400 N. Hence, this study reports on low to very low speed collision. Further work is required to investigate moderate to high speed collisions.

REFERENCES

(1) Szabo Thomas J. and Welcher J., Biodynamic Engineering Inc., "Dynamics of low speed crash test with energy absorbing bumper", SAE technical papers (921573). pp. 1-9.

(2) David J. King, Gunter P. Siegmund, and Mark N. Bailey, MacInnis Engineering Associates Ltd., "Automobile Bumper Behavior in Low-Speed Impacts", SAE technical papers (02-11),1993, pp. 1-18.

(3) Brach R.M., University of Notre Dame; Brach R.M, Tnodyne Inc., "A review of impact models for vehicle collision", SAE technical papers (870048), 1987.

(4) Patrick M. Glance, Concept Analysis Corporation, "Measuring the Phenomenon of Bumper Impact", SAE technical papers (01-3187), 1999, pp. 1-10.

(5) Heinrichs Bradley E., Lawrence J.M., Allin B.D., Bowler J.J., Wilkinson C.C, Ising K.W., King D.J. (Macinnis Engineering Associates), Ptucha S.J. (Westport Research Inc.), "Low-speed impact testing of pickup truck bumpers", SAE technical papers (01-0893), 2001.

(6) Howrad R.P., Bomar J. and Bare C., Biodynamic Research Corp., "Vehicle restitution response in low velocity collisions", SAE technical papers (931842), 1993, pp.1-10.

(7) Tanner B.C., Wiechel J.F., Bixel R.A., Cheng P.H. (S.E.A Inc), Guenther D.A (Ohio State Univ.), Cassidy M.P. (Daimler Chrysler Corp.). "Coefficients of restitution for low and moderate speed impacts with non-standard impact configurations", SAE technical papers (2001-01-0891), 2001.

(8) Cannon J.W. (Washington and Jefferson College), "Dependence of a coefficient of restitution on geometry for high speed vehicle collisions", SAE technical papers (2001-01-0892).

(9) David A. Sindrey, Stelco Inc., "Steel Bumper Systems for Passenger Vehicles and Light Trucks", SAE technical papers (01-1007), 1999, pp. 1-9.

(10) Adolfsson J., SAAB Automobile, Sorqvist E., Outokumpu Stainless, Trollhattan, "Lighter Stainless Steel bumper Contributes to Improve Fuel Efficiency in Cars", 2005.

(11) Plastics and Today's Automobile, American Plastics Council, http://www.plastics-car.com.

(12) Suddin M.N., Salit M.S., Ismail N., Maleque M.A. and Zainuddin S., "Total design of polymer composite automotive bumper fascia", Suranaree J. Sci. Technol. 12(1), 2004, pp. 39-45.

(13) Rawson Janet M, GE plastics, "Comparison of analysis results to physical testing performance of engineering thermoplastic bumper beams", SAE technical papers (940168), 1994.

(14) Evans D., GE plastics; Morgan T., GM small car division, "Engineering thermoplastic energy absorbers for bumpers", SAE technical papers (1999-01-1011), 1999.

(15) (Chaudhari M.K., Sandhu S.S. and Raghu R., The automotive Research Assn. of India, "Design, development, testing and evaluation of energy absorbing bumpers", SAE technical papers (93-1843), 1993.

(16) Gilliard B, GE Plastics; Bassel W., Haque E., Lewis T., Azdel Inc.; Featherman D., Altair Engineering;Johnston C., Continental Structural Plastics, "I-section bumper with

improved performance from new mineral-filled glass mat thermoplastic (GMT) composite", SAE technical papers (1999-01-1014), 1999.

(17) Zaouk A.K., Bedewi N.E., Kan C. and Marzougui D., "Validation of a no-linear finite element vehicle model using multiple impact data", International Mechanical Engineering Congress and Exposition, 1996.

(18) Gioutsos T.; Breed Technologies Inc., "Important issues in crash severity sensing", SAE technical papers (2002-01-0182), 2002.

(19) Gioutsos T. and Tabar D.; Breed Technologies Inc., "Determination of crash severity using a ball-in-tube and accelerometer sensing system (BASS)", SAE technical papers (1999-01-1326), 1999.

(20) Foo A., TRW Automotive Electronics; Ridella S.A., TRW Automotive, Occupant Safety Systems, "Advancements in crash sensing", SAE technical papers (2000-01-C036), 2000.

(21) Dargahi J., Parameswaran and Payandeh S., "Micro machined piezoelectric tactile sensor for an endoscopic grasper-theory, fabrication, and experiments", Journal of Micromechanical Systems, Vol. 9, No. 3, 2000, pp. 329-335.

(22) Dargahi J., "Piezoelectric and pyroelectric transient signal analysis for detection of the temperature of a contact object for robotic tactile sensing", Sensors and Actuators, A-71, 1998, pp. 89-97.

(23) Dargahi J., "A piezoelectric tactile sensor with three sensing elements for robotic, endoscopic and prosthetic applications", Sensors and Actuators (80), 2000, pp. 23-30.

(24) EHAG Electronics Hardware AG, *"Piezo film sensors technical manual"*, http://www.ehag.ch.

(25) APC International, Ltd, *"Piezoelectric ceramics: principles and applications"*, Mackey Ville, PA, [c2002].

(26) Chatigny J.V. and Robb L.E., *"Piezo Film Sensors"*, Pennwalt Corporation.

(27) Dargahi J., Phd Thesis, "The application of Polyvinylidene Fluoride as an robotic tactile sensor", Glasgow Caledonian University, Glasgow, UK, April 1993.

(28) Gregorio R. Jr and De Souza Nociti N.C.P., "Effect of PMMA addition on the solution crystallization of the α and β phases of Polyvinylidene Fluoride (PVDF)", J.Phys.D: Appl. Phys.,Vol. 28, 1995, pp. 432-436.

(29) Furukawa T. and Wang T., *"The Application of Ferroelectric Polymers"*, T. Wang, J. M. Herbert, A. M. Glass, Eds, Newyork: Blackie, 1988.

(30) Dargahi J., Sokhnavar S., Packirisamy M., "Theoretical and experimental techniques in using Polyvinylidene Fluoride (PVDF) films as a transducer in sensor systems", No.01-CSME-44, Vol. 28/ Issue no. 2B, 2004, pp. 291-307.

(31)Kepler R.G. and Anderson R.A., "Piezoelectrcity and pyroelectricity in Polyvinylidene Fluoride", Journal of Applied Physics, Vol.49(8), 1978

(32) Gerlicszy G. and Betz R., "SOLEF PVDF biaxially oriented piezo and pyroelectric films for transducers", Sensors and Actuators, Vol. 12m, 1987, pp. 207-223.

(33) Dario P., Bardelli R., De Rossi D., Wang L.R., Pinotti P.C., Sensor Review, 1982, pp. 194-198.

(34) Ounaies Z., Harrison J.S. and Rich J., "Piezoelectric materials for sensor and actuator application at NASA LARC", ICASE, Vol. 8, No. 2, 1999.

(35) Code of Federal Regulations (CFR).Title 49, Volume 5, Parts 400 to 999, Revised as of October 1, 1999.From the U.S. Government Printing Office via GPO Access.pp.824.

(36) American Iron and Steel Institute, "Steel Bumper Systems for Passenger Vehicles and Light Trucks", Revision Number Two (Feb 15, 2003).

(37) Smith John J., Smith Raymond P. and Associates Inc., "Why Injuries Occur in Minor Vehicle Damage Collision".

(38) Good fellow Sensors, England, http://www.goodfellow.com/csp/active/gfHome.csp

(39) Kato T., Yamamoto A., Higuchi T., "Shape recognition using piezoelectric thin films", IEEE, 0-7803-7852, pp.-112-116.

(40) Dargahi J., Najarian S. and Zheng X.Z., "Measurements and modeling of compliance using novel multi sensor endoscopic grasper", Sensors and Materials, Vol.17, No.1, 2005, pp.7-20.

APPENDIX – A

Base Frame Design

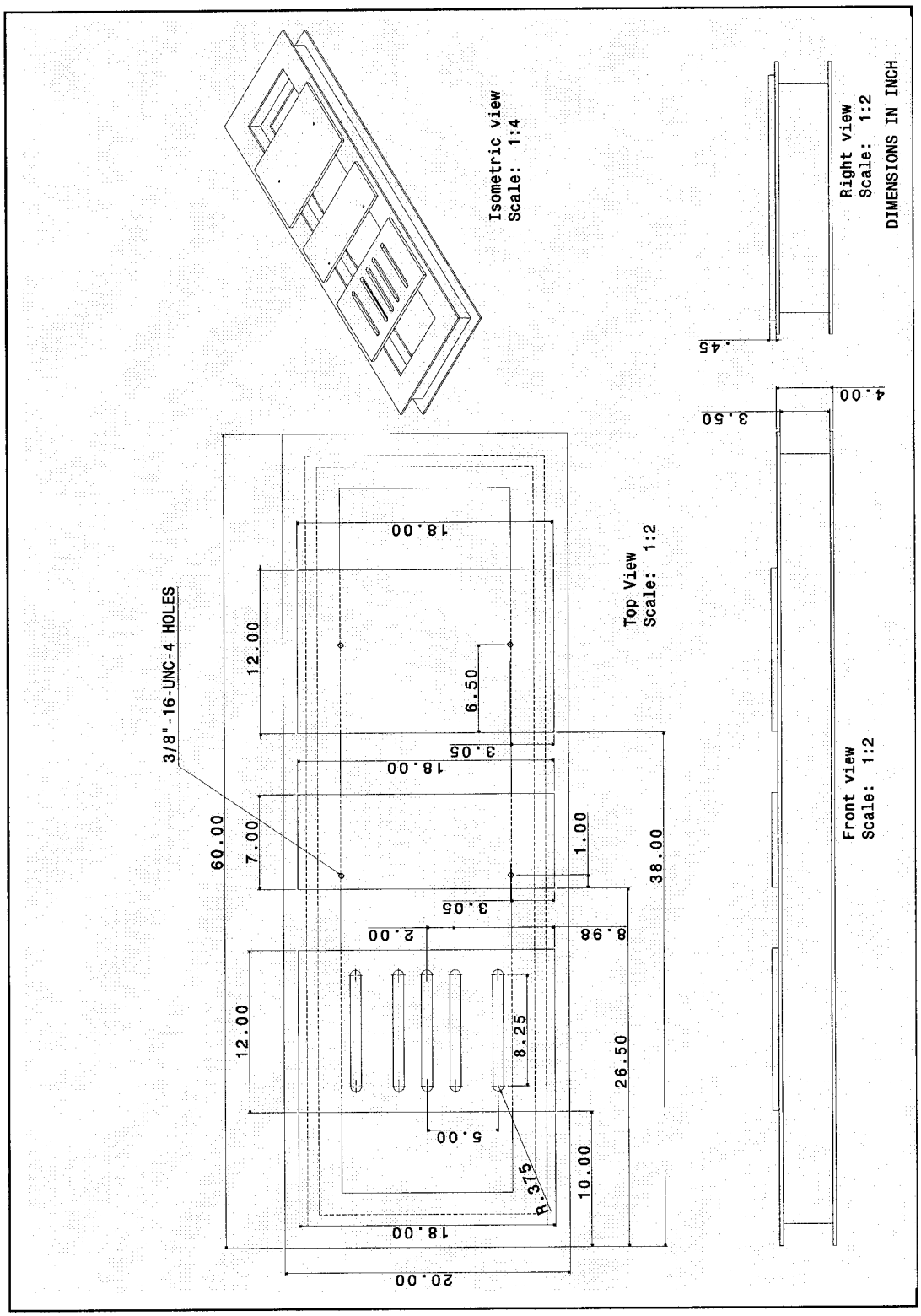

Bumper Holder Design

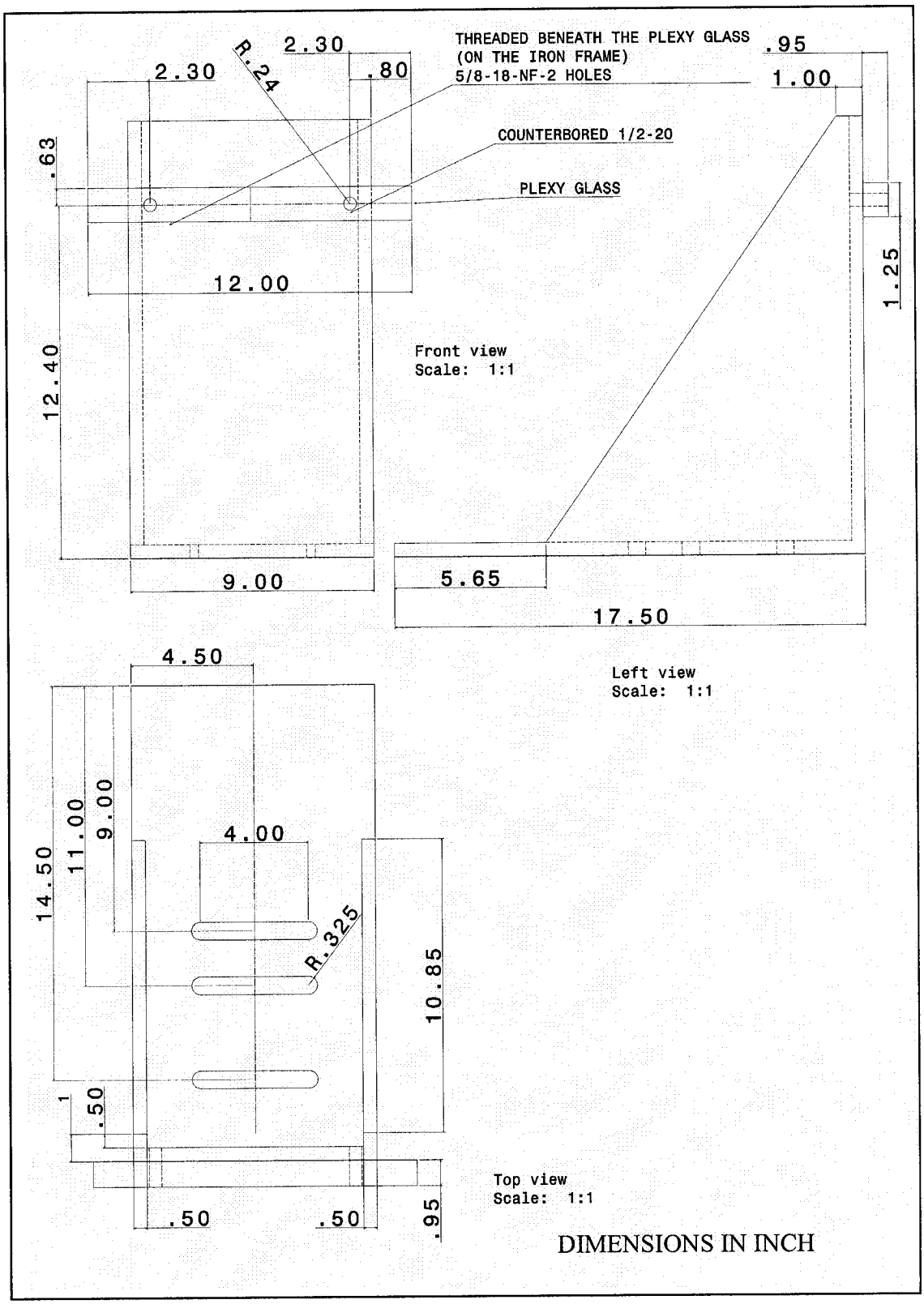

Probe with Removable Head Design

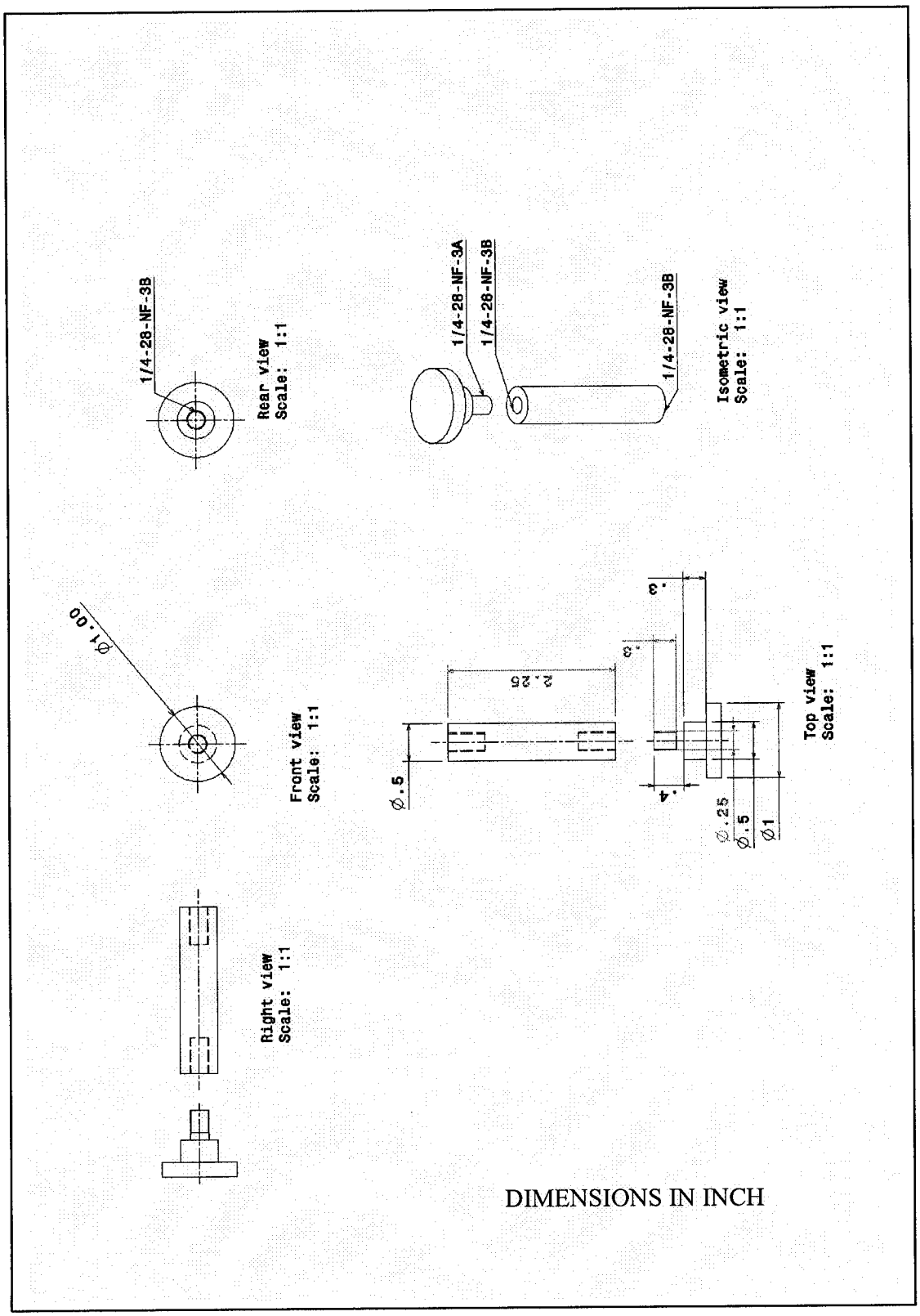

APPENDIX-B

Sample Calculation of Collision Detection Design 1

To test the entire procedure of collision detection a known load of 300 N is applied in a known position of 20.32 mm away from sensor 3. The highest peak values of output voltages were recorded. These two outputs value were inserted in to the system to obtain the corresponding load and position like the real life situation. The two-sensor method for force and position (graphically and analytically) detection and approximation method were justified.

It is assumed that a collision has occurred. The signal analyzer in the car detects that the highest peak is from the sensor 3 and is 6.31 V and that the second highest peak is from sensor 2 and is 5.67 V. It is clear that the impact occurred between these two sensors. The sum of the two peak values is 11.98 V. To determine the magnitude and position of the impact load, the following calculation will be conducted:

From equation 5.2, which is $y = 0.0371x + 0.8479$ where y is the sum of the two highest peak voltages and x is the impact force in Newton. Hence, the impact force is 300 N. For a 300N impact load, from Figure 5.8 the position is found to be 21.2 mm away from sensor 3. The position equation developed in Figure 5.10 for a 300 N load by sensor 3 was found as

$$y = -0.0001x^2 - 0.0429x + 7.0989$$

So using this equation x value was found to be 18 mm.

The *approximation method* could be used to detect the position of the above collision.

Using the equations developed in Figures 5.11, 5.12 and 5.13, the coefficient of the quadratic equation i.e. $y = Ax^2 + Bx + C$, can easily be found according to the applied load. By considering 300N load in the equations of approximation method the coefficients result as following.

$A = -2.78 \times 10^{-4}; B = -31.7 \times 10^{-3}; C = 7.15;$

So the equation becomes,

$y = -2.78 \times 10^{-4} x^2 - 31.7 \times 10^{-3} x + 7.15$

The highest peak value from sensor 3, y = 6.51 V as mentioned earlier so the position of impact can be obtained as: x = 17.52 mm away from sensor 3.

Collision force and its corresponding positing can also be evaluated in Collision Detection Design 2 by using the same procedure.